Title of Thesis

CFD Simulation of Silica Gel and Water Adsorbent Beds Used in Adsorption Cooling System

By

JOHN WHITE

Student No: 1068698

Project Supervisors: Dr. R. K. Al-Dadah and Dr Michael Ward

A THESIS SUBMITTED

FOR THE DEGREE OF DOCTOR OF PHILOSOPHY

DEPARTMENT OF MECHANICAL ENGINEERING

THE UNIVERSITY OF BIRMINGHAM

2012

ABSTRACT

Adsorption cooling systems are considered to be an important alternative to conventional heating and cooling systems, however at present it has had limited commercial applications. This is because of the low thermal heat transfer during its operations cycle from heat exchanger to adsorbent packing. The main objective of this study is the design and CFD simulation of a new compact copper wire woven fins heat exchanger and silica gel adsorbent bed used as part of an adsorption cooling system. This type of heat exchanger has a large surface area because of the wire woven fins design but can still be design as a small compact heat exchanger. It is proposed that this will help improve the coefficient of performance (COP) of the cycle and improve the heat transfer rate in the system. The porous adsorbent bed is the core component of an adsorption cooling system. Its heat transfer performance has a control on the adsorption/desorption of vapour refrigerant capacity of the system. The porous materials used as packing in the adsorbent bed are the fundamental building blocks for the adsorption cooling system but despite its importance as a packing in an adsorbent bed, very little is known about flow dynamics in porous media. One reason for this is because of the difficulty of measuring the heat transfer between porous media and heat exchanger fins, and adsorption/desorption of water vapour in a full bed. This has restricted the design and development of this technology, therefore, in order to investigate the heat transfer between the fins and porous adsorbent, Computational Fluid Dynamics (CFD) Solidworks COSMOS CFD FLOW Simulation software was used. The software Solidworks COSMOS FLOW developed by DASSAULT SYSTEMES, has CFD heat transfer, porous material and gas two phase simulation capability and uses the Finite Volume (FVM) method approach and hybrid surface modelling method to develop CFD models and assemblies. The software described are incorporated into Solidworks as add on programs making this CFD programs more users friendly.

This study used flow simulation CFD high resolution to better understand the vapour flow through complex porous media, adsorbent beds, both sizes of porous media, and arranged and random sphere packing.

This thesis CFD simulation comprises experimental data derived from using a Dynamic Vapour Sorption (DVS) adsorption test rig in the Department of Chemical Engineering University of Birmingham and material published on various types of adsorbent beds, adsorption cooling systems, technical papers and peer-reviewed journals, leading to the concept design of an adsorbent bed test rig with a copper wire woven fins heat exchanger. The purpose for this adsorbent bed design with the use of copper wire woven fins was for two main reasons:

(i) To help increase the surface area of the heat exchanger without increasing the size of the heat exchanger.

(ii) To help increase the heat transfer from the heat exchanger to the silica gel adsorbent which is an associated problem linked to the adsorption cooling systems low heat transfer.

The wire woven heat exchanger has a larger surface area due to the copper wire woven fins which help to increase the heat transfer coefficient, enabling it to be used as part of the of an adsorbent bed.

ACKNOWLEDGEMENTS

I would like to thank the following people for their guidance and advice during the course of this project:

Dr. R. K. Al-Dadah, Project Supervisor, Lecturer in Thermofluids, School of Mechanical Engineering. University of Birmingham

Dr Michael Ward Senior Lecturer, School of Mechanical Engineering University of Birmingham.

I would like to acknowledge the advice and assistance of Mr Paul Kerby, Director of P.A.K Engineering Ltd.

Finally, I wish to express my gratitude to my family and friends for their help and encouragement, support, understanding and love.

Publications

White, J. (2012) "Computational Fluid Dynamics Modelling and Experimental Study on a Single Silica Gel Type B", *Modelling and Simulation in Engineering*, Hindawi Publishing Corporation. Published online January 2012, vol. 2012, Article ID 598479, 9 pages,

This publication is incorporated as chapter four of this thesis

White, J. (2012) "A CFD Simulation on How the Different Sizes of Silica Gel Will Affect the Adsorption Performance of Silica Gel", *Modelling and Simulation in Engineering*, Hindawi Publishing Corporation. Published online January 2012 vol. 2012, Article ID 651434, 2 Pages

This publication is incorporated as chapter five of this thesis

White, J and Al-Dadah, R.K. (2012) "The Adaption of Wire Woven Fins to Improve Heat Transfer and Reduce the Size of Adsorbent Beds*",* ***In Progress***

White, J., and Al-Dadah, R.K. (2012) "Using CFD Media Approach to Study Performance in Adsorbent Beds" ***In Progress***

White, J., and Al-Dadah, R.K (2012) "Compact Adsorbent Bed Design using Wire Woven Fins", ***In Progress***

TABLE OF CONTENTS

Chapter 1

Chapter 2:

Literature Review

Chapter 3:

First principles of computational fluid dynamics

Chapter 5:

A CFD Simulation on how the different sizes of silica gel used in an adsorbent bed will affect the adsorption performance of silica gel

I hereby declare that all information in this document has been obtained and presented in accordance with academic rules and ethical conduct. I also declare that, as required by these rules and conduct, I have fully cited and referenced all material and results that are not original to this work.

Name, Last name: John White ……

Signature ……..

Date ……..

LIST OF TABLES

LIST OF FIGURES

Chapter 2

Chapter 3

Chapter 4

Chapter 5

Chapter 6

Chapter 7

Chapter 8

Nomenclature

a	:	Surface area of silica gel	(m^2)
C_0	:	Inlet concentration	(kg m^{-3})
C	:	Bed concentration	(kg m^{-3})
C_2	:	Inertia resistance coefficient	(m)
c_p	:	Specific heat	(kJ kg^{-1} K^{-1})
COP	:	Coefficient of performance	(-)
D	:	Molecular diffusivity	(m^2 sec^{-1})
D_p	:	Particle diameter	(m)
D_e	:	efficient water diffusivity	(m^2/s)
h_m	:	Surface mass transfer coefficient	(kg kPa $^{-1}m^{-2}$ s^{-1})
h_{fg}	:	Latent heat of vaporisation of water	(kJ kg^{-1})
Htc	:	Heat transfer coefficient	KW/(m^2K)
k	:	Mass transfer coefficient	(sec^{-1})
LMTD	:	Log mean temp difference	(°C)
P	:	Partial pressure	(Pa)
Pr	:	Prandtl number	(-)
q	:	Adsorbent capacity	(mmol g^{-1})
q_s	:	Maximum capacity	(mmol g^{-1})
R	:	Thermal resistance	(k/kw)
R_{cont}	:	Contact thermal resistance	(k/kw)
SCP	:	Specific cooling power	(kw/kg)

t	:	Time	(sec)
τ	:	The tortuosity factor	(-)
u	:	Water vapour velocity (x-direction)	(m sec^{-1})
U	:	Heat loss coefficient	(w/m^2 °C)
v	:	Water vapour velocity (y-direction)	(m sec^{-1})
w	:	Water vapour velocity (z-direction)	(m sec^{-1})
wl	:	Weight loss percentage	(w/w%)
ΔH	:	heat of adsorption (J/mole)	(-)
ρ	:	the fluid density	(kg/m^3)
α	:	Linear thermal expanding coefficient	(K^{-1})
λ	:	Thermal conductivity	(kW m^{-1} K^{-1})
Δx	:	Distance between nodes	(m)
Δm	:	net flow between nodes	(kg s^{-1})
μ	:	Viscosity	(kPa s)
ṁ	:	total mass flow flux of water vapour	(kg/sm^2)

Greek symbols

ε : Bed fraction (Porosity)

ρ_s : Particles Density (kg m^{-3})

ρ : Fluid Density (kg m^{-3})

α : Viscous resistant coefficient (m^{-1})

μ : Fluid Viscosity (Ns m^{-2})

Abbreviation

CFD： Computational Fluid Dynamics

LDF： Linear Driving Force

UDS： User’s Defined Scalars

UDF： User’s Defined Functions

CHAPTER 1

1.1. Introduction

Over the years Computational Fluid Dynamics (CFD) has become a standard simulation tool for the design, analysis, system performance and analysis of engineering systems concerning fluid flows [1-7]. This increase has been driven by the progress of computer speed, affordable systems and the ease of availability of new commercial CFD software leading to the steady decrease in the costs of CFD simulation compared to prototype experiments [2].

A good understanding and an accurate description of adsorption/desorption, water vapour velocity flow, heat and mass transfer are necessary for the modelling of adsorbent beds as part of adsorption cooling systems [3-5]. Accurate modelling of porous adsorbent packed - beds is difficult, due to the existence of wall effects across the entire radius of the bed, flow outlet, heat and mass diffusion and complex flow structures generated by the internal geometry of the porous adsorbent packed region. With new methods such as CFD it is possible to get an in-depth view of the system [6,8].

1.2 Problem Statement

Adsorbent beds are an essential part of the adsorption cooling system as they are used for the adsorption/desorption of water vapour from the evaporator chamber with the help of a heat exchanger and porous adsorbent material [1, 3-7]. To improve the modelling of these systems a more fundamental understanding of the adsorption/desorption of water vapour on to porous media and the heat transfer from heat exchanger fins to porous media processes taking place in an adsorbent bed is required [3-8].

This is an area where (computational fluid dynamics) CFD can give a lot more information; using CFD we can identify heat transfer and water vapour velocity flow patterns inside the

adsorbent bed and look at the effects of silica gel adsorption/desorption of water vapour on different size silica gel granules used as packing in adsorbent bed [3-7].

Some of these studies of fluid dynamics and heat transfer in adsorbent beds date back to the early twentieth century Augier .F et al [1]. These early investigations of flow in porous media packed beds provided mainly bulk information such as pressure drop correlations, Mueller, G. E [2] predict pressure loss for flow in adsorbent beds.

Rahim and Mohseni [3] used CFD to provide an innovative approach to model and analyse the local flow and the effect of silica gel size on adsorption performance of a packed bed. CFD simulation of porous media local flow and heat transfer based on CFD technique has increasingly been reported in recent years in fields of packed bed flow and heat transfer modelling [7] CFD simulation is based on fundamental principles of diffusion and adsorption/desorption of porous materials Murakami et al [4].

1.3 Adsorbent Bed Modelling

When attempting to model an adsorbent bed, it is necessary to have a good understanding of the packing structure, porous adsorbent granule size, porosity, particle distribution and void fraction and chemical nature [4]. This is of prime importance when evaluating adsorption/desorption rates in porous adsorbent packed beds, and vapour flow heat and mass transport phenomena between porous adsorbents and fins [5].

1.4 Wire Woven Fins Heat Exchanger used as Part of the Adsorbent Bed

Wire woven fins heat exchangers have been extensively used in heating and cooling applications such as engine oil cooler and air heating system but has not yet been adapted for the application of adsorption cooling system. This type of heat exchanger can be adapted to be used as part of the adsorbent bed to help solve the problems adsorption system has with

the oversize adsorbent bed. This type of heat exchanger has continuous wire loops and therefore offers good heat transfer efficiency because of the large surface area made by using wire fins. The advantage of this type of heat exchanger is that it can be designed as a compact heat exchanger making the adsorbent bed smaller in size [4].

1.5 The Wire Wound Fins Heat Exchanger Characteristics

1. Good heat transfer enabling the design of a compact heat exchanger unit to be used as part of an adsorbent bed.
2. The above advantage makes it possible to design a heat exchange smaller in size compared with any other type of fin tubes.
3. Wire wound fin heat exchanger is made from loops of wire spirally wound over a tube and soldered throughout the length of the tube giving this type of heat exchanger large surface area.

Geometrical characteristics of the adsorbent bed (its length and diameter) together with the packing structure will influence the flow behaviour and also the heat and mass transport mechanisms. Modelling of an adsorbent bed is a difficult task due to the number of problems that have to be solved in order to obtain a practical model. Existing models for adsorbent bed heat transfer lump several transport mechanisms into each effective parameter, causing simulation models to be not descriptive enough. In the published literature no conformity concerning transport behaviour in porous adsorbent beds can be reached to date.

1.6 Aims of Research

Using a natural refrigerant for adsorption cooling technology is acknowledged as extremely important from the stand point of the environment, waste heat or solar adsorption cooling are methods which makes use of natural refrigerant and porous material. Many studies have been

carried out in the past few decades to prove the value of this technology for cooling. These efforts have inspired this study.

Present research through experimental testing and CFD simulation offers a practical strategy for the adaptability and utility of an adsorption cooling system. This study involved the design of a wire woven fins and silica gel pack adsorbent bed and data collection from the experiments conducted on the test rig. It was concerned with the determination of the interface of individual components constituting the adsorption test rig, thereby, helping the assessment of the performance of the complete system. The study involved preparation of CFD simulation model of the full adsorption cooling test rig and the CFD validation of the model from test results.

This research was also involved in the conceptual development of new wire woven fins with silica gel packing for incorporation in the CFD simulation model. The CFD simulation of adsorption cooling system showed that this new design could have beneficial effects on the performance of the system.

CFD analysis of wire fin and silica gel allowed micro analysis of the water vapour flow and heat transfer processes occurring in the adsorption bed. This micro study of the adsorption bed under adsorption and desorption of water vapour allowed an insight into the physical process that happens inside an adsorbent bed. The CFD study provided knowledge about the heat transfer attainable by fins and silica gel packing.

Finally, based on a validated model of the adsorption cooling system suggestions were made regarding the new design of the adsorption cooling system.

1.7 Research Objectives

Having outlined the aims of this study it is possible to state its main objectives as follows:

1. The design of a copper wire woven finned heat exchanger to be used as part of an adsorbent bed.
2. The use of CFD modeling as a research and design tool in the field of adsorption cooling system.
3. To suggest additional research issues form this present study.

1.8. Solving the Problem

Adsorption cooling systems which run on thermal heat cycle obtained from renewable sources could be an environmentally friendly alternative to conventional mechanical compressor systems, if the size of the heat exchanger could be reduced to a smaller size and the heat transfer between porous adsorbent and heat exchanger improved [2-3]. It is hoped that the concept design of the new wire woven fin heat exchanger proposal in the area of adsorption cooling will eventually be used as a common heat exchanger adsorbent bed design.

Many studies have been undertaken to evaluate the benefits of flat plate fin heat exchanger adsorbent bed in the adsorption cooling system. However, very few studies have been done to examine the wire woven fin heat exchanger [7-8]. There is a lack of experimental and CFD simulation data concerning the use of wire fins as part of an adsorption cooling system. This study aims to assess the potential of experimental and CFD simulation of silica gel and wire fin heat exchangers, used as part of an adsorption cooling system [2,4-8].

1.9 Scope of the Research

The aim of this work is to establish and validate CFD simulation methodologies for solving fluid flow and heat and mass transfer phenomena in three-dimensional models of adsorbent porous packed beds, and apply this strategy as a design tool for adsorbent bed used in adsorption cooling systems.

In order to accomplish this aim, the following specific objectives were established at the beginning of the study:

1. Literature review on adsorbent bed design, development and a revision of previous simulation strategies and approaches to this type of system.

2. Review of particle-to-fluid heat and mass transfer phenomena using water vapour fluid and silica gel particles through CFD simulations.

3. Validation of the flow velocity field prediction in an adsorbent porous packed bed through the comparison of CFD simulations against experimental results obtained from experimental testing.

4. Validation of temperature fields and heat transfer parameters prediction in an adsorbent bed as part of an adsorption cooling system through the comparison of CFD simulations against published data.

1.10 Research Methodology

This thesis CFD simulation is based on three sources of data. These are experimental data done on a Dynamic Vapour Sorption (DVS) adsorption test rig in the Department of Chemical Engineering University of Birmingham; a wire woven fins heat exchanger

adsorption test rig which was used to generate experimental data for the CFD simulation, and data from published research material on several adsorbent and adsorption cooling systems.
An experimental adsorption test was done on different size of porous adsorbent. The experiments gave a good insight into the working of water vapour adsorption of different size of porous media used as packing in adsorbent bed.

Also, an adsorbent bed test rig was designed with a copper wire woven heat exchanger. The purpose for this adsorbent bed design was for two main reasons (i) was to help reduce the size of the heat exchanger as this is one of the main problems of the adsorption cooling system. (ii) To help increase the heat transfer from the heat exchanger to the silica gel adsorbent, this is also one of the main problems with heat exchanger used at present. This type of heat exchanger has a large surface area due to the copper wire woven fins which help to increase the heat transfer coefficient, enabling the design of a compact heat exchanger unit to be used as part of an adsorbent bed.

A 3D model was prepared in CFD flow simulation. Prior to simulation of this 3D component model it was necessary to ensure the reliability of the CFD. Accordingly, a validation study was carried out, which proved the reliability of the CFD simulation model and encouraged further use of CFD in the modelling of new concept design of an wire woven fins adsorbent bed design.

1.11 Structure of the Thesis

This thesis covers design and experimental and CFD simulation studies on adsorption cooling system. The thesis is divided in nine chapters. These are:

Chapter 1, the present chapter, discusses the background of the research work. It outlines the factors which led to the start of this investigation. It also summarizes the goal of the research methodology.

Chapter 2 is mainly concerned with the review of relevant research work done in the general area of adsorption cooling technology. The research works reviewed includes theses written in the area of adsorption cooling, research articles discussing different aspects such as energy saving, configuration, economics, components and outlines the fundamentals of adsorption process with reference to silica gel, an important porous material. In this connection isotherms of porous materials are discussed in some detail and the adsorption cycle is described. The theory of adsorption explained in some details as well as the potential of CFD simulation.

Chapter 3 discusses the fundamentals of computational fluid dynamics.

Chapter 4 gives an account of Dynamic Vapour Sorption (DVS) experimental study and CFD modelling of on silica gel. The model validation curves and their discussions are also given here along with the simulation results. This chapter was published online in January 2012.

Chapter 5 provides a detailed CFD (Computational fluid dynamics) analysis of adsorbent beds and how different sizes of silica gel will affect the adsorption and desorption rate, the use of Solidworks flow simulation software is also given here. The information obtained from the CFD analysis about the heat transfer and flow behaviour is discussed in detail. This Chapter was published online in January 2012.

Chapter 6 CFD simulation comparison study have been carried out on a wire woven copper coil fin and a flat plat fin heat exchanger comparing the heat transfer performance. The CFD boundary conditions and properties are taken from experimental test rig data, research papers and heat transfer text books.

Chapter 7 discusses the experimental work performed on the adsorption cooling test rig. This chapter begins with the introduction of test rig design, its constituting components and data

acquisition system. Performance curves of system components such as the evaporator, condenser and adsorbent beds are discussed. This chapter also outlines the system behavior under different operating conditions and a full system CFD simulation.

Chapter 8 discusses the conclusions and suggestions for further work. This includes some guidelines about using adsorption-cooling system in conjunction with other cooling methods.

1.12 Conclusion

A great deal of research covering all important aspects of the adsorption cooling system has been undertaken in the past few decades; however a major portion of these studies have been concerned with the mild climate of Europe, China and North America. Few studies have been conducted for the hotter climates but now there is an increasing requirement to investigate the performance of adsorption cooling systems due to the need to conserve energy and find sustainable alternatives. This requirement has been brought about by increasing environmental concerns of using fossil fuels.

CHAPTER 2

LITERATURE REVIEW

Abstract

The main purpose of this chapter is to provide essential understanding of the solar energy or waste heat power adsorption cooling systems and to give a useful procedure regarding design parameters of adsorbent beds used in adsorption cooling. Adsorption cooling technology can meet the needs for cooling requirements such as air-conditioning and food preservation [9-13]. They have almost no moving parts and are environmentally friendly. For these reasons there is a growing interest in the development and use of adsorption cooling technology owing to their various environmental benefits.

2.1. Introduction

Industrial design and development of adsorption cooling systems started in the 1920s by using silica gel and sulfur dioxide, Miller [9]. However, because of the new development of CFC refrigerants and the development of mechanical vapour-compression the adsorption cooling technology was abandoned until the 1970s when IGT [10] conducted a technical feasibility study of water vapour adsorption cooling system. However, this technology was not as popular as the mechanical vapour compression driven cooling system in the 1970s. A design and development researcher Tchernev 1979 [11] started work on adsorption working pairs to be used in adsorption cooling systems. This was used for the cooling of vaccines in developing countries. However, because of this development the interest in this type of technology started to grow rapidly in the 1980s with many cooling system researchers worldwide working on a variety of adsorption cooling system. A company called Nishiyodo Kuchou Manufacturing Company (Japan) in 1986, designed and manufactured the first

industrial adsorption cooling system see figure.2.1. Since then, the adsorption chiller has been used and closely evaluated in a wide area of applications in Japan, Europe and USA with high initial acceptance.

2.1.1 The Adsorption Cooling Technology

The adsorption cooling technology utilises the physical adsorption process where the molecules of the water vapour or gas are bound to the surface of the porous adsorbent by Van-der-Waal forces [9,12-20]. These adsorbents are porous materials like silica-gel, zeolites and activated carbons. The main structural feature of the porous adsorbent and refrigerant pair is the amount of adsorbed fluid per unit of dry porous adsorbent.

2.1.2 The Main Advantages of Adsorption Cooling Technology

- It is a robust technology with no risk of crystallization, no danger of damage due to temperatures.
- The materials used today (zeolite, silica gel) are environmentally friendly
- Very low intrinsic electricity consumption due to the lack of a pump. Electricity is only required for the switching valves and the control unit.
- Very little moving parts with the potential of low maintenance effort and costs.
- High potential of cost reduction in mass production due to the small number of individual parts.

2.1.3 The Main Disadvantages are

- High requirements for vacuum tightness of the container.
- Slightly lower COP than comparable absorption technology.
- Cyclic temperature variation in the hydraulic circuits requires careful design of the external hydraulic circuits.

- Commercially available machines are expensive and only some suppliers are on the market.

2.1.4 Design and Development in Adsorption Cooling Technology to date

The next section of this chapter will describe the recent developments in the field of adsorption cooling technology, heat and mass transfer, working pairs, component developments.

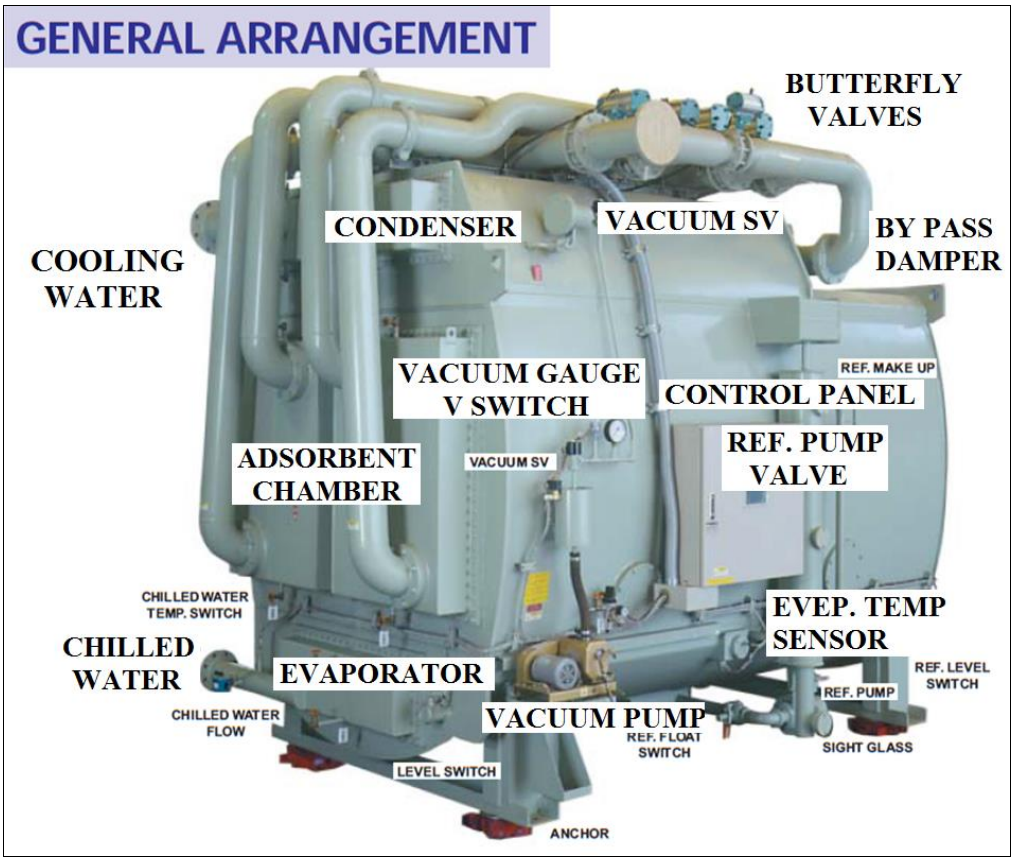

Figure 2.1.Adsorption cooling system design by Nishiyodo Kuchou Manufacturing www.emissionless.com.

The adsorption cooling system is still limited by four main technological problems that have not yet been solved, as follows:

1. Have low coefficient of performance (COP) values.
2. Intermittently working principles.
3. Require high technology and special designs to maintain high vacuum.

4. Have large volume and weight relative to traditional mechanical heat pump systems.

In the following section of this literature review an attempt is made to give a brief discussion on the attempts made to design an adsorption cooling system with good coefficient of performance (COP). Sakoda and Suzuki [13] designed and studied a silica-gal water pair adsorption cooling system. Sakoda and Suzuki [14] then designed and built a small silica-gal water cooling system and proposed a simple CFD simulation model which could interpret the experimental results. Their research showed that the heat transfer area between the porous adsorbent packed bed and its heat exchanger had a considerable effect on the COP. Gurgel [15] designed and studied an adsorption cooling drinking fountain using silica gel/water pair. Cho and Kim [16] designed a tested and developed a CFD simulation code to study the effects of heat exchangers and heat transfer rate on the cooling capacity of a silica-gal/water adsorption cooling system. Kluppel and Watabe and Yanadori [17] designed and studied the cooling characteristic of silica gel /ethanol. Saha et al.[18] studied analytically the performance of a three-stage silica-gal/water adsorption cooling system to temperatures the waste heat used was between 55°C to 85°C.

Boelman et al. [19] studied the influence of thermal capacitance and heat exchanger UA-value on the cooling capacity, power density, and COP of a silica gel-water chillier.

Alam et al. [20] investigated the effect of adsorbent bed on the performance of silica gel adsorption refrigeration systems. Anyanwu and Ezekwe [21] designed and studied experimentally an active carbon/methanol adsorption cooling system. This system had three major components a collector adsorber, condenser and evaporator.

The collector was designed as a flat plate type collector adsorber and used clear plane glass sheet of effective exposed area of 1.2 m^2. Connected to steel condenser tube this tube was immersed in a water tank. The evaporator was designed as a spirally coiled copper tube immersed in water. Adsorbent cooling during the adsorption process was by solar heat. According to the study the ambient temperatures during the adsorbate generation and adsorption process varied over 18.5–34°C.

The refrigerator yielded evaporator temperatures ranging over 1.0–8.5 °C from water initially in the temperature range 24–28 °C. (See figure.2.2)

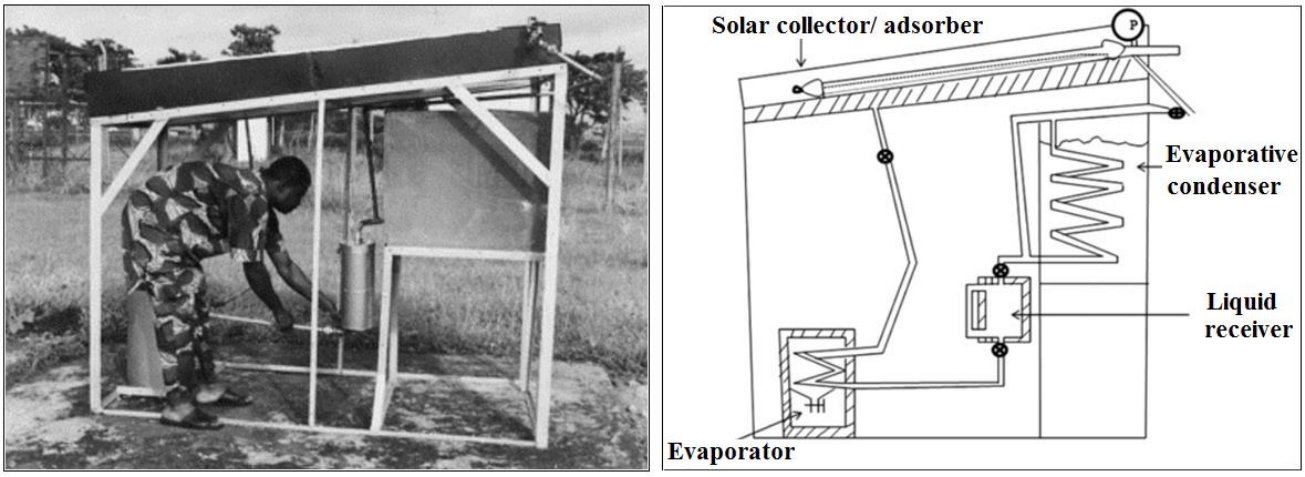

Figure 2.2 Active carbon/methanol adsorption cooling system Anyanwu and Ezekwe [21]

R. Wang et al. [23] designed and carried out a study on the energy efficiency of a new solar energy adsorption cooling system. They found that the new system had higher solar energy conversion efficiency than the conventional solar thermal power generation system. The energy efficiency increased to 58.0% from 10.2%.

Parameters	Performance	Unit
Cooling power	8.5	kW
Chilled water	10	°C
Chilled water flow rate	1.5	t/h
Cooling water inlet	32	°C
Cooling water flow rate	5	t/h
Hot water inlet	85	°C
Hot water flow rate	3.6	t/h
COP	0.4	
Weight	1.5	t
Power AC	2Φ-220V-50Hz	

Figure 2.3 Photograph of silica gel–water adsorption chillier and performance table R. Wang et al [23].

Anyanwu et al. [24] investigated the effects of the heat transfer of a new heat exchanger design parameter on the switching frequency, and the results showed that the optimum switching frequency was very sensitive to the heat exchanger's design parameters, and increases with the increase of adsorbent granules packing.

Chang et al [25] designed and tested an adsorption cooling system with silica gel as the adsorbent and water as the adsorbate. They aimed to reduce the manufacturing costs and simplify the construction of the adsorption cooling system. A vacuum tank was designed to contain the adsorption bed and evaporator/condenser. Flat-tube type heat exchangers were used for adsorption beds in order to increase the heat transfer area and improve the heat transfer ability between the adsorbent and heat exchanger fins. Under the standard test conditions of 80°C hot water, 30°C cooling water, and 14°C chilled water inlet temperatures, a cooling power of 4.3 kW and a coefficient of performance (COP) for cooling of 0.45 were achieved. It provided a specific cooling power (SCP) of about 176 W/(kg adsorbent). With lower hot water flow rates, a higher COP of 0.53 was achieved (see figure.2.4).

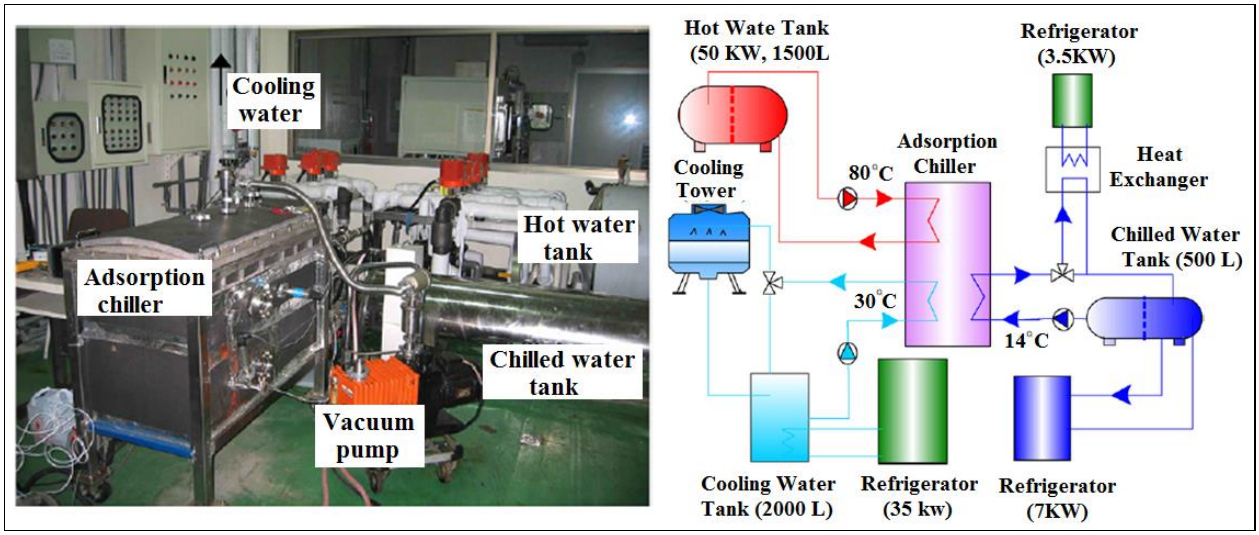

Figure 2.4 (a) Photograph of experimental facility (b) Schematic of experimental facility Chang et al [25].

Dr. Uli Jakob and Walter Mittelbach [26] developed a system consisting of two identical modules. Each module contains a heat exchanger for the adsorption material and a second heat exchanger for evaporation and condensation of the process water. Both heat exchangers are assembled into one single vacuum tight container forming a sealed unit that is connected to the surroundings only by hydraulic piping.

This type of design configuration helped to lower the material, weight and volume of the adsorption cooling system which is one of the problems effecting the development of this type of system. At the present stage of development the adsorption design heat exchanger surface is coated with silica gel using epoxy resin as adhesive. This helps with a faster heat transfer, another recognised problem in this type of system.

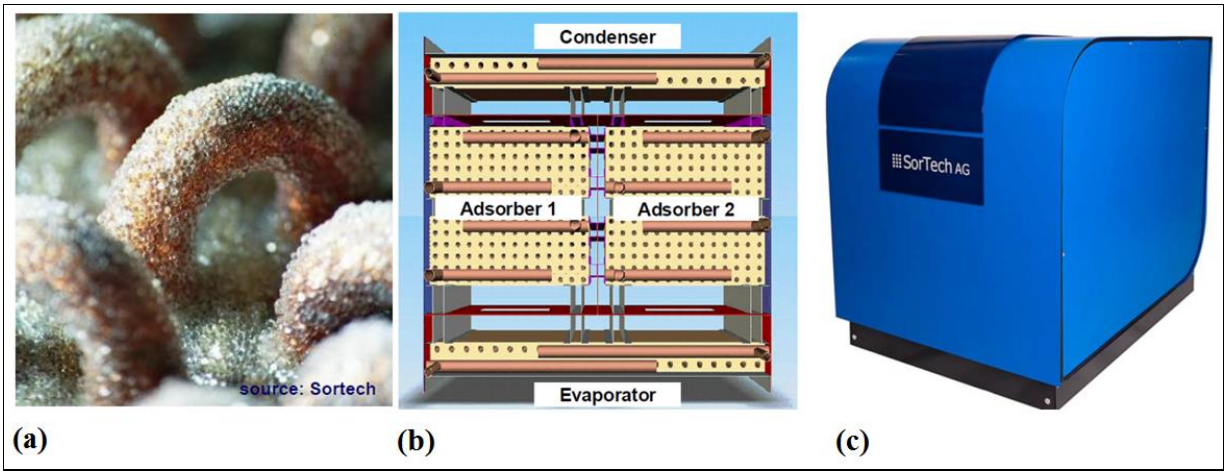

Figure.2.5 (a) Heat exchanger surface coated with silica gel using epoxy resin as adhesive (b) The vacuum envelope design helps reduce the amount of material use giving the system less weight. (c) full system design model ACS 08 (source: SorTech) Dr. Uli Jakob and Walter Mittelbach [26].

2.2. The Operating Principle of an Adsorption Cooling System

The adsorption cooling system generates cold through the process of adsorption on porous material.

Step 1: Desorption drying of the adsorbent (zeolite or silica gel) is dried by heat input. [9, 11-25] Water vapour flows into the condenser and is condensed under heat emission. When the adsorbent is dry, the hot water input is stopped and the condenser valve closes.

Step 2: Adsorption water vapour is adsorbed on the surface of the adsorbent. After a cool down phase the reverse reaction and the evaporation of the liquid condensate start. The valve to the evaporator opens and the dry adsorbent aspirates water vapour. In the evaporator, water evaporates and generates cold, which can be used for air-conditioning. During the adsorption process heat is rejected which has to be dissipated. In a final phase, the condensate is returned to the evaporator and the circuit closed [15, 16-48]. In order to achieve a continuous cold production two adsorption beds work in combination, i.e. one adsorption bed desorbs while the other adsorber generates cold by adsorbing in the meantime see figure.2.6

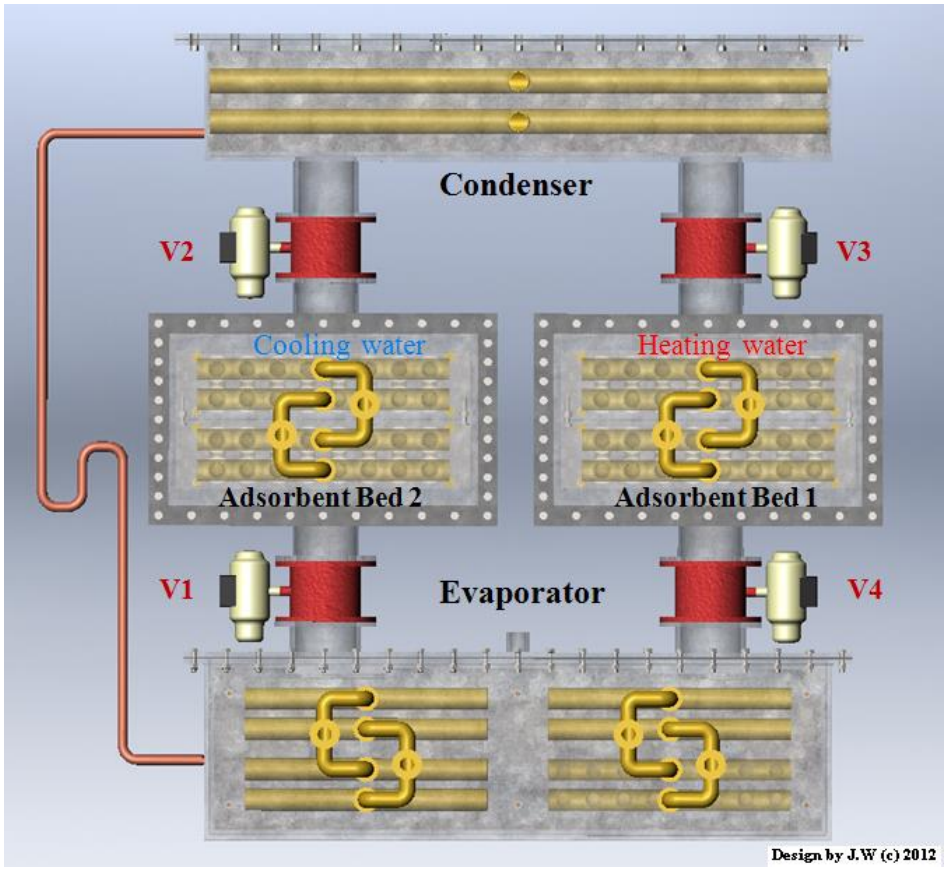

Mode (A) Switching period

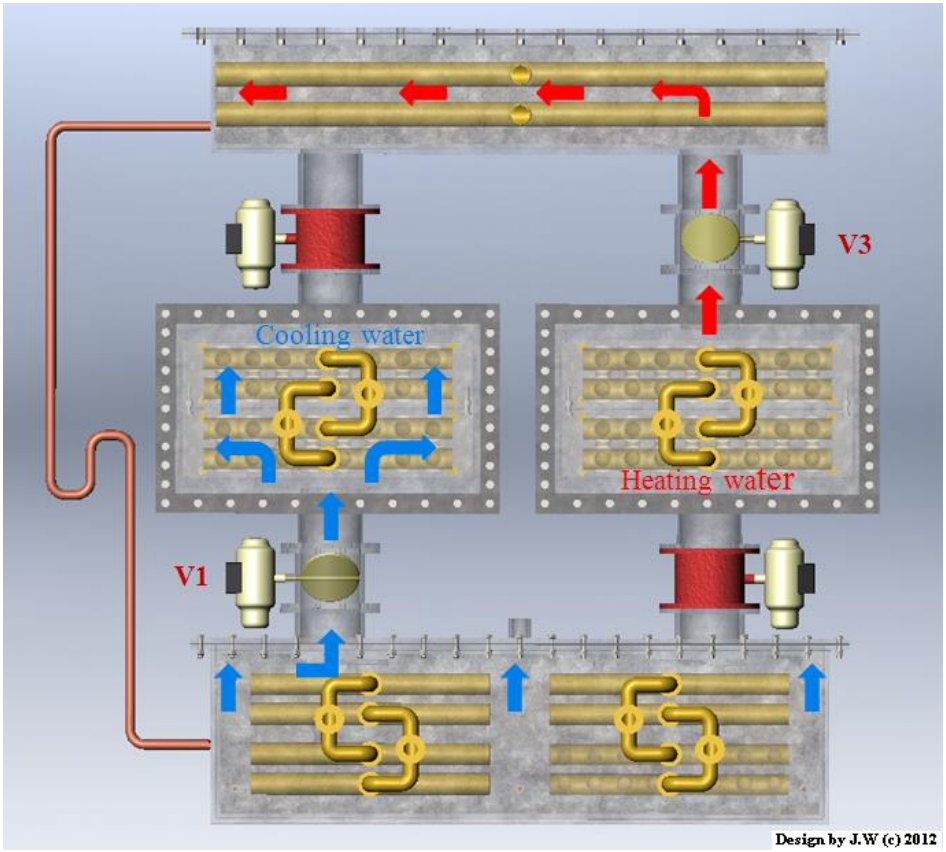

Mode (B) adsorption/desorption

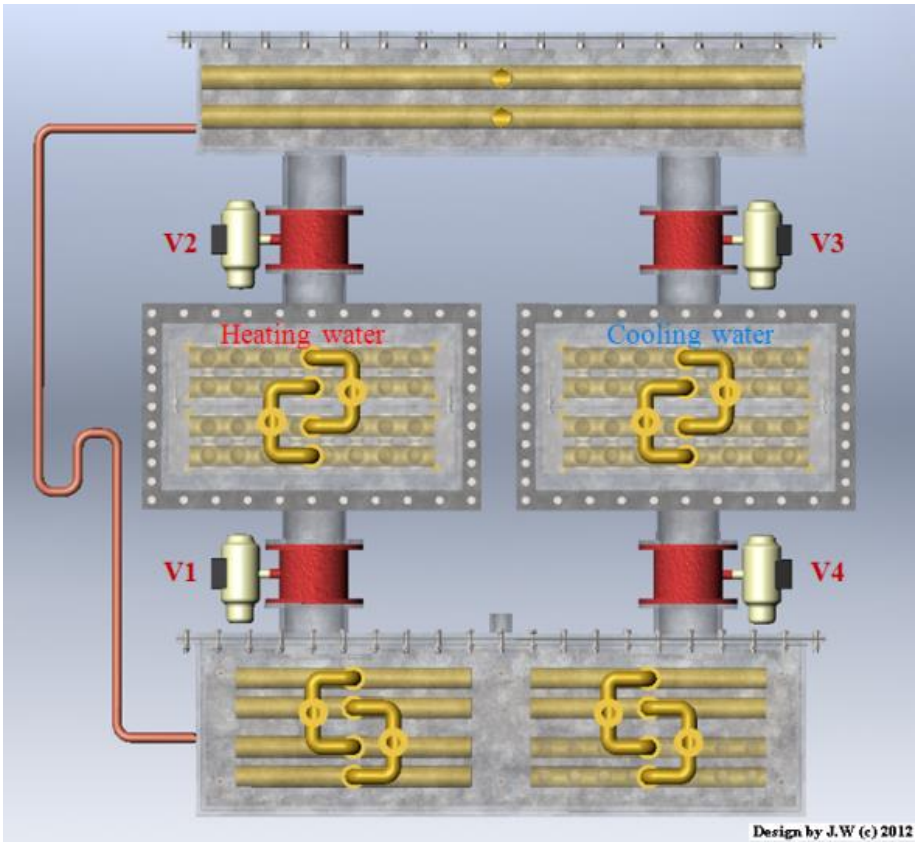

Mode (C) reversing the heating / cooling

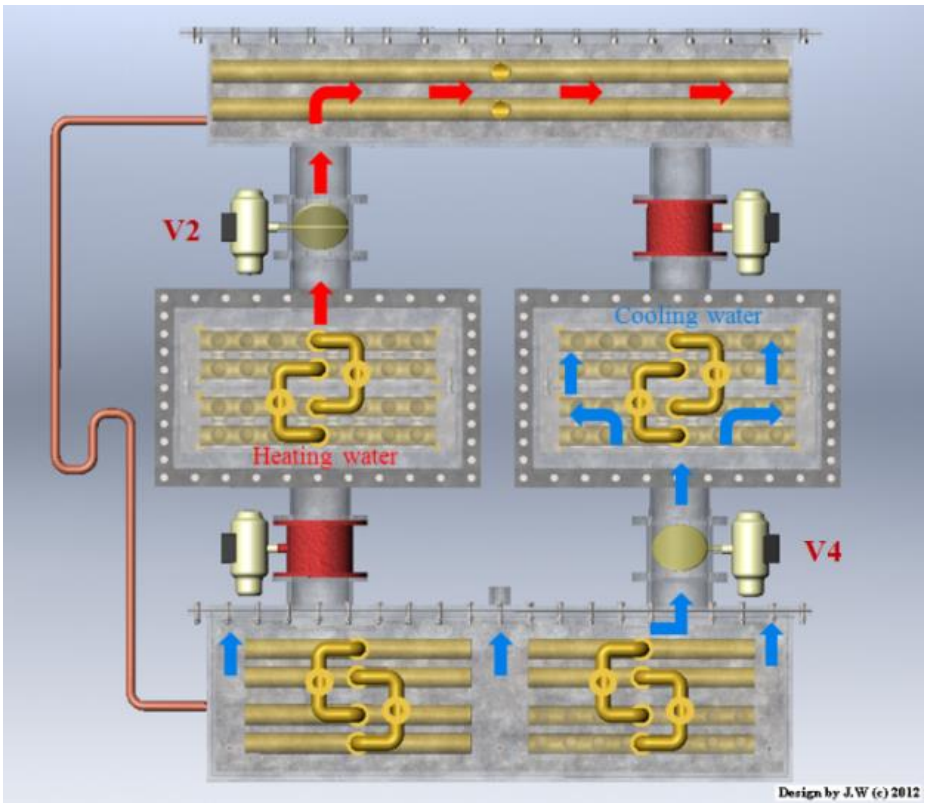

Mode (D) adsorption/desorption

Figure 2.6 Operating Cycle of the adsorption cooling system by J.W © 2012

2.3. Porous Adsorbent Materials

Almost all porous adsorbents materials have the capacity to adsorb water vapour and gases by physical and or chemical forces. The porous media materials used on adsorb purpose are called the adsorbents. The moisture or gases adsorbed can be driven out from the adsorbent by heating, and the cooled 'dry' adsorbents can adsorb moisture or gases again. The popular adsorbents are silica-gel, zeolite, and activated carbon [15,16-26].

These porous media materials can be subdivided into 3 categories, set out by IUPAC [27]:

- Microporous materials: 0.2–2 nm
- Mesoporous materials: 2–50 nm
- Macroporous materials: 50–1000 nm

The common porous adsorbents used as packing in a adsorption bed cooling system are silica gel, zeolite and activated carbon see figure.2.7.[26-27].

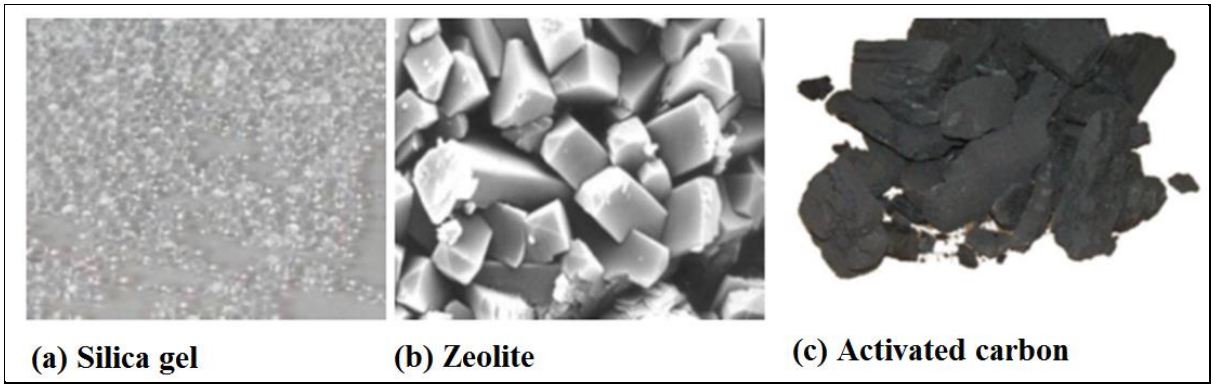

Figure.2.7. The common porous adsorbents used as packing in an adsorption bed [27].

2.3.1 Silica Gel

Silica gels have been the object of many studies in adsorption cooling in recent years. This is due to the adsorption capability of water vapour because of the physical porous structure of silica gel and its large surface area. It has the adsorption capability to adsorb 50% of its mass of vapour without changing its mass (Figure.2.8) [27]. The adsorption ability of silica gel

increases when the polarity increases. One hydroxyl can adsorb one molecule of water. Each kind of silica gel has only one type of pore, which usually is confined in narrow channels. The pore diameters of common silica gel are 2, 3 nm (A type) and 0.7 nm (B type), and the specific surface area is about 100–1000 m^2/g. Type A- silica gel is a fine pore silica gel it has a large internal surface area [27]. Having a high moisture-adsorbing capacity at low humidity and is used as an adsorbent in adsorption cooling systems. Type B contains large pores so type B adsorbs water vapour at low temperature and releases it at high temperature so this type of silica gel would be more practical for system design to desorbs water vapour at high humidity and adsorbs at low humidity [26, 27]. Type C silica gel is also fine pore silica gel. It is known as macro-pored silica gel available in spherical shape this type will also work as a good adsorbent in adsorption cooling system. It is important to compare the adsorption capacity of different types of silica gels as this will help to determine which silica gel has the best performance for the different design configurations [27].

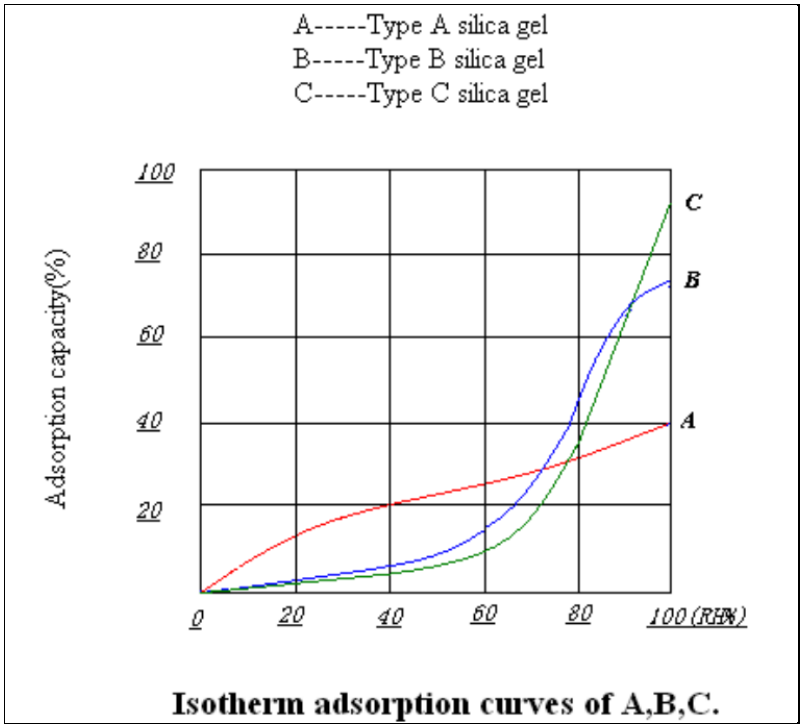

Figure 2.8 The isotherm adsorption curves of silica gel type A, B and C [27].

2.3.2 Zeolite

Zeolite is a highly porous adsorbent material, which belongs to the class of alumina-silicates. This adsorbent is characterised by a three-dimensional pore structure. The corresponding crystallographic structure is formed by crystal of (AlO4) and (SiO4) [27, 28]. These crystals are the fundamental construction for various zeolites such as zeolites A and X, the commonly used adsorbents in the application of adsorption cooling systems. The porosity of the zeolite is between 0.2 and 0.5. [27]. There are about 40 types of natural zeolite.

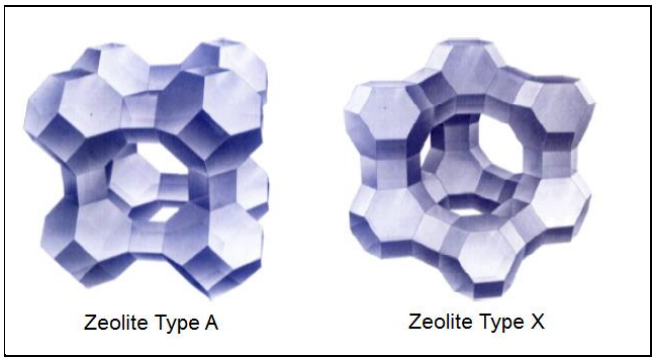

Figure.2.9 Crystal cell unit of zeolite: (a) crystal cell unit of type A zeolite; (b) crystal cell unit of type X, Y zeolite [27,28].

13X zeolite adsorbents is the main type used for adsorption cooling systems. The adsorption and desorption heat of zeolite pairs are high, and the desorption temperature of these pairs is also high at about 250–300°C. The zeolites are usually employed in adsorption cooling system with a heat source between 200 and 300°C.

2.3.3 Activated Carbon

Activated carbons have been a key adsorbent material in adsorption cooling technology for many years due to their porous surface. The structure of activated carbon is shown in Figure 2.10. The specific surface area of activated carbon is between 500 and 1500 m^2/g. [29-30]**.** Activated carbon comes in three forms: powder, granular and extruded. Each form is available in many granule sizes [29, 30].

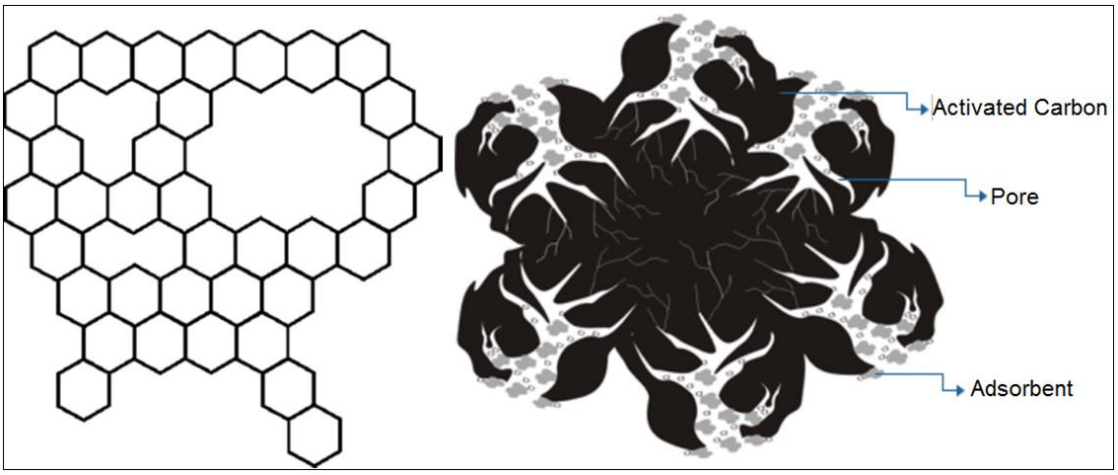

Figure.2.10. Structure of activated carbon. [www.activatedcarbonindia.com]

The net structure of activated carbon pores is composed of irregular channels, which have larger pore area at the surface of the grain, and narrow pore area within the grain [26, 27-30]. The difference between activated carbon and other types of adsorbent is the surface feature. The whole surface of activated carbon is covered by an oxide matrix and by some inorganic materials, and therefore, it is non-polar or has a weak polarity. The adsorption heat of activated carbon pairs is lower than that of other types of physical adsorbent pairs. Pores in Activated Carbon are classified into three types: Micropores (pore dia less than 20 nm), Mesopores (pore dia 20-200 nm) and Macropores (200 nm & above)[27,29-30].

2.4. New types of Adsorbents

Over the last five years a number of new adsorbents have been developed. A number of these may lead to improvement in absorbent bed due to their good adsorption and desorption capabilities. Those that appear to offer improvements are discussed in this section.

2.4.1. Attapulgite Clay Adsorbents

Attapulgite Clay is a promising material for adsorption systems. This is clay-based adsorbent, which is chemically inert, resistant to deterioration, commercially available in large quantities and has many industrial and environmental applications. Attapulgite clay (see figure.2.11) has some of the main requirements for adsorption cycles; it has an ideal water loading of about 0.20 kg/kg as well as good containing ability for water due to its highly porous structures [31]. The $CaCl_2$ impregnated attapulgite presents similar performance as other mesoporous materials confined with hygroscopic salt hydrates.

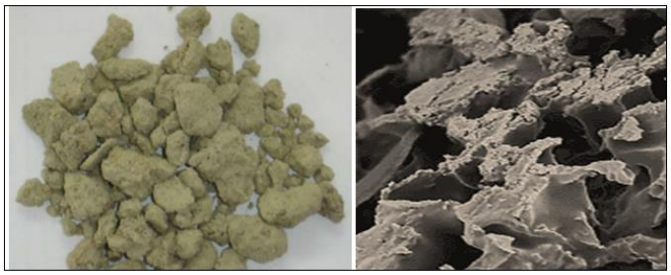

A B

Figure.2.11 Attapulgite clay materials [31].

Clay based $CaCl_2$ and $SrCl_2$ composites have been proposed and have shown advanced performance for cooling and air-conditioning systems driven by low temperature waste heat or solar energy [32]. More recent research has been done in this area and the results have shown that: at higher relative humidity, water loading on AT–CiCl (20%) can be as high as 0.60 kg/kg, while at relative humidity 20%, the loading can be 0.30 kg/kg, which is higher than commonly used 13X Zeolite and silica gel [15,18,19].

The composites obtained can be effectively regenerated between 160°C - 180°C and reused. Though $CaCl_2$ is the most ordinary desiccant, LiCl is also well known for its particular hydrophilic property and has been widely used in the dehumidifier and in desiccant cooling

systems. Consequently, properties of attapulgite-based LiCl composites deserve closer investigations.

2.4.2 Silica from Micelle Template

There are several kinds of new adsorbent porous media proposed in the literature. New research on new types of Mesoporous materials with regular geometries have recently gained much attention owing to their greater potentials in practical applications such as adsorption cooling system [9,10-33].

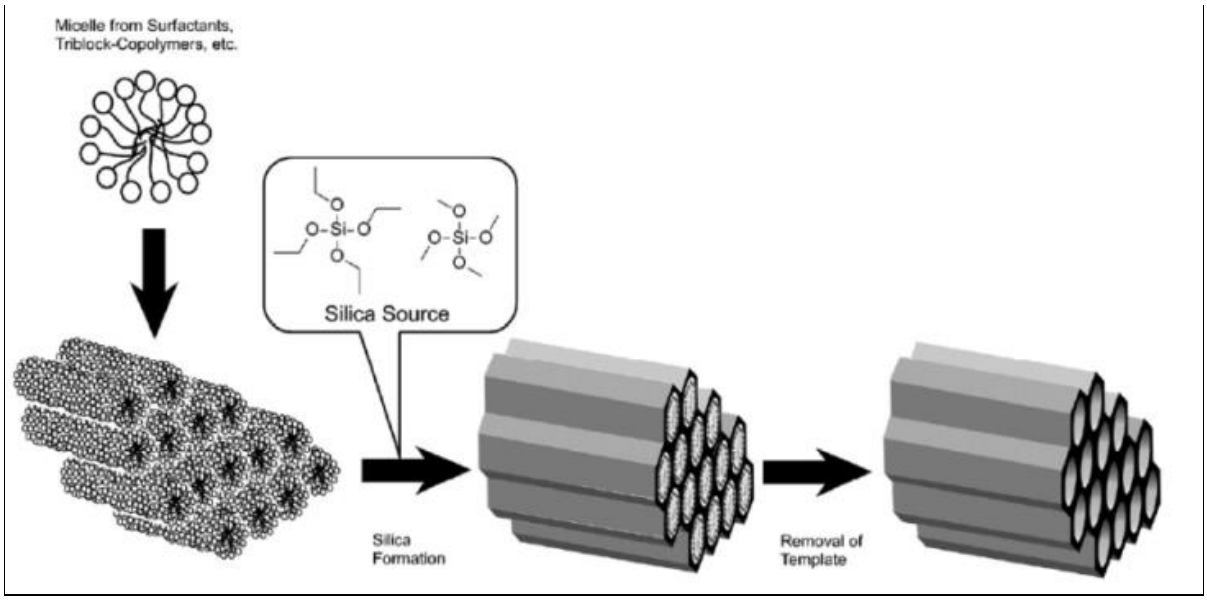

Figure.2.12 General Concept for synthesis of mesoporous silica from micelle template [33].

2.4.3 Metal-Organic Framework Adsorbent Materials

Metal Organic Frameworks (MOFs) are new adsorbent materials that seem to becoming promising as suitable alternatives as porous media for different industrial applications within catalysis and adsorption cooling technology. These adsorbents have been designed to overcoming many of the limitations of zeolites and silica gel porous adsorbents. These adsorbents can be designed to have both micro and meso-pores which give this type of adsorbent an advantage [36].

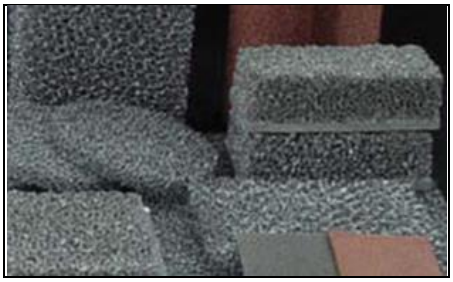

Figure 2.13 Metal–organic framework adsorbent materials [36].

2.5. Types of Working Adsorbate and Adsorbent Pairs

At present, three types of working adsorbate and adsorbent, respectively, are favoured for pairing for use in adsorption refrigeration technology: ammonia, methanol and water for adsorbate and activated carbon, silica-gel and zeolite for adsorbent see table.2.1 [15,16-33].

Table.2.1 **Working pairs for adsorption systems**

Working pairs	
Sorbate	**Adsorbent**
Sulphur dioxide	**Silica gel**
Water	**Silica gel**
Ammonia	**Silica gel**
Methanol	**Activated carbon**
Ammonia	**Activated carbon**
Ammonia	**Calcium chloride**
Water	**Zeolite (Metal-Alumo-Silicate)**

The selection of any pair of adsorbent/adsorbate depends on certain desirable characteristics these are listed below:

(i) Evaporation temperature below 0°C.

(ii) Small size of molecules such that it can easily be adsorbed into the adsorbent.

(iii) Microspores of diameter less than 20nm.

(iv) High latent heat of vaporization and low specific volume.

(v) Thermally stable with the adsorbent at the cycle operating temperature ranges.

(vi) Non-toxic, non-corrosive and non-flammable.

(vii) Low saturation pressures (above atmospheric) at normal operating temperature.

Silica Gel–Water

Silica gel–water belongs to low temperature working pairs, which can be driven by heat sources of between 60°C and 85°C under low pressure [9-33].

2.5.2 Zeolite-Water

For zeolite-water working pairs, the adsorption isotherm is flat. The latent heat of water is much larger than methanol or other traditional refrigerants because of the high desorption temperature. The temperature lift of this system is higher than 70°C. The adsorber can be directly heated by waste heat such as solar panels. Therefore, the zeolite-water system is simpler than one driven by the hot water [12-34].The desorption temperature is higher than 200°C but the adsorption temperature might be lower than 80°C. The thermal stress of the adsorber metal will be difficult to release, especially when the adsorber is just switched between heating and cooling. Therefore, there is a higher manufacturing cost to adsorbent beds due to the risk of leakage bed [33, 34].

The zeolite–water adsorption refrigeration system has been used where the temperature variation speed of adsorbent bed is slow, such as in the intermittent adsorption air conditioning using a tubular solar collector as an adsorber. A zeolite-water system is only suitable for air conditioning because water cannot evaporate at the temperature below 0°C. Low evaporating pressure of water causes a slow adsorption process, and the high desorption temperature increases the sensible heat of the adsorber [33]. Therefore the SCP of the zeolite-water system is not very high. It has been pointed out that the mass transfer performance in a

zeolite-water adsorption refrigeration system is the main factor to influence the improvement of its performance [9-33].

2.6. Principles of Adsorption and Desorption

The first part of this chapter provides reviews of the different design configuration of adsorption cooling technology and different adsorbent and adsorbate pairs used in adsorption cooling technology. This section will serves as an essential background of vapour adsorption phenomenon before the design and CFD modelling study on this type of system. It aims to demonstrate the fundamental principles of the adsorption phenomenon which explain the adsorptions and desorption of water vapour in an adsorption cooling system.

2.6.1 Adsorption Phenomenon

Adsorption phenomenon has fascinated engineers and scientists since the beginning of the 19th century because this phenomenon has been adapted and used in a large number of technological and extremely important practical applications over the years. Some examples are in catalytic used in purification of water, sewages, air and adsorption cooling technology. Despite the developments in this area, scientists are still mystified when it comes to the phenomenon of adsorption and desorption. One reason for this is that the knowledge and innovation achieved over time was more through trial and or, rather than through science [9-22].

The fundamental understanding of the scientific principles of adsorption phenomenon is underdeveloped, in part, because the study of adsorption of vapour requires extremely careful experimentation if meaningful results are to be obtained. In recent years substantial effort has been progressively directed toward closing the gap between practice and theory. Mainly through the expansion of new approaches by means of CFD computer simulation methods and owing to new methods which study surface layers. These sections of this review will

present, in brief, adsorption and desorption and highlight the theoretical description of the phenomenon under consideration [16, 34-35].

2.6.2 Historical overview of adsorption/desorption

The phenomenon of adsorption/desorption was discovered over two centuries ago by C. W. Scheele in 1773 and by the F. Fontana in 1777. In 1785, they found that when they heated charcoal contained in a test tube it desorbed gases. The gases then adsorbed back when the charcoal was cooled [37].

The nature of adsorption/desorption has always been a controversial one throughout the nineteenth century. In a paper Faraday (1834) discussed the possibility that gases are held onto the surface by an electrical force and suggested that gases could react more easily once they were in the adsorbed state. However, Berzelius (1836) noted that the best adsorbent was highly porous materials. Therefore, Berzelius proposed that adsorption was a process where surface tension or some other force caused gas to be condensed into the pores of a porous media [37-39].

The idea that most adsorption/desorption processes were really just pore condensations was actively debated in the literature in the 1850s to 1920s. Magnus (1825, 1853) and Magnus [1929] showed that pore condensation does occur. However, other investigators found there were some data that were not in accord with the idea that pore condensation alone explained adsorption/desorption [37-39].

2.6.3 Types of Adsorption

Types of adsorption will depend upon the vacuum pressure present between vapour or gas molecules and porous adsorbent, adsorption is classified into two types [12-18]:

1. **Physical adsorption (Physisorption):**

If a force of attraction existing between adsorbate and porous material surface, this is the Vander Waal's forces, the adsorption is physical adsorption. In physical adsorption the attraction between the vapour or gas and porous material surface are weak, hence this type of adsorption can be easily reversed by heating [15].

2. **Chemical adsorption (Chemisorption):**

If the forces of attraction existing between vapour or gas and porous material surface have the same strength as chemical bonds, this type of adsorption is named chemical adsorption. In chemisorption the force of attraction is strong therefore chemisorption adsorption cannot be easily reversed [15].

2.6.4 Factors Affecting Adsorption

The rate of adsorption is governed by the following factors [12-17]:

1. Type of adsorbate and adsorbent.
2. The surface area of adsorbent.
3. Experimental conditions.

2.6.5 Types of Adsorption Isotherms

Adsorption isotherms measured on a range of gas - solid systems have a variety of forms, and can be grouped into one of six types according to the International Union of Pure Applied Chemistry (IUPAC) Classification 1994 [27] with the majority resulting from physisorption, figure. 2.15 shows the six types of isotherms, which only hold for the adsorption of a single component gas within its condensable range, and are very useful for the study of porous materials.

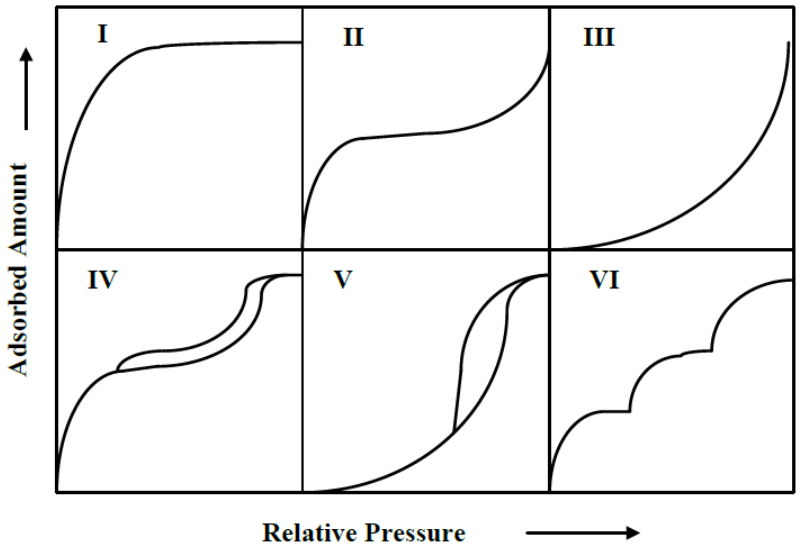

Figure 2.14 The six main types of isotherms, according to the IUPAC classification [27]

Type 1

This isotherm is characterised by its concave shape to the relative pressure (P/P_0) axis. The curve rises sharply at low relative pressures until it reaches a plateau after which the amount of fluid adsorbed by a unit mass of solid (n^a/m^s) approaches a limiting value as P/P_0 goes to 1. Strong adsorbate – adsorbent interactions occur in micropores of molecular dimensions, hence a decrease in pore width below 2 nm will lead to an increase in adsorption energy as well as a decrease in the relative pressure at which micropore filling occurs. According to IUPAC classification [27] the narrow range of relative pressure necessary to attain the plateau in Type 1, signifies the existence of a limited range of pore size. The appearance of a nearly horizontal plateau is an indication of a very small horizontal pore surface area in terms of pore width and this is typical of microporous solids.

Type II

The Type II isotherm is also concave to the P/P_0 axis initially, then almost linear and finally convex to the P/P_0 axis. The Type II isotherm is an indication of the formation of an adsorbed layer, whose viscosity increases gradually with accumulative relative pressure as

P/P_0 approaches one layer. Figure 2.15 signifies the completion of a monolayer and the onset of multilayer adsorption. This point yields an estimate of the amount of adsorbate required to cover the unit mass of solid surface to a monolayer capacity. Complete reversibility of the sorption isotherm must be met for normal monolayer-multilayer adsorption on an open and stable adsorbent. The Type II isotherm is associated with non-porous and macroporous adsorbents which permits monolayer-multilayer adsorption at high values of relative pressure (P/P_0) [27].

Type III

This is convex to the relative pressure axis, over the whole range. According to Sangwichien et al [38] this is characteristic of weak adsorbent - adsorbate interactions, and more so, true Type III isotherms are not common.

Type IV

This isotherm exhibits a similar concave shape to the P/P_0 axis as Type II but differs in that it levels off at high relative pressures. The main characteristic of this isotherm is its incomplete reversibility. This forms what is known as a hysteresis loop which varies from one system to another. Hysteresis loops in Type IV isotherms are associated with capillary condensation, which governs the filling and emptying of pores.

Type V

The Type V isotherm is convex to the P/P_0 axis in a similar manner to the Type III, and is also formed due to weak adsorbent and adsorbate interactions. The main characteristic difference is that the Type V isotherm exhibits a hysteresis loop which is due to the mechanism of pour filling and emptying by capillary condensation.

Type VI

This has been more recently observed, and is termed the stepped isotherm.

2.6.6 Adsorption Equations

There are many mathematical equations used to describe adsorption isotherm. Some of these equations are derived from experimental data with a finite amount of empirical parameters. In this study the BET approach is used.

The BET equation is an accepted equation applied to the explanation of the physical adsorption process. The adsorption method which the BET equation is based describes the multilayer physical adsorption on the basis of the kinetic method proposed by Brunauer, Emmett, and Teller in (1938) [34,35] see figure.2.15.

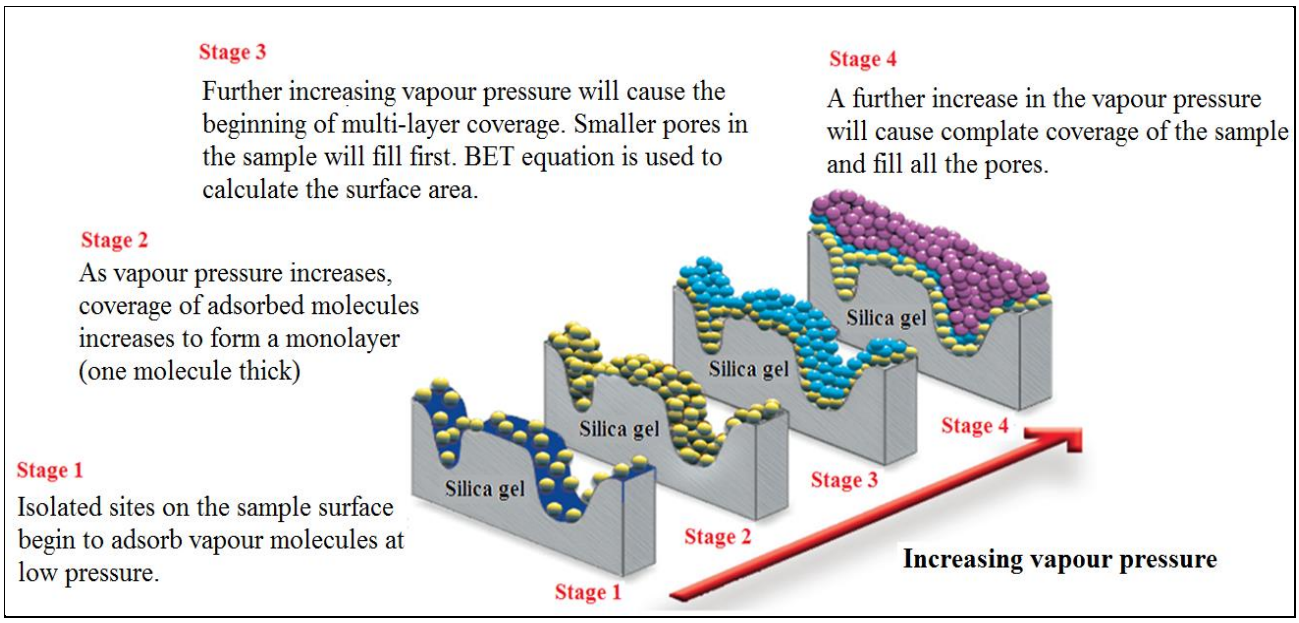

Figure 2.15 The BET adsorption multi-layer model [34-35].

The BET adsorption theory is an adaptation of the Langmuir theory, which is the theory for monolayer to multilayer adsorption with the following [34-35]:

(a) Vapour or gas molecules physically adsorb on to a porous adsorbent in layers.

(b) The BET equation is applied to each layer of vapour or gas molecules. The resulting BET equation is expressed by (1):

$$\frac{1}{v[(P_0/P)-1]} = \frac{c-1}{v_m c}\left(\frac{P}{P_0}\right) + \frac{1}{v_m c} \qquad (2.1)$$

P and P_0 are the balance and the saturation pressure of adsorbents at the temperature of adsorption, v is the adsorbed gas or vapour and v_m is the adsorbed vapour amount. c is the BET constant which is (2.2):

$$c = \exp\left(\frac{E_1 - E_L}{RT}\right) \qquad (2.2)$$

E_1 is the of adsorption for the vapour layer one and E_L is for the vapour layer two and upper layers.

2.6.7. Adsorption Measurement Method

Adsorption measurement is to establish the adsorption features of adsorbent and adsorbate working pair, together with isotherm, kinetics and heat of adsorption data. All these key parameters are essential for CFD simulation and modelling of any adsorption process. At present the available adsorption measurement techniques can be found in the literature [16,34,39]. They are grouped into three types, i.e. gas flow [41] volumetric [43] and gravimetric [38].

2.6.8 Gas Flow Method

This type of adsorption measurement method was first proposed by Nelsen and Eggertsen [41]. This test rig used helium as the transporter gas and a flow meter was used to calculate the pressure of the vapour or gas. The adsorbed gas volume is determined from the peak area in the adsorption/desorption chart recorded by a potentiometer over a period of time. This test rig is inexpensive and easy to operate. However, the measurement of this adsorption method is not accurate. This method is usually useful for fast single point determinations of the specific surface area. Multipoint measurements of isotherms need a more accurate method of measurement in order to be used in CFD simulation.

2.6.9 Gas Adsorption Volumetric Method

The volumetric gas adsorption method was first proposed by Emmett [41], in which the gas adsorption was measured by a mercury burette and manometer. The quantity of gas adsorbed was measured by the gas volume change in the burette. However, the mercury burette is no longer used because of the concerns of element toxicity and has led to mercury burettes being phased out of use.

Gas Adsorption Gravimetry

In gas adsorption gravimetry, the adsorbed mass, adsorption pressure and temperature are measured directly and independently. This adsorption method is a more accurate method and is becoming more popular in the adsorption measurement of silica gel adsorbent [25-38].

2.7. Enhancement Methods Used in Improving Adsorbent Bed Design

The choice of the adsorbent has a significant impact on the performance of adsorption refrigerators. Detailed reviews about adsorbents and working pairs for heat transformation

processes have been published recently. There are several adsorbent beds configuration designs that can be found in the literature [40, 45, 48-51] these are:

•Unconsolidated (fixed bed),

•Consolidated adsorbent beds

•Coated adsorbent beds

2.7.1. Unconsolidated Fixed Beds

An unconsolidated fixed bed is an adsorbent bed with random pack granules with no binder or adhesives the disadvantage of the unconsolidated fixed bed shown in figure 2.16 suffers from is a poor thermal contact of the adsorbent granules to the heat exchanger fins surface (point contact) resulting in a low heat transfer coefficient and slow heat transfer limited adsorption kinetics. Various attempts to improve the transfer properties of unconsolidated adsorber beds are carried out using different methods [41]:

1. Mixing together adsorbent of various grain sizes in a multimodal distribution.
2. Using metal inserts.
3. Using composite adsorbents with additives.

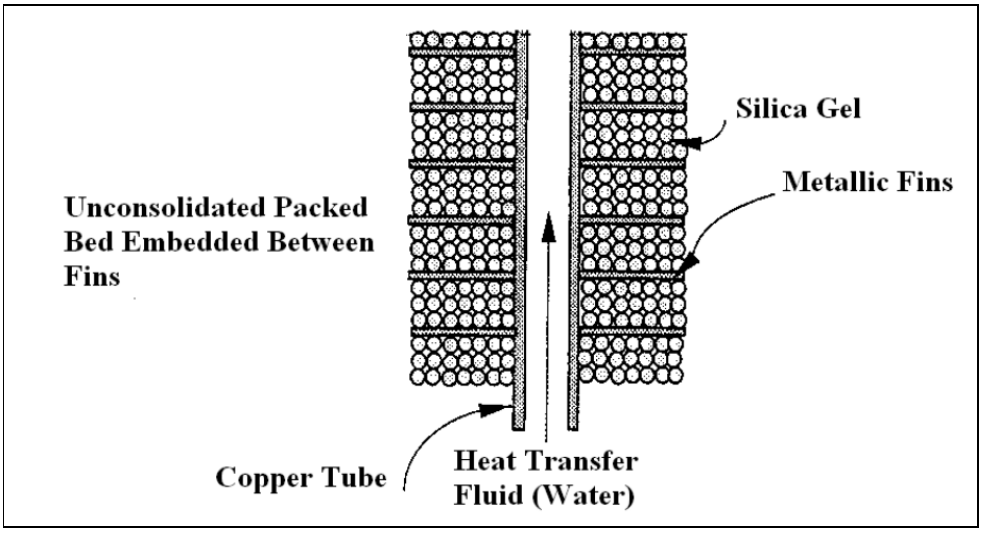

Figure 2.16 Example of an unconsolidated fixes bed [40].

2.7.2 Consolidated Adsorbent

To produce mechanically stable pellets, a binder such as silica, alumina or clay is generally necessary. However, the use of a binder and the fixed bed arrangement involves some essential drawbacks [40-51]. Binder used may influence the adsorption performance, reduce the amount of adsorbent per volume and hinder the access to the porous system of the adsorbent [40-51].

Marletta et al. [45], used a thin adsorbent coating, based on zeolite (consolidated with an inorganic binder) bound around a copper tube, See figure 2.17 They reported that this bound structure allows an increase in the adsorbent thermal conductivity.

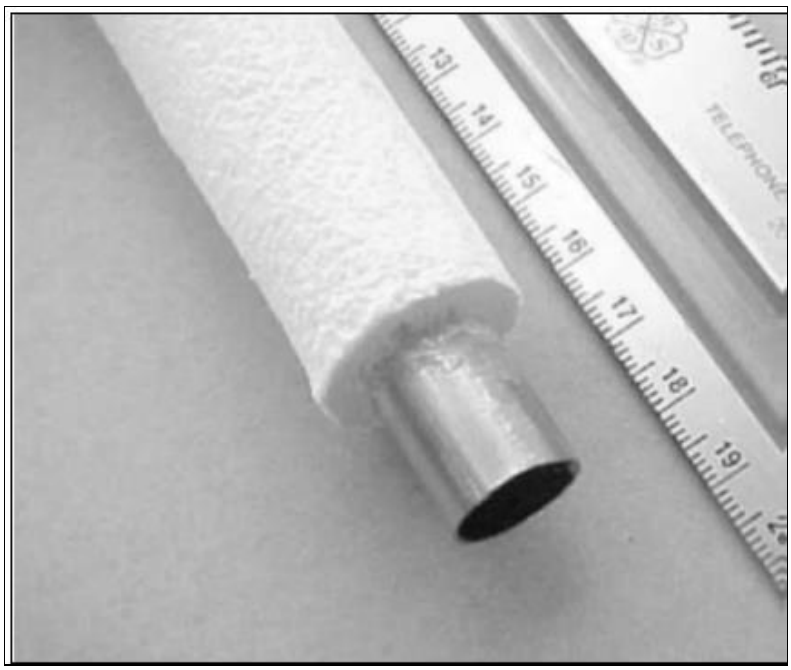

Figure 2.17 Consolidated adsorbent onto tube Marletta et al [45].

2.7.3. Coated Adsorbents

Another approach is the coating of the heat exchanger surface with the active material (silica gel or zeolites) See figure 2.18

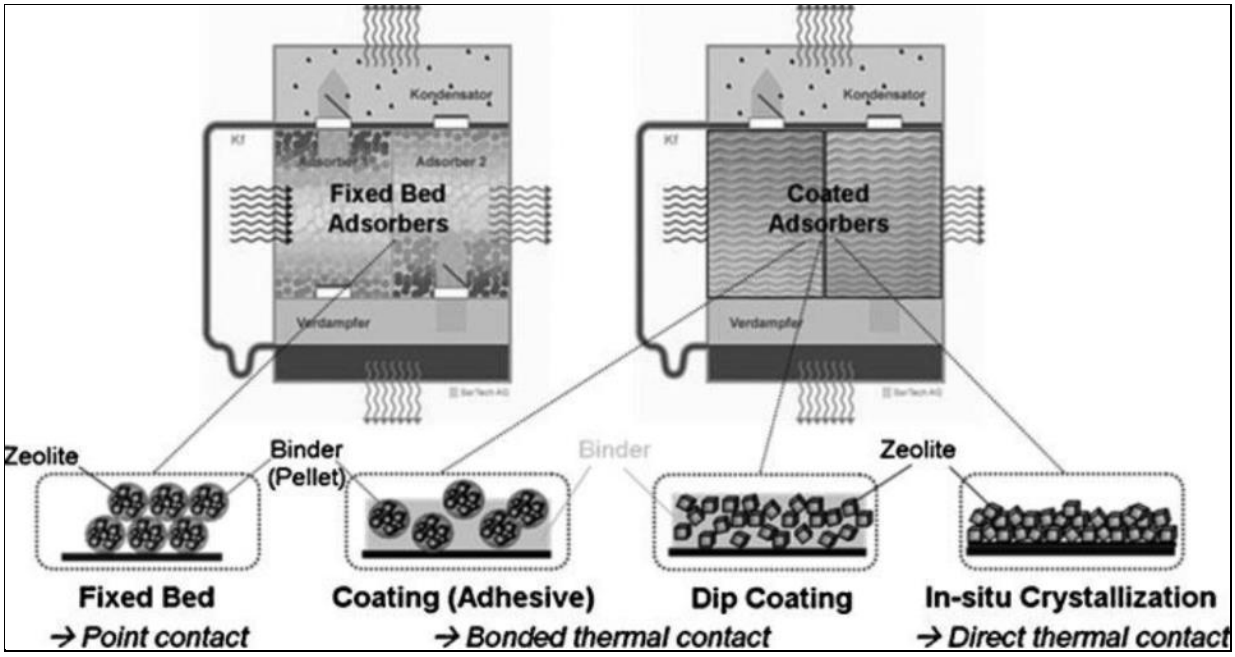

Figure 2.18 Dr. Uli Jakob [48], SorTech AG researched and developed a method.

AG researched and developed a method, which enables them to attach silica gel granules to a heat exchanger surface with the aid of epoxy resin figure 2.19 without blocking the entrance pores of the granule. According to their research paper all types of granulate can be applied by this technique [48].

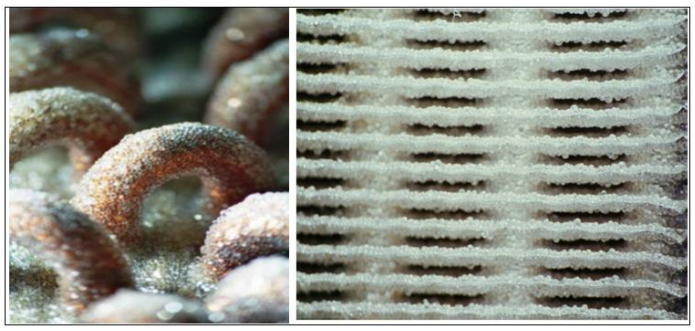

Figure 2.19 Photo of a silica gel coated tube and fin adsorber heat exchanger (source: SorTech) [48].

The epoxy resin bonding advantages are:

- Improved speed of heat transfer
- Improved vapour transport
- Less volume and weight
- Significantly increased power density

2.7.4. Direct Crystallisation Zeolite

This coating technique uses the direct synthesis of zeolite on the heat exchanger surface and because of the coalescence of zeolite and the metal very compact layers without the need of binding agents are created [49]. Thereby, a large contact area and a good mechanic stability of the boundary layer is achieved, see figure 2.20

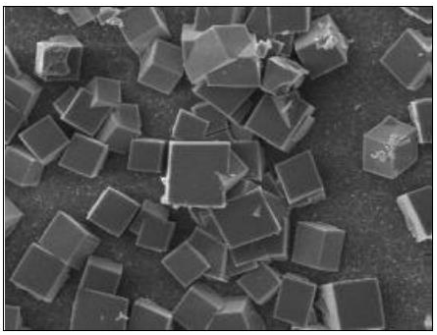

Figure 2.20 Direct crystallization with zeolite [48].

2.8. Conclusion

From this literature review it can be concluded that the prospect of using adsorption cooling technology is an alternative to mechanical vapour refrigeration system. The adsorption cooling system compared to the mechanical system has low maintenance and the absence of moving components is also a very important feature that makes this type of system suitable for numerous other applications such as air-conditioning and cooling food storage units.

The environmental benefits are also impressive, when compared to conventional compressor cooling technology.

The absence of harmful or hazardous products such as CFCs, together with a substantial reduction of CO2 emissions due to very low consumption of electricity, creates an environmentally safe technology. Low-temperature waste heat or solar energy can be converted into a chilling capacity as low as 5°C. However, the adsorption cooling technology is restricted by the poor thermal conductivity of porous media and large heat exchanger used in this system. There are two ways one could solve these problems, one is to develop a new adsorbent material which would have a better adsorption capacity; another, could be to redesign the construction of the adsorbent bed with the help of CFD modelling in order to improve the heat transfer to the porous material used as the adsorption packing.

CHAPTER 3

FIRST PRINCIPLES OF COMPUTATIONAL FLUID DYNAMICS

Abstract

This chapter focuses on the principles of Computational Fluid Dynamics (CFD), flow phenomena in porous media, and mathematical models for water vapour and heat transfer processes in adsorbent bed used in adsorption cooling system. Five areas of relevant literature were reviewed: (a) general modelling methodology; (b) basic principles of CFD; (c) porous media approach; (d) modelling of water vapour; (e) modelling of heat transfer in adsorbent beds.

3.1Introduction

Computational Fluid Dynamics (CFD) is the term given to the task of solving the fluid flow and governing equations by a computer. However the equations governing fluid flow have been known for over 100 years major advances in CFD were hindered until the 1970s when digital computers became accessible to the scientific researchers and the public [53-59]. The speed of modern computers and relatively low price and the new commercial CFD codes now accessible makes CFD a very suitable tool for researcher and designers engineers [52].

Currently there are several widely used commercial CFD tools such as COMSOL MULTIPHYSICS, SolidWorks COSMOS FLOW SIMULATION, PHOENICS, FLUENT, CFX, and STAR-CD.

3.1.1 History of Computational Fluid Dynamics CFD

In the eighteenth and nineteenth century engineer and mathematicians mathematically describe the motion of fluids [126]. Daniel Bernoulli derived the famous Bernoulli s equation (1738) and Leonhard Euler proposed the Euler equations which describes the conservation of

momentum for fluid flow, and conservation of mass. He also proposed the velocity potential theory. Two important contributors to the field of computational fluid dynamics were Claude Louis Marie Henry Navier and the Irishman, George Gabriel Stokes who introduced viscous transport into the Euler equations, which resulted in the now famous Navier-Stokes equations.

These forms of the differential mathematical equations that they proposed nearly 200 years ago are the foundation of the modern computational fluid dynamics (CFD) simulation modelling they include expressions for the conservation of mass, momentum, energy and turbulence. However it was not until the arrival of modern computers in the 1960s and 1970s that they could be resolved for real flow problems within a reasonable timescales. It was at this point in time considerable amount of work was carried out on development of the theories of boundary layers and turbulence in CFD fluid flow.

3.2 CFD governing equations

The fundamental governing equations of fluid dynamics are the mass, momentum and energy equations as mention above. These three equations are the fundamental principles upon the computational fluid dynamics are based [76, 77].

- Mass
- Momentum
- Energy

The first law states that mass cannot be created nor destroyed. The second law states that the rate of change of momentum equals the sum of the forces on a fluid particle, and is described by Newton's second law. The third law states that the rate of change of energy is equal to the rate of change of heat addition and work done on a fluid particle, and is the first law of thermodynamics. If the motion of a fluid is only affected by phenomena on a macroscopic

scale and molecular effects can be ignored, it is regarded as a continuum. A fluid element therefore represents an average of a large enough number of molecules in a point in space and time [101].

Mass
$$\frac{\partial \rho}{\partial t} + \nabla.(\rho \mathbf{V}) = 0 \tag{3.1}$$

Momentum
$$\rho \frac{D\mathbf{V}}{Dt} = \nabla.\boldsymbol{\tau}_{ij} - \nabla p + \rho \mathbf{F} \tag{3.2}$$

Energy
$$\rho \frac{De}{Dt} + p(\nabla.\mathbf{V}) = \frac{\partial Q}{\partial t} - \nabla.\mathbf{q} + \boldsymbol{\Phi} \tag{3.3}$$

Where $\boldsymbol{\rho}$ is the fluid density, $\boldsymbol{V}$ is the fluid velocity vector τ_{ij} is the viscous stress tensor, $\boldsymbol{p}$ is pressure, $\mathbf{F}$ is the body forces, e is the internal energy, $\boldsymbol{Q}$ is the heat source term, $\boldsymbol{t}$ is time, Φ is the dissipation term**,** and $\nabla.\mathbf{q}$ is the heat loss by conduction. Fourier's law for heat transfer by conduction can be used to describe $\mathbf{q}$ as:

$$\mathbf{q} = -k\nabla T \tag{3.4}$$

where $\boldsymbol{k}$ is the coefficient of thermal conductivity, and $\boldsymbol{T}$ is the temperature. Depending on the nature of physics governing the fluid motion one or more terms might be negligible. For example, if the fluid is incompressible and the coefficient of viscosity of the fluid, μ, as well as, coefficient of thermal conductivity are constant, the mass, momentum, and energy equations reduce to the following equations:

$$\nabla.\mathbf{V} = 0 \tag{3.5}$$

$$\rho \frac{D\mathbf{V}}{Dt} = \mu \nabla^2 \mathbf{V} - \nabla p + \rho \mathbf{F} \tag{3.6}$$

$$\rho \frac{De}{Dt} = \frac{\partial Q}{\partial t} + k\nabla^2 T + \mathbf{\Phi} \tag{3.7}$$

Presence of each term and their combinations determines the appropriate solution numerical procedure.

3.3 Turbulence Modelling

Water vapour turbulence in an adsorbent bed is a three-dimensional time dependent motion in which causes vapour velocity variations. Turbulence is one of the most complex phenomena in an adsorbent bed. Some of the reasons for the complexity are [68]:

1. Intrinsic randomness: Turbulent flows are extremely sensitive to small disturbances due to which turbulent flows inherently have no repeatability
2. Intermittency: Turbulence can interact with non-turbulent fluid flow and can appear intermittently in time at certain location.

Although turbulence is a very complex flow phenomenon it can be computed by using the Reynolds Averaged Navier -Stokes (RANS) methods. This method predicts the flow perfectly in many simulated circumstances.

Compiling the Navier-Stokes equations into the RANS equations makes it possible to simulate practical flow simulation in an adsorbent bed. The assumption (known as the Reynolds decomposition) behind the RANS equations is that the time-dependent turbulent velocity variations can be separated from the mean flow velocity. This transform then introduces a set of unknowns called the Reynolds stresses, which are functions of the velocity variations and which require a turbulence model (e.g. the two-equation k-epsilon model) to produce a closed system of solvable equations. The reduced computational requirements for the RANS equations while still significant are orders of magnitude less than that required for the original Navier-Stokes equations. Another advantage of using the RANS equations for

steady fluid flow simulation in a adsorbent bed is that the mean flow velocity is calculated as a direct result without the need to average the instantaneous velocity over a series of time steps [78].

It is a relatively straightforward process to produce an unsteady variant of the RANS equations (sometimes referred to as URANS) for transient flows, while still solving for the mean flow velocity separately from the turbulent velocity fluctuations.

Combining the RANS equations with assumptions that enforce the conservation of mass and energy produces the mainstream approach used within CFD to simulate a wide variety of practical fluid flows. CFD breaks down a fluid domain into discrete cells (a mesh) and then solves the RANS and conservation laws in each cell. The accuracy of a typical CFD simulation is primarily determined by the mesh resolution (usually the higher the better but at the cost of more computing resources and slower turnaround times Fig .3.4.[81]

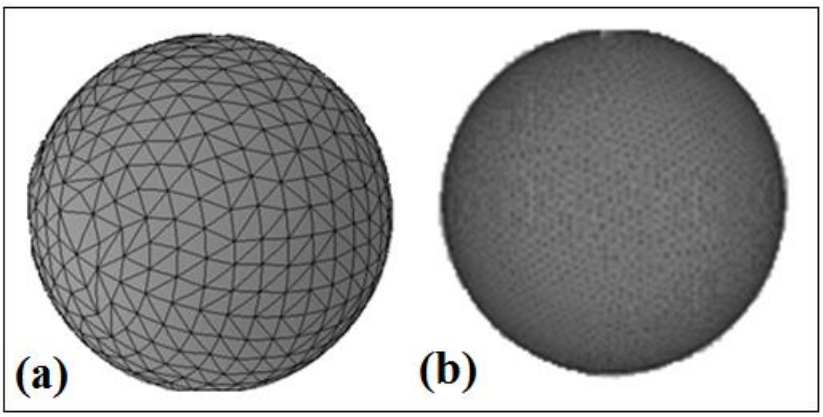

Figure 3.1 (a) Silica gel mesh resolution low (b) Silica gel mesh resolution high.

The time averaged Navier-Stokes equations are given as:

$$\rho U_j \frac{\partial U_i}{\partial x_j} = -\frac{\partial P}{\partial x_i} + \mathbf{F}_i + \frac{\partial}{\partial x_j}\left(\mu\left(\frac{\partial U_i}{\partial x_j} + \frac{\partial U_j}{\partial x_i}\right) - \rho\overline{u_i' u_j'}\right) \tag{3.8}$$

The $\overline{u_i' u_j'}$ term is an unknown quantity, which originates due to averaging a nonlinear term. It is called Reynolds stresses. Similarly the Reynolds averaged equations for a mean scalar field (neglecting source term) is:

$$\frac{\partial(\rho T)}{\partial t} + \frac{\partial(\rho U_j T)}{\partial x_j} = \frac{\partial}{\partial x_j}\left(\Gamma \frac{\partial T}{\partial x_j} - \rho \overline{u_i' T'}\right) \tag{3.9}$$

Where Γ is the thermal diffusivity of the fluid the $\overline{u_j' T'}$ term is called passive scalar-flux and is an unknown quantity, which originates due to averaging a nonlinear term in transport equation of total scalar field. This is analogous to Reynolds stresses. The RANS models can be categorised as eddy viscosity based models (EVM) and non-eddy viscosity based models, called second moment closure models [80].

3.3.1 The standard $\kappa - \varepsilon$ model

The simplest of turbulence models are two-equation models in which the solution of two separate transport equations allows the turbulent velocity and length scales to be independently solved. The standard $\boldsymbol{\kappa - \varepsilon}$ model falls within this class of turbulence model and has become the common used turbulence equations for practical CFD flow simulations.

3.3.2 The RNG $\kappa - \varepsilon$ model

The **RNG** $\boldsymbol{\kappa - \varepsilon}$ model is derived using a rigorous statistical method called renormalization group (**RNG**) theory. It is similar in form to the standard $\boldsymbol{\kappa - \varepsilon}$ model, but consists of the following modifications:

1. The **RNG** model has an additional term in its $\boldsymbol{\varepsilon}$ equation that significantly improves the accuracy for rapidly strained flows.
2. The effect of swirl on turbulence is included in the **RNG** model, enhancing accuracy for swirling flows.

3. The **RNG** theory provides an analytical formula for turbulent Prandtl numbers, while the standard $\boldsymbol{\kappa - \varepsilon}$ model uses user-specified, constant values.
4. However the standard $\boldsymbol{\kappa - \varepsilon}$ model is a high-Reynolds-number model, the **RNG** theory provides an analytically-derived differential formula for effective viscosity that accounts for low-Reynolds-number effects.

These features make the **RNG** $\boldsymbol{\kappa - \varepsilon}$ model more accurate and reliable for a wider class of flows than the standard $\boldsymbol{\kappa - \varepsilon}$ model.

3.3.3 The realizable $\boldsymbol{\kappa - \varepsilon}$ model

The realizable $\boldsymbol{\kappa - \varepsilon}$ model is a relatively recent development and differs from the standard $\boldsymbol{\kappa - \varepsilon}$ model in two significant ways:

1. The realizable $\boldsymbol{\kappa - \varepsilon}$ model contains a new formulation for the turbulent viscosity.
2. A new transport equation for the dissipation rate, $\boldsymbol{\varepsilon}$, has been derived from an exact equation for the transport of the mean-square viscosity fluctuation.

The term "*realizable*" means that the model fulfils certain calculated constraints on the Reynolds stresses consistent with the physics of turbulent flows. Neither the standard $\boldsymbol{\kappa - \varepsilon}$ model nor the RNG $\boldsymbol{\kappa - \varepsilon}$ model is realizable [67-79].

One of the advantages of the realizable $\boldsymbol{\kappa - \varepsilon}$ model is that it can accurately predict the diffusion rate on sphere object. It also can provide superior performance for flows involving rotation, boundary layers under strong adverse pressure gradients, separation, and recirculation. Both the realizable and RNG $\boldsymbol{\kappa - \varepsilon}$ models have shown substantial improvements over the standard $\boldsymbol{\kappa - \varepsilon}$ model where the flow features include strong streamline curvature vortices and rotation. Since the model is still relatively new, it is not clear in exactly which instances the realizable $\boldsymbol{\kappa - \varepsilon}$ model consistently outperforms the RNG model.

3.3.4 Near-wall treatments for wall-bounded turbulent flows

Turbulent flows are considerably affected by the presence of walls the mean velocity field is affected through the no-slip condition that has to be satisfied at the adsorbent bed wall. Also the turbulence is also changed by the presence of the heat exchanger fins. Very close to the wall, viscous damping reduces the tangential velocity fluctuations while kinematic blocking reduces the normal fluctuations. Toward the outer part of the near-wall region however the turbulence is rapidly increased by the production of turbulence kinetic energy due to the large gradients in mean velocity [60-79].

The near-wall modelling significantly impacts the conformity of numerical solutions as walls and heat exchanger fins are the main source of mean viscosity and turbulence. After all it is in the near-wall region that the solution variables have large gradients and the momentum and other scalar transports occur most vigorously. Therefore accurate representation of the flow in the near wall region determines successful predictions of wall-bounded turbulent flows. The $\boldsymbol{\kappa - \varepsilon}$ models are primarily valid for turbulent core flows (i.e., the flow in the regions fairly far-off from the adsorbent beds walls).

3.3.5 Flows in Porous Media

Porous media are treated in CFD simulation modelling as distributed resistances to fluid flow therefore, the porous matrix act on the fluid flowing through it via the S_i, $S_i u_i$ and (if heat conduction in porous solids is considered) *QH* terms in Eqs. (3.11) and (3.12), whose components related to porosity are defined as:

$$\frac{\partial \rho}{\partial t} + \frac{\partial}{\partial x_i}(\rho u_i) = 0 \tag{3.10}$$

$$\frac{\partial \rho u_i}{\partial t} + \frac{\partial}{\partial x_j}(\rho u_i u_j) + \frac{\partial p}{\partial x_i} = \frac{\partial}{\partial x_j}(\tau_{ij} + \tau_{ij}^R) + S_i \quad i = 1,2,3$$

(3.11)

$$\frac{\partial \rho H}{\partial t} + \frac{\partial \rho u_i H}{\partial x_i} = \frac{\partial}{\partial x_i}\left(u_j(\tau_{ij} + \tau_{ij}^R) + q_i\right) + \frac{\partial p}{\partial t} - \tau_{ij}^R \frac{\partial u_i}{\partial x_j} + \rho\varepsilon + S_i u_i + Q_H,$$

$$H = h + \frac{u^2}{2},$$

(3.12)

where ***u*** is the fluid velocity, ***ρ*** is the fluid density, is a mass-distributed external force per unit mass due to a porous media resistance **(S_i^{porous})**, a buoyancy **($S_i^{gravity} = -\rho g_i$**, where g_i is the gravitational acceleration component along the *i*-th coordinate direction), and the coordinate system's rotation **($S_i^{rotation}$),** i.e., $S_i = S_i^{porous} + S_i^{gravity} + S_i^{rotation}$, *h* is the thermal enthalpy, Q_H is a heat source or sink per unit volume, τ_{ik} is the viscous shear stress tensor, is the diffusive heat flux. The subscripts are used to denote summation over the three coordinate directions. For calculations with the High Mach number flow option enabled, the following energy equation is used:

$$\frac{\partial \rho E}{\partial t} + \frac{\partial \rho u_i \left(E + \frac{p}{\rho}\right)}{\partial x_i} = \frac{\partial}{\partial x_i}\left(u_j(\tau_{ij} + \tau_{ij}^R) + q_i\right) - \tau_{ij}^R \frac{\partial u_i}{\partial x_j} + \rho\varepsilon + S_i u_i + Q_H,$$

$$E = e + \frac{u^2}{2},$$

(3.13)

Where *e* is the internal energy. For Newtonian fluids the viscous shear stress tensor is defined as:

$$\tau_{ij} = \mu\left(\frac{\partial u_i}{\partial x_j} + \frac{\partial u_j}{\partial x_i} - \frac{2}{3}\delta_{ij}\frac{\partial u_k}{\partial x_k}\right)$$

(3.14)

Following Boussinesq assumption, the Reynolds-stress tensor has the following form:

$$\tau_{ij}^{R} = \mu_t \left(\frac{\partial u_i}{\partial x_j} + \frac{\partial u_j}{\partial x_i} - \frac{2}{3}\delta_{ij}\frac{\partial u_k}{\partial x_k} \right) - \frac{2}{3}\rho k \delta_{ij} \tag{3.15}$$

Here δ_{ij} is the Kronecker delta function (it is equal to unity when $i = j$, and zero otherwise), μ is the dynamic viscosity coefficient, μ_t is the turbulent eddy viscosity coefficient and k is the turbulent kinetic energy. Note that μ_t and k are zero for laminar flows. In the frame of the ***k***-ε turbulence model, μ_t is defined using two basic turbulence properties, namely, the turbulent kinetic energy ***k*** and the turbulent dissipation ***ε***,

$$\mu_t = f_\mu \frac{C_\mu \rho k^2}{\varepsilon} \tag{3.16}$$

Here f_μ is a turbulent viscosity factor. It is defined by the expression

$$f_\mu = \left[1 - \exp\left(-0.025 R_y\right)\right]^2 \cdot \left(1 + \frac{20{,}5}{R_T}\right) \quad ,$$

$$\text{where } R_T = \frac{\rho k^2}{\mu\varepsilon} \quad , \quad R_y = \frac{\rho\sqrt{k}\,y}{\mu} \tag{3.17}$$

and y is the distance from the wall. This function allows us to take into account laminar-turbulent transition. Two additional transport equations are used to describe the turbulent kinetic energy and dissipation,

$$\frac{\partial \rho k}{\partial t} + \frac{\partial}{\partial x_i}\left(\rho u_i k\right) = \frac{\partial}{\partial x_i}\left(\left(\mu + \frac{\mu_t}{\sigma_k}\right)\frac{\partial k}{\partial x_i}\right) + S_k \quad , \tag{3.18}$$

$$\frac{\partial \rho \varepsilon}{\partial t} + \frac{\partial}{\partial x_i}\left(\rho u_i \varepsilon\right) = \frac{\partial}{\partial x_i}\left(\left(\mu + \frac{\mu_t}{\sigma_\varepsilon}\right)\frac{\partial \varepsilon}{\partial x_i}\right) + S_\varepsilon \quad , \tag{3.19}$$

where the source terms S_k and S_ε are defined as

$$S_k = \tau_{ij}^R \frac{\partial u_i}{\partial x_j} - \rho\varepsilon + \mu_t P_B \tag{3.20}$$

$$S_\varepsilon = C_{\varepsilon 1} \frac{\varepsilon}{k}\left(f_1 \tau_{ij}^R \frac{\partial u_i}{\partial x_j} + \mu_t C_B P_B \right) - C_{\varepsilon 2} f_2 \frac{\rho\varepsilon^2}{k} \quad . \tag{3.21}$$

Here P_B represents the turbulent generation due to buoyancy forces and can be written as

$$P_B = -\frac{g_i}{\sigma_B}\frac{1}{\rho}\frac{\partial \rho}{\partial x_i} \tag{3.22}$$

where g_i is the component of gravitational acceleration in direction x_i, the constant $\sigma_B = 0.9$, and constant is C_B defined as: $C_B = 1$ when $P_B >$, and 0 otherwise;

$$f_1 = 1 + \left(\frac{0.05}{f_\mu}\right)^3 \quad , \quad f_2 = 1 - \exp\left(-R_T^2\right) \tag{3.23}$$

The constants $C_\mu, C_{\varepsilon 1}, C_{\varepsilon 2}, \sigma_k, \sigma_\varepsilon$ are defined empirically. In the simulation the following typical values are used:

$$C_\mu = 0.09,\ C_{\varepsilon 1} = 1.44,\ C_{\varepsilon 2} = 1.92,\ \sigma_\varepsilon = 1.3,$$
$$\sigma_k = 1 \tag{3.24}$$

Where Lewis number Le=1 the diffusive heat flux is defined as:

$$q_i = \left(\frac{\mu}{\mathrm{Pr}} + \frac{\mu_t}{\sigma_c} \right) \frac{\partial h}{\partial x_i} \quad , i = 1, 2, 3. \tag{3.25}$$

Here the constant σ_c = 0.9, Pr is the Prandtl number, and *h* is the thermal enthalpy. These equations describe both laminar and turbulent flows. Moreover, transitions from one case to another and back are possible. The parameters *k* and μ_t are zero for purely laminar flows.

3.4 CFD Modelling

3.4.1 Computational Fluid Dynamics

Using CFD to create a better understanding of porous media flow processes is an essential step as it will provide data that cannot be obtained in any other way. It is therefore essential to further explore the concept of CFD**.**

Computational Fluid Dynamics is a method [67, 68] that has become more popular in the modelling of porous media systems in many fields. CFD simulation makes it possible to solve flow, mass and energy balances in complex flow like porous media. The CFD results can show specific flow and heat transfer and velocity flow of water vapour that are hard to obtain experimentally or with conventional modelling methods. CFD numerically solves the Navier-Stokes equations and the energy and species balances. The differential forms of these balances are solved over a large number of control volumes. These control volumes are small volumes within the flow geometry, all control volumes properly combined to form the entire flow geometry. The size and number of control volumes is user determined and will affect the accuracy of the results. After boundary conditions have been implemented the flow and energy balances are solved numerically [3,65,69].

3.4 Mesh Specifics in Silica Gel Packed Bed Modelling

For all types of geometries the creation of the mesh has different obstacles. In the meshing of Silica gel packed bed geometry the major issue is resolving the areas where two solid surfaces touch the contact points. This is because it is not possible to incorporate actual

contact points of the spheres with each other or the wall when turbulent flow needs to be resolved. By having two solid faces touch in one only point in a flow geometry, certain control volumes in the fluid zone that are located near the contact point are created with infinitely small edges, resulting in tangential points (control volumes belonging to the solid and fluid phase simultaneously) that lead to an irresolvable simulation condition[53-55].

In this study to include real contact points the silica gel granules had be modelled overlapping by 1% as shown in figure.3.2 of their diameters with the adjacent surfaces in the geometric model.

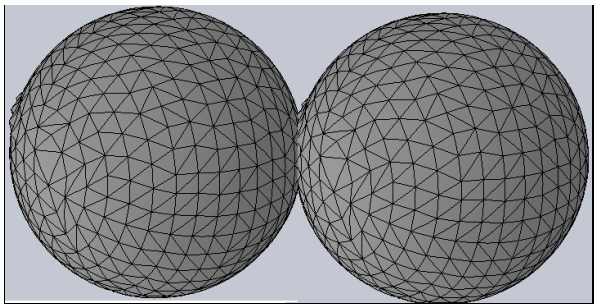

Figure 3.2 3D Dimensional display and detail of the control volumes in the fluid region near particle-to particle contact points.

One of the most problematic and time consuming part of the CFD is the mesh generation it becomes complex when the simulation model has various voids and openings as is the case of adsorbent granules packet beds CFD simulation modelling. Mesh generation is essentially the discretization of the computational domain [54]. The meshing method used in finite difference included a fixed set of nodes points. The finite volume method uses a points system that forms a set of volumes which are called cells [54-77]. These cells define the boundaries of the control volumes while the computational node lies at the centre of the control volume [67,77]. The advantage of finite volume method is that the integral conservation is solved accurately over the control volume. The finite element methods use a set of sub-volumes elements which have nodes where the variables are defined [54]. Constant

variables such as temperature can be represented over the finite element by a linear combination of polynomials called interpolation functions.

The universal types of mesh elements used in CFD solvers are the tetrahedral, hexahedral and pyramidal as shown in Figure 3.3 [54-75].

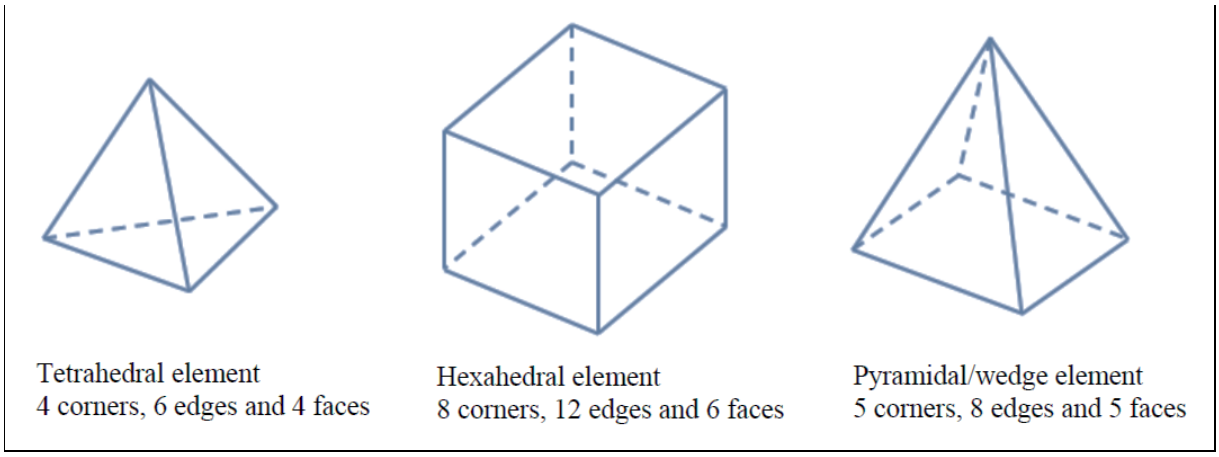

Figure 3.3 Mesh element types for CFD analysis.

The methods of mesh elements depend on the abilities of the CFD solver structured mesh codes use quadrilaterals in 2D and hexahedra in 3D flows. Unstructured mesh solvers often use triangles in 2D or tetrahedral in 3D.

3.5.1 Structured Meshes

A structured mesh is characterized by regular connectivity that can be expressed as a two or three dimensional array. This restricts the element choices to quadrilaterals in 2D or hexahedra in 3D as shown in figure 3.4 are a structured mesh. This type of mesh procedure is quite tedious if it involves complex 3D geometry.

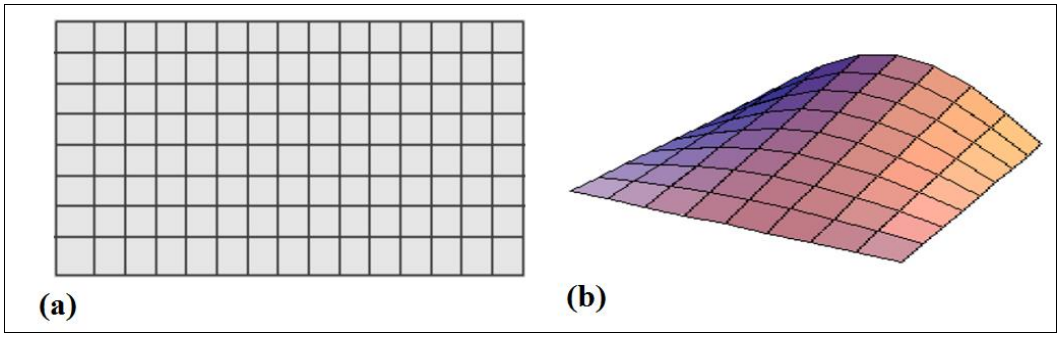

Figure 3.4 Structured meshes (a) 2D mesh (b) 3D mesh.

Tetrahedral meshing method allows fairly easy meshing of complex geometries. A surface mesh consisting of hexahedral elements is first created this is then used to mesh the inside of the geometry.

3.5.2 Unstructured Meshes

An unstructured mesh is characterized by irregular connectivity this type of mesh can be expressed in two or three dimensional models see figure 3.5. The advantage of this type of mesh is it can be adapted to accommodate complex CFD models wherever required. This is based on the fact that the control volume can be of any unstructured mesh shape. Unstructured mesh reduces the time which is required for meshing as a result of mesh generation being quicker and easy.

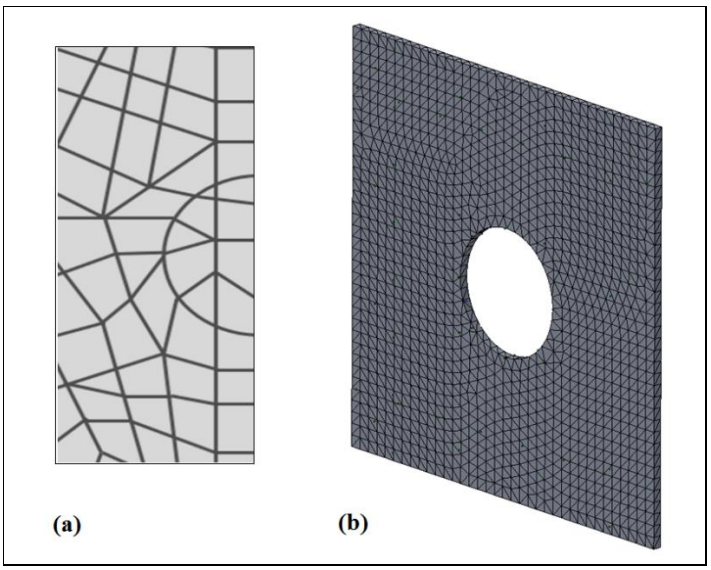

Figure 3.5 Unstructured meshes (a) 2D mesh (b) 3D mesh.

3.5.3 Hybrid Meshes

A hybrid mesh is a mesh that contains structured portions and unstructured portions as shown in figure 3.6. This type of mesh was designed to achieve the advantage of both unstructured and structured mesh. Hybrid mesh contain tetrahedral, hexahedral and pyramid elements in 3D and quadrilaterals in 2D.

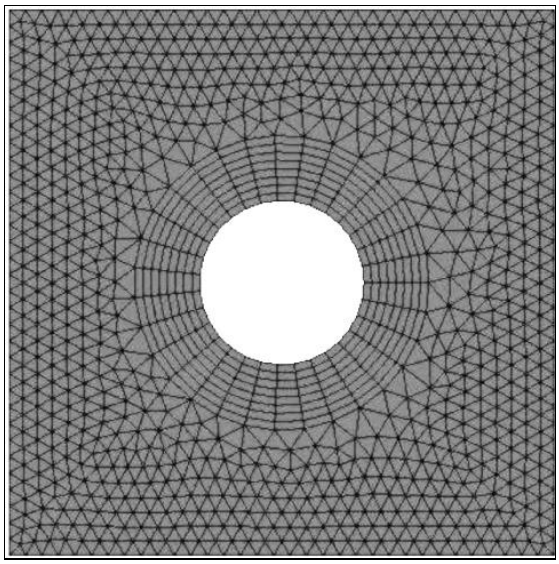

Figure 3.6 Cartesian hybrid mesh [121].

The mesh quality has a strong influence on the accuracy of the CFD simulation where a poor quality mesh will affect the numerical accuracy.

3.6 Commercially Available CFD Method

In order for one to solve the CFD equations of computational fluid dynamics first their numerical data must be generated. This is done by a method so-called discretization. In the discretization method, each term within the equation describing the fluid flow is written in a way the computer can be programmed to solve the equations. There are various methods for CFD numerical discretization. In this section of the thesis three of the universally used methods will be introduce, namely: (1) the finite difference method, (2) the finite element method and (3) the finite volume method [67, 68 -75].

Commercially available widespread CFD codes use one of three basic methods:

Finite differences method (FDM) (**Structured meshes**)

Finite volumes method (FVM) (**Unstructured meshes**)

Finite elements method (FEM) **(Structured meshes)**

3.6.1 The finite differences Method (FDM)

The finite difference method is one of the earliest methods to be used in numerical solution. This method is thought to have been developed by Euler in (1768) [67, 74-75] which was used to develop numerical solution for differential equations by hand. This method was then adapted for CFD simple codes. In theory the finite difference methods can be applied to any type of mesh system. However this method is more commonly applied to structured meshes since it requires a mesh having a high degree of uniformity [68,75]. This method has a set of finite points, so-called nodes, and the Navier-Stokes equations are enforced at these points. The equations take the shape of templates which describe velocity and pressure values at one node to the values at neighbouring nodes. Creation of the templates needs that the nodes be attached in a arranged finite mesh, so that each node recognize its neighbour's see figure 3.7.

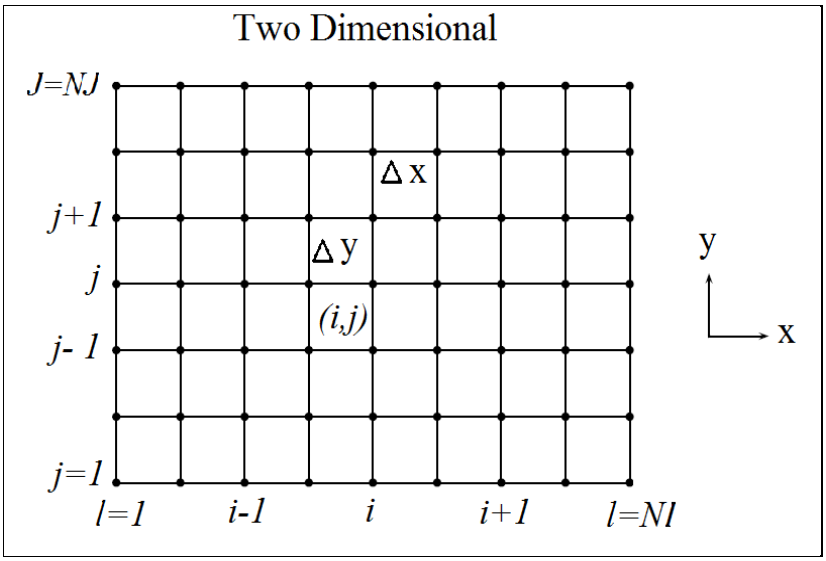

Figure 3.7 Illustration of a two dimensional equally distributed mesh for the finite difference method.

3.6.2 Finite Volumes Method (FVM)

The finite volume method was developed by researchers such as McDonald and Mac Cormack (1971) and (1972) [67, 68] for the solution of two dimensional time- dependent Euler equations and was later extended to three dimensional flows by Inouye and Rizzi (1973) [67, 68]. The advantage of the finite volume method is that it is not limited to one mesh method because it works with control volumes and has the capacity to accommodate any type of mesh. Including unstructured meshes allows it to have a large number of options for the definition of shape and location of control volumes. This method offers greater flexibility for handling complex geometries. Another attractive feature is that this method requires no transformation of the equation in terms of body fitted coordinate system as shown in figure.3.8.

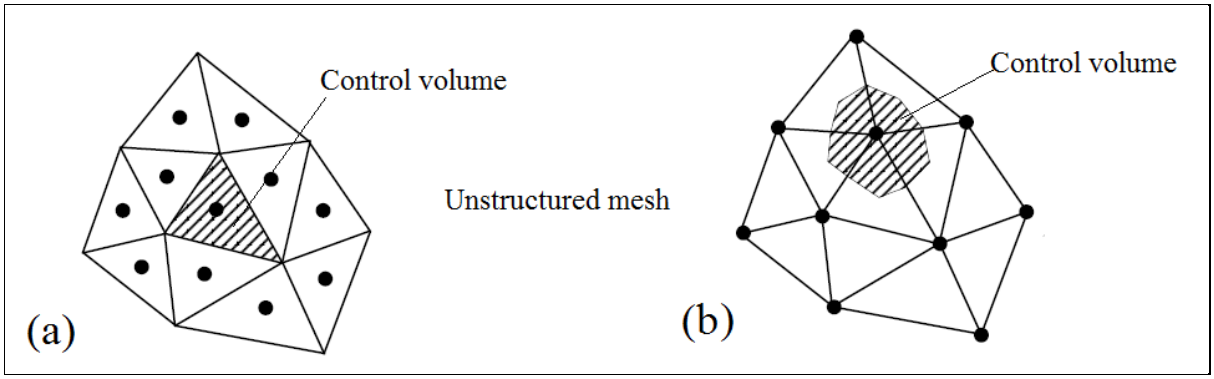

Figure.3.8 (a) Mesh and dual mesh of cell FVM (b) Mesh and dual mesh of vertex FVM.

3.6.3 Finite Elements Method (FEM)

The finite element is one of the earliest use was by Courant (1943) [67] for solving a torsion problem. The method was then refined significantly in the 60's and 70's, mostly for analysing structural mechanics problem. FEM analysis of fluid flow was developed in the mid- to late 70's. One of the advantages of this method it has a high accuracy on coarse mesh it can also be used for diffusion dominated problems (viscous flow) and viscous, free surface problems.

Disadvantages of this method slow performance for large simulation problems and is not well suited for turbulent flows simulation modelling figure.3.9.

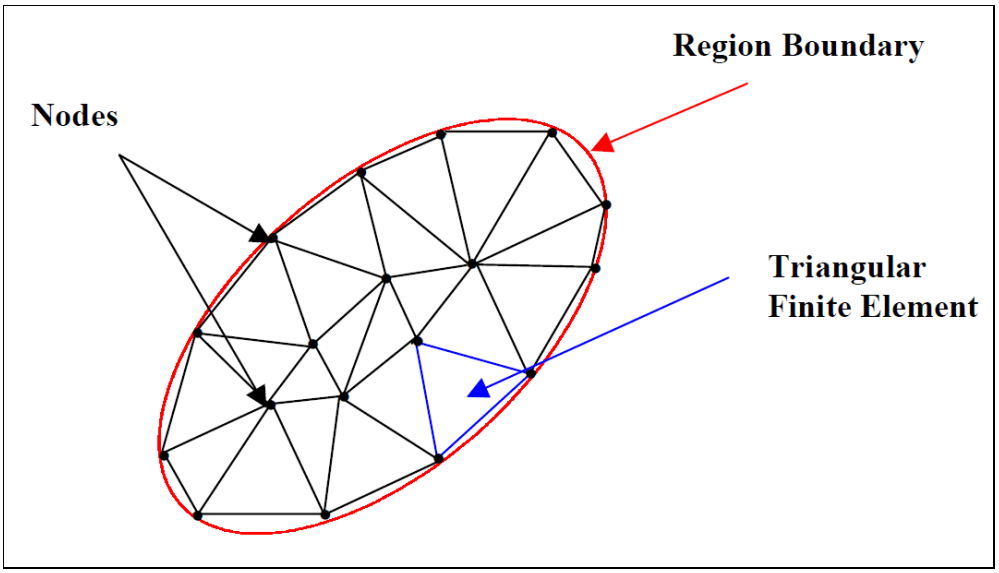

Figure.3.9 Two-dimensional region subdivided in finite elements.

3.6.4 Comparison of the Different CFD Methods

The main differences between the above three methods include the followings. The finite difference method and the finite volume method both produce the CFD numerical equations at a given point based on the values at nearby points while the finite element method creates equations for each element separately of other elements. Only when the finite element equations are composed together and accumulated into the global matrices that the communication between elements are taken into account [54-68]

3.7 The three main CFD elements

Enclosed in all CFD software codes are three main elements: (1) a pre-processor, which is used to input the flow parameter and the boundary conditions of the intended model. (2) A flow solver, which is used to solve the governing equations of the flow data subject to the

setting provided. (3) A post-processor, which is used to manipulate the data and show the results in graphical and easy to read layout [77-79].

1. Pre-processor
2. Solver
3. Post processor

The functions of these three elements will be examined in more detail in this part of the thesis see figure 3.10

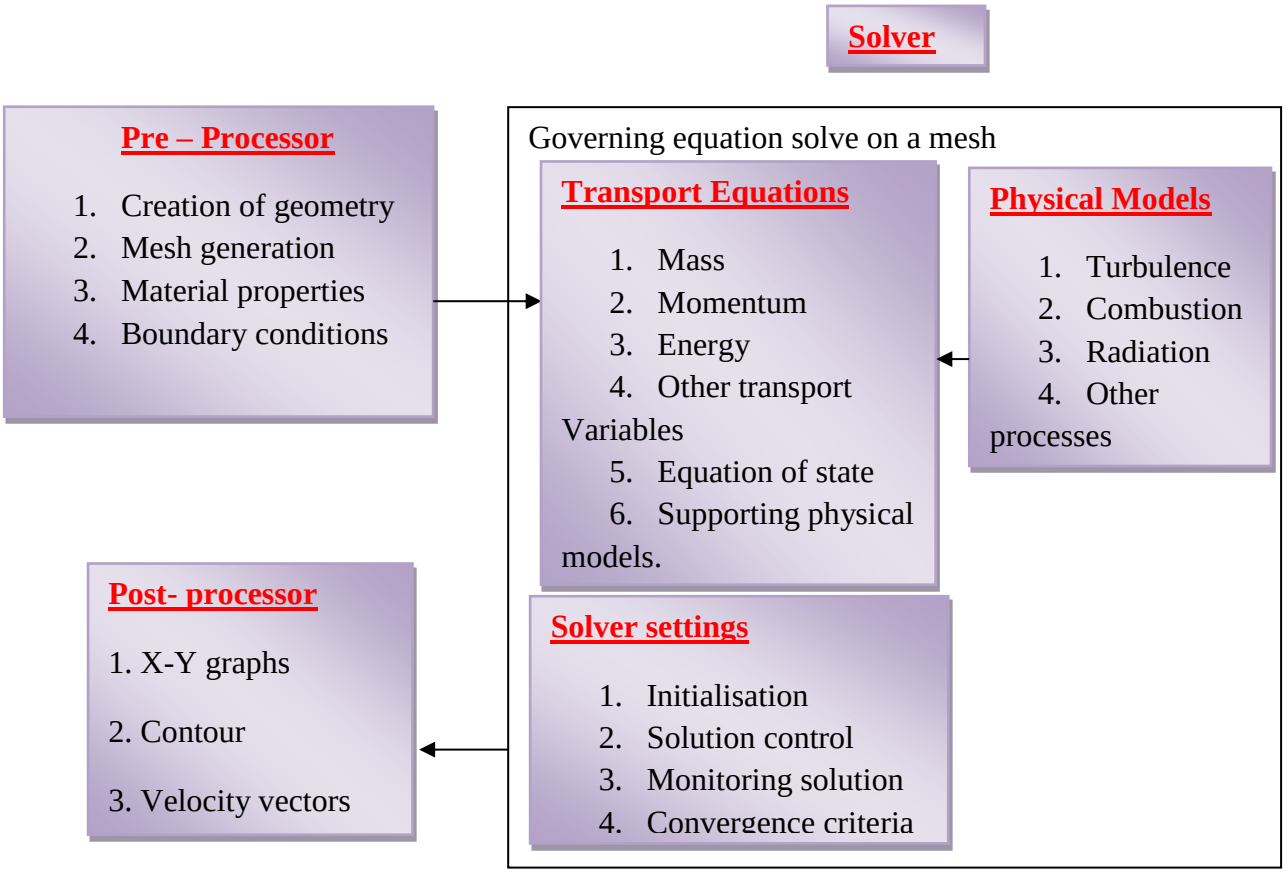

Figure 3.10 The inter connectivity functions of the three main elements within a CFD analysis framework.

3.7.1 Pre-processing

All the tasks that take place before the numerical solution process are called pre-processing. This includes problem assessment, meshing and generation of a computational model.

Problem assessment is the first stage in using CFD in this stage the engineer considers the flow problem, the second stage is meshing. Where the engineer create the geometry of the domain that needs to be analysed. Then the problem domain is sub-divided into smaller cells, also known as volumes or elements [65-79].

3.7.2 Solver

When a mesh is completed with its grid density and all other complications resolved, the actual computational part of the CFD can be started. At this point the completed geometry can be imported into the solver and the CFD simulation is started. Again, a series of steps are to be performed; first, the boundary conditions on the system need to be set and next the process iteration parameters need to be set. With the boundary conditions defined the simulation can be performed. The final step in obtaining the desired data is the post-processing of the data in which the desired data sets are taken from the simulation data [67-76].

3.7.3 Post-processing

The post-processing program is used to evaluate the data generated by the CFD analysis.
When the simulation has converged the last data set is stored as a final solution. This data set has a record of the status of all elements in the model, temperature, densities, pressures, flow aspects etc. To be able to interpret the data it needs to be ordered and reduced to comprehensible sizes [67-69]. This displaying of the data is called post-processing and makes it possible to compare the different simulations with each other and with external data. There are as many ways of displaying the data as there are data points so it is important to select the data representation that is required for the desired data comparison. Some of the standard visualization options available are contour plots and velocity vector plots. Contour plots will give a plot in a defined collection of control volumes which can be a plane or a volume, of

contours of another variable. For example a plane can be defined as a constant x-coordinate plane (y-z plane); we can then make a contour plot showing temperature contours in this plane.

In the same plane a velocity contour plot can be made showing absolute velocities of the fluid in the defined plane [60-77]. Other variables that can be used for contour plots are magnitude of velocity components turbulence components and local pressure. Velocity vector plots can be made to get an insight into the flow patterns in the overall geometry or detailed at specific locations. The density and magnification of the velocity vectors in the specified field can be manually changed to get a most optimal picture [60-73].

The field density has a maximum limitation, the amount of elements in the model. Besides these qualitative data export methods it is also possible to export the numerical data in many different forms [3,73]. Direct export of selected data sets is facilitated for a number of external applications. It is also possible to export data in Parasolid format for further manipulation. Another method for exporting the numerical data is the two-dimensional plot function in which two data sets can be plotted against each other [54-80]. This function is useful when, for example, radial velocity or temperature profiles need to be compared. From different simulations, identical plots can be created and a direct comparison of the numerical data is possible [75-80].

3.8 CAD Geometry Design

In this phase of the model design the major topological entities are defined. The outer wall to the model is established as well as the internal structure, solid particles and fluid regions. Several entities, such as cylinders or spheres, are ready made parts that can be added to the geometry. Before exporting the fundamental geometry it is important all curves are defined as so-called B-Spline curves, these are mathematical descriptions of the specific curves. This

conversion is necessary to be able to have the surface mesh form to the exact contours of the created geometry.

3.9 Imposing Boundary Conditions Inlet and Outlet

The boundary conditions take into account numerous elements that affect the behaviour of fluids and help to visualize them through 3D simulation. Some of these elements consist of mass transfer, heat flow, and changes in gas to liquid and liquid to gas phases. Boundary conditions contribute to the understanding of what results are possible at the inlet and outlet of a model [54].

External Faces

1. Flow inlet and exit boundaries: pressure inlet, velocity inlet pressure outlet, outflow.
2. Wall repeating and boundaries: wall symmetry
3. Internal zones: fluid
4. Internal face boundaries porous media silica gel interior

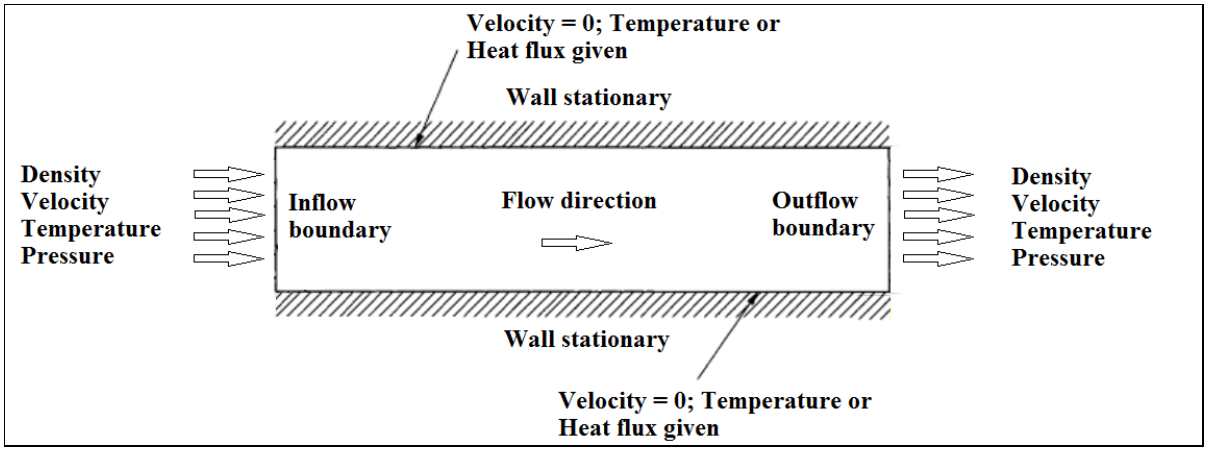

Figure.3.11 Establishing by setting the iteration parameters.

3.10 Validating CFD against Experimental Data

This study has used CFD for detailed modelling of heat and mass transfer in an adsorption system adsorbent bed. One of the major questions in CFD simulation modelling is whether it

can be used to describe system performance well enough to be considered an alternative to experimental data gathering [73,74].

For this, validation of CFD data against experimental data is desired. In this project a 3D adsorbent bed was designed and data gathered from research papers and experimental test rigs and a 3D CFD model. A comparison of the experimental data was made in order to validate the CFD results. Simulated tests of the effect of adsorbent size and properties of silica gel were done using the porous media approaches by application of modified Navier-Stokes equations and the continuity equations. In these equations, an additional term was used to describe the porosity distribution in order to take into account the porous media packing geometry, and in order to design an efficient adsorbent bed, flow and temperature, adsorption information was needed [78-80].

3.10.1 Experiments vs. CFD Simulations

CFD gives an insight into flow patterns that are difficult, expensive or impossible to study using traditional experimental techniques. Table 3.1 Experiments vs. CFD simulation

EXPERIMENTS	**CFD SIMULATIONS**
Quantitative description of flow phenomena using measurements	Quantitative prediction of flow phenomena using CFD software
• For one quantity at a time.	• For all desired quantities.
• At a limited number of points and time instants.	• With high resolution in space and time.
• For a laboratory scale model	• For the actual flow domain
• For a limited range of problems and operating conditions	• For virtually any problem and realistic operating conditions
Error sources measurement errors, flow disturbances by the probes.	Error sources modelling, discretization, iteration, implementation.

CFD will not replace the experimental measurements completely but the amount of experimentation and the overall cost will be reduced in time.

Table 3.2 Experiments vs. CFD simulation

Table 3.2 highlights the characteristics of experiments to CFD

EXPERIMENTS	SIMULATIONS
• Expensive	• Inexpensive
• Slow	• Quicker
• Sequential	• Parallel
• Single purpose	• Multiple purpose

3.11 The Computational Fluid Dynamics Software Used in This Thesis

The CFD software used in this thesis is Solidworks COSMOS CFD Flow Simulation previously called Cosmos Flow.

3.11.1 The advantages of using CFD

CFD commercial software is useful tools to visualize the adsorption phenomena in porous media and have provided valuable insight into microscopic behaviour not obtainable through core experiments. Several methods have been developed to include adsorption of water vapour and porous media in CFD simulations [1,3,4,59]. The applications of CFD simulation of adsorption are increasingly becoming established in adsorbent bed and chemical processes as an alternative to the conventional techniques [59,66].

CFD codes describing porous adsorbent surface adsorption of gas or vapour appears to be the most suitable from the point of view of accuracy. CFD models can be used to describe the effects of surface multilayer vapour adsorption on porous adsorbent this phenomena need to be considered when modelling realistic adsorption of water vapour [35,53]. The Navier-Stokes, vapour diffusion, Lattice Boltzmann and **Brunauer -Emmett-Teller (BET)** equations describing adsorption in CFD simulation are well established[3,4,35].

3.11.3 The limitation of CFD modelling when dealing with chemical adsorption of vapour

CFD commercial software has the capability to model physical surface adsorption of vapour transport within porous adsorbent regions [6,7]. However, this capability is somewhat limited when extended to chemical adsorption phenomena of vapour in porous adsorbent regions. This restricts the modelling of adsorption to mainly physical surface modelling of the adsorption of vapour or gasses [59,72].

This is not a problem when studying adsorption cooling systems because the adsorption taking place in the adsorption cooling system is of a physical surface adsorption phenomenon only. However, this can be more difficult when attempting the simulation of a chemical adsorption system. There are hybrid CFD software packages specifically developed for modelling complex chemical adsorption such as CHEMKIN [131], CANTERA [132], DETCHEM [133], which also offer CFD codes for special reactor configurations such as channel flows and monolithic reactors. These kinetic packages also have a variety of user written subroutines for modelling complex reaction a variety of multi-purpose and specialized CFD codes.

Another limitation of CFD adsorption simulation of vapour is the computer power needed to correctly model adsorption, which limits CFD simulation to only to small section of an adsorbent bed.

3.12 The Different Types of CFD Simulation Software Package

When selecting a CFD simulation software package you are faced with a large selection of options. There is a vast range of computational fluid dynamic systems available, from general-purpose CFD software through to very specific application software. There are some CFD programs that will provide results for pipe systems only whilst others will work only

with 2D CFD Simulation methods. Some general purpose CFD software can be versatile in different area of CFD modelling but not specialist.

There are three types of CFD simulation areas:

3.12.1 Commercial off the Shelf CFD Simulation Software Packages

These are CFD packages developed and supported by commercial organizations the leading general purpose products are:

- **COSMOS FLOW SIMULATION**
- **COMSOL MULTIPHYSICS**
- **STAR-CD**
- **FLUENT**
- **CFX**

Each software program has advantages and disadvantages.

3.12.2 Custom-built CFD Simulation Specialist Software

The advantages of custom built CFD simulation software over general-purpose CFD simulation software both industrial and academic develop CFD programmes in-house for their own user base. Large industrial establishments, for instance, have a tendency to rely greatly on custom-built CFD system because they need high accuracy results.

3.12.3 CFD Freeware Software

- **Open FOAM**

OpenFOAM is a universal CFD code written in C++ the package comprises of modules for a wide range of CFD simulation procedures. OpenFOAM was written by Henry Weller and others at Imperial College. This is just one of the several CFD freeware software that can be download from the internet.

3.13 Conclusion

At presently CFD simulation method is largely used in engineering application to provide data that is complementary to experimental and theoretical results. This simulation method is becoming more common in academic establishments and government research laboratories. One of the reasons for this can be partially accredited to the rapid evolution of CFD methods especially through the availability of multipurpose commercial CFD computer programs. Also with the decreasing costs of computer hardware and fast computing speed engineers are increasingly relying on this reliable simulation tool. In conclusion to this chapter one can continue to believe as the future unfolds CFD simulation and its modelling methods will continue to remain at the forefront of increasing research and development as long as the vast majority of complex fluid flow solution remains unanswered.

CHAPTER 4

COMPUTATIONAL FLUID DYNAMICS MODELLING AND EXPERIMENTAL STUDY ON A SILICA GEL TYPE B

Abstract

The last chapter has provided reviews of basic underlying principles of CFD this will serve as an essential knowledge for this chapter. The application of computational fluid dynamics (CFDs) in the area of porous media and adsorption cooling system is becoming more practical due to the significant improvement in computer power. The results from previous studies have shown that CFD can be useful tool for predicting the water vapour flow pattern, temperature, heat transfer and flow velocity and adsorption rate. This chapter investigates the effect of silica gel granular size on the water adsorption rate using computational fluid dynamics and gravimetric experimental (DVS) method.

4.1 Introduction

The adsorption properties of silica gel have been studied for many years as silica gel is used in many industries including adsorption cooling systems. Past research have shown experimentally that the adsorption rate of silica gel granules depend on their size. The purpose of this work was to study the effect of granule size on the adsorption properties of silica gel by using CFD and comparing the simulation results to those obtained experimentally. (CFD) Computational Fluid Dynamics is a field that has developed over the years because of the new development of computers and CFD simulation. CFD is also used a simulation tool in refrigeration and air conditioning industry. In this chapter CFD simulation have been used for modelling of heat and mass transfer in a adsorption tube with silica. One of the questions in CFD modelling is can this type of technology be used as an alternative to experimental data gathering. For this hypothesis a confirmation of CFD data against

experimental data is desired. In this chapter a 3D silica gel and tube structured model have been developed for this purpose. Data will be gathered from experimental study of identical CFD model. This data will be compared to experimental and CFD results. The effects of silica gel size and properties have been studied using the porous media approaches by application of modified Navier-Stokes equations and the continuity equation. In this set of equations, an additional term is used describing the porosity distribution in order to take into account the porous media packing geometry.

To design an efficient adsorbent bed, flow and temperature information is essential. Studies of fluid dynamics and heat transfer in adsorbent beds date back to the early twentieth century [6]. The early investigation of flow in porous media packed beds provided mainly such bulk information as pressure drop correlations. For example, Ergun [82] Andersson suggested a pressure loss equation, in which parameters like porous media particle diameter and fluid physical properties were used to correlate the pressure drop. Similar correlations were proposed by Molerus [63].

These three empirical correlations rather well predict pressure loss for flow in adsorbent beds but provide nothing more about local flow fields our adsorption/desorption on porous media. On the other hand, of the many investigations of heat transfer in adsorbent beds in the last several decades, effective parameter methods were applied to predict temperature distribution [3,83].

CFD (computational fluid dynamics) provides an innovative approach to model and analysing the local flow and the effect of silica gel size on adsorption performance of a packed bed. Numerical simulation of porous media local flow and heat transfer based on the CFD technique has increasingly been reported in recent years in fields of packed bed flow and heat transfer modelling [84]. In this work, a finite volume formulation based on the

Chimera meshing technique is used to simulate the local flow and heat transfer in a silica gel packed bed, which contains 120 randomly packed spheres.

4.2 Experimental Apparatus Description

There are numerous methods used for measuring the adsorption uptake of an adsorbent and the most widely reported procedures are the gravimetric method and the volumetric method. The experimental apparatus used in this chapter is the gravimetric method (TGA) developed by Micromeritics instrument corporation this system is designed to measure adsorption/desorption of porous media materials see Figure.4.1 and Figure.4.2 for Schematic layout of the of the (DVS) instrument.

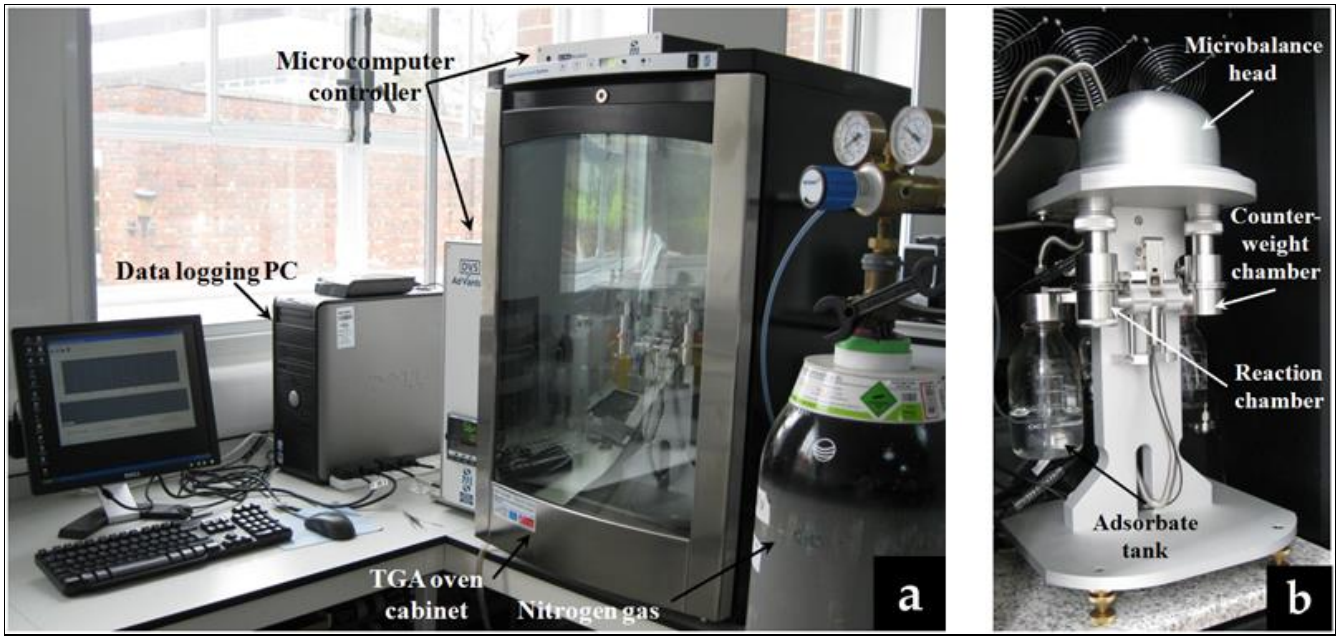

Figure 4.1 Pictorial view of the used DVS instrument.

This system measures the change in weight of a silica gel sample as it is heated for desorption of water and cooled for the adsorption of water vapour or held at a constant temperature.

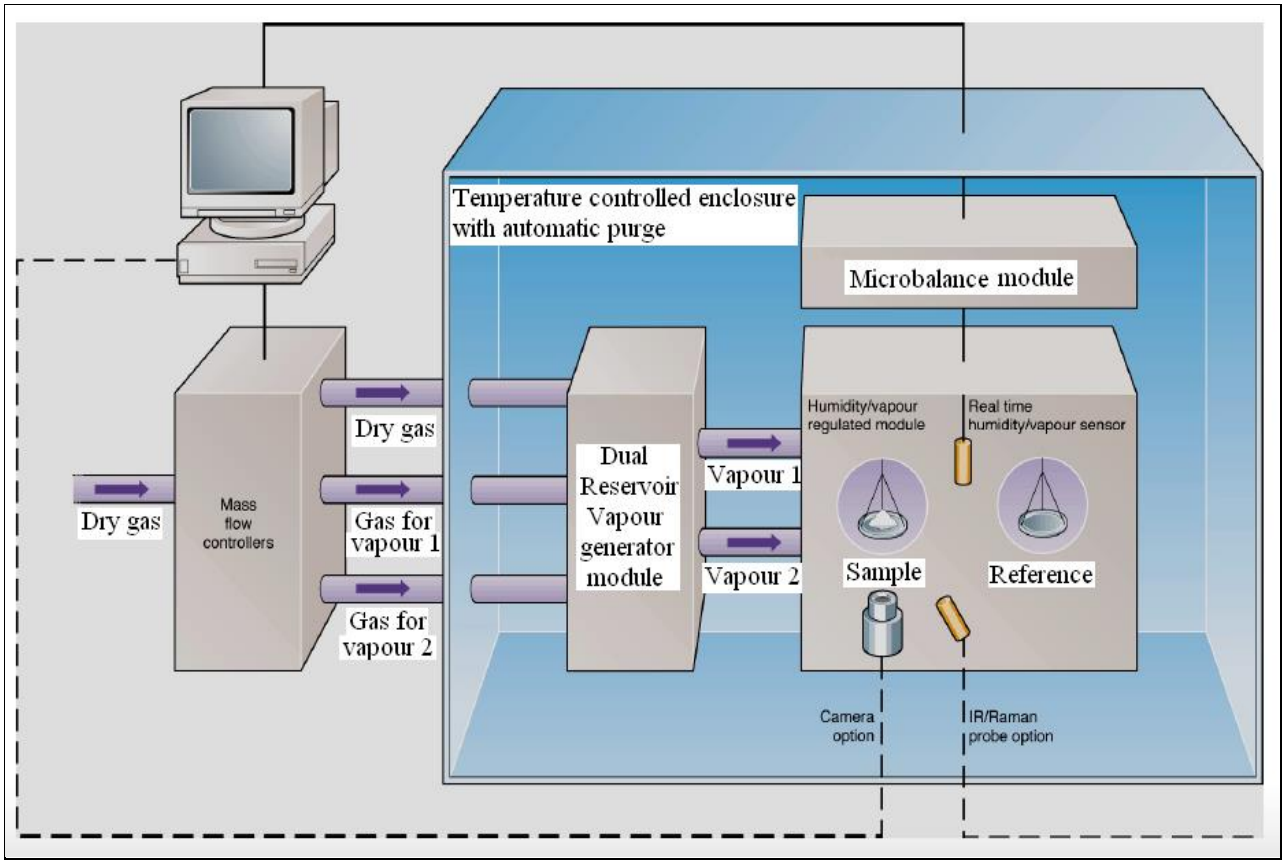

Figure 4.2 Schematic of the (DVS) instrument.

4.2.1 Experiment Setup and Procedure

The Dynamic Vapour Sorption (DVS) method is used for isotherm, kinetics adsorption experiments due to the high accuracy, ease of control of the pressure and temperature of the experiment. DVS gives a direct measurement of the quantity of adsorbate adsorbed throughout the uptake process. A microbalance device is used where the adsorbent mass is measured as a function of temperature and time. In the DVS, the sample containers are suspended on an extension wire that is connected to the microbalance see figure.4.3.

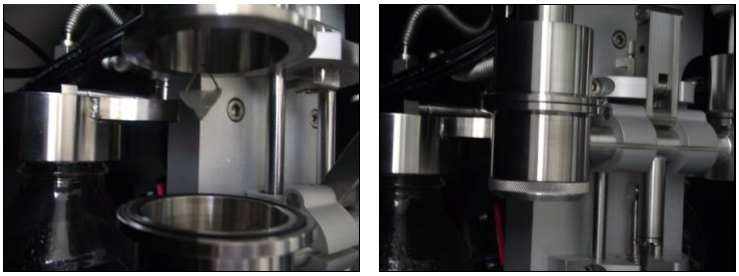

Figure 4.3 Sample container suspended on an extension wire.

The micro-balance measures the weight of sample and it can detect weight changes of the sample in a very short time. Its measurement ranges are between 0 to 150mg with readability up to 0.1μg. The Control software screen shot displays and controls the functions of the micro furnace, balance and thermocouple this run on a computer connected to the DVS's thermal gas analysis station. During the experiment, the time, weight and temperature are recorded continuously at defined intervals and the data are stored on the computer. Silica gel granules sample used in the experiment was Fuji type B size 3.5mm mesh 10-40 see table.4.1.

Figure 4.4 One silica gel size 3.5mm type B.

In Figure.4.4 shows a single silica gel size 3.5mm type B The purpose of testing one silica gel adsorption / desorption was to generate experimental data to be used in a CFD module. The advantage of studying a single granule of silica gel is very useful when designing a 3D adsorption bed simulation prediction model.

4.3. DVS Experimental Results

The adsorption isotherms of the Fuji Davison silica gel-water systems are known to exhibit zero hysteresis. Hence, in the spirit of confirming the reliability of the analyser, experiments are carried out from low vapour exposure to high vapour exposure (low-high process) and then from high coverage back to low exposure (high-low process). Figure.4.5 shows a typical adsorption the isotherm plot for water vapour adsorption on the type B size 3.5mm silica gel

(specific surface area is around 800 m^2 g^{-1}). Figure.4.6 presents the water vapour adsorption uptake on the type B silica gel size 5mm following the low-high process at 25°C. The adsorption temperature fluctuation is about 0.5°C, which is controlled by the microcomputer controller, see figure 1, Pictorial view of the used DVS instrument.

4.3.1 The Isotherm Plot for Silica Gel Size 3.5 mm

The adsorption/desorption isotherm plot for silica gel size 3.5mm for temperature 25°C in figure.4.5 shows a typical water adsorption result from a DVS experiment. The Isotherm plot adsorption kinetic data shows the change in mass and humidity as over a function of time. From the kinetic results, the rate of water uptake and water diffusion coefficients can be determined. The balance mass values at each vapour phase were used to calculate the adsorption and desorption isotherms [82].

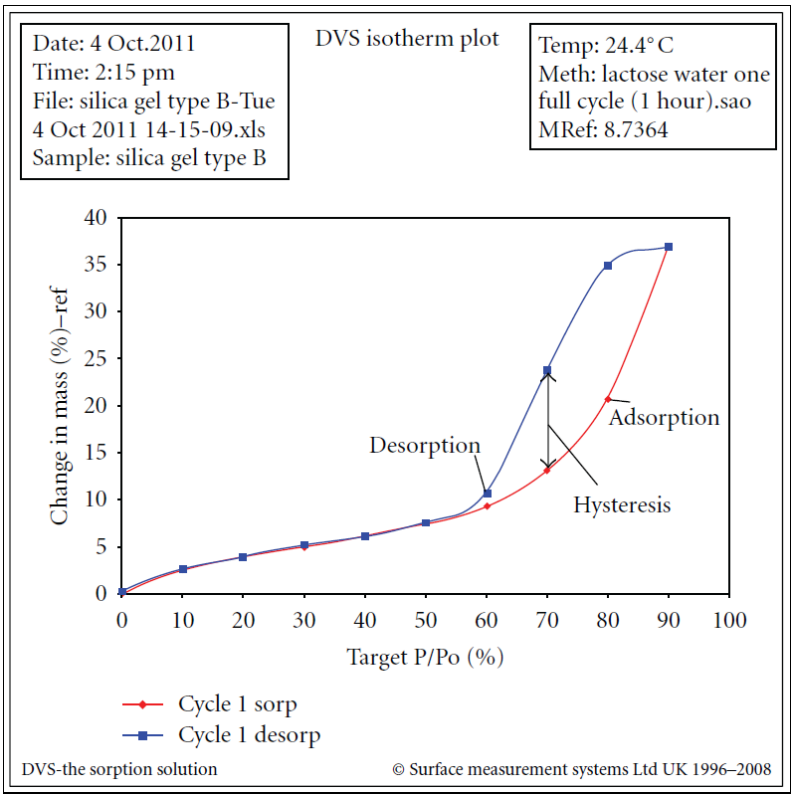

Figure.4.5 Moisture sorption behaviour of silica gel type B size 3.5mm at 25ºC 1-cycle experiment.

Figure.4.5 shows two isotherms, one obtained by wetting a sample from a dry state and the other obtained by drying a sample from wet state. Water adsorption (red) and desorption (blue) isotherms at 25 °C measured on silica gel. The moisture content at each water activity is higher during desorption (drying from high moisture content) than adsorption (wetting from low moisture content).

4.3.2 The Isotherm Plot for Silica Gel Size 5mm

In fig. 6 the isotherm plot is for silica gel size 5mm. The plot begins at water performance near zero and 1°C. The shape and location of the isotherm hysteresis gives the information about the adsorption method and sample porosity. Temperature of water vapour in the adsorbent sample chamber is at a constant 25°C. The isotherm plot will be used to assist in determining drying rates and optimal endpoints. The isotherm also shows whether the silica gel exhibits hysteresis and what impact that will have on water activity after drying to a given moisture content drying curve, for silica gel type B, size 5mm. Figure.4.6, shows two isotherms, one obtained by wetting the silica gel sample from a dry state and the other obtained by drying the silica gel sample from a wet state.

The water adsorption is shown (red) and desorption is shown (blue), isotherms at a temperature of 25°C. In this isotherm plot the moisture content at each water activity is higher during desorption (drying from high moisture content) than adsorption (wetting from low moisture content). The isotherm plot represents the limits or bounding isotherms since they begin at water performance near zero and one degree centigrade. The shape of the isotherm hysteresis gives the information about the adsorption mechanism and sample porosity of the 5mm silica gel.

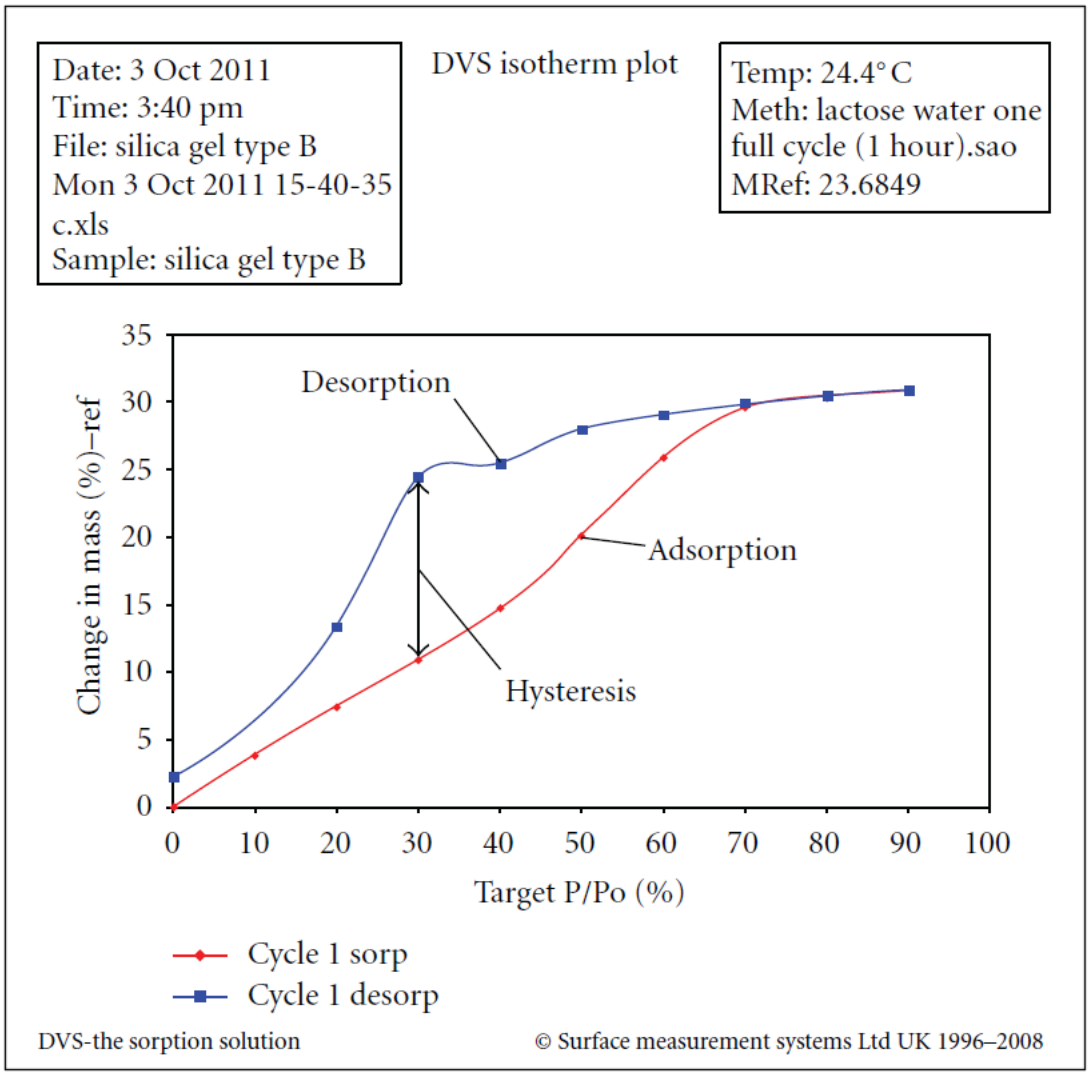

Figure 4.6 Moisture sorption behaviour of silica gel type B size 5mm at 25°C 1-cycle experiment.

The shape and location of the isotherm hysteresis for silica gel type B size 5mm temperature of water vapour in the adsorbent sample chamber is at a constant 25°C.

4.3.3 Physical Properties

The adsorption performance of silica gel is influenced by the physical properties such as surface area, pore size, pore volume and pore distribution, porosity, and density as shown in Table.4.1.

Table.4.1 Thermophysical Properties

	Type B
Specific surface area (m^2/g)	450
Porous volume (mL/g)	0.85
Average pore diameter (A)	22
Apparent density (kg/m^3)	730
pH value	5.0
Water content (wt.%)	<2.0
Specific heat capacity (kJ/kg K)	0.921
Thermal conductivity (W/m K)	0.174
Mesh size	10–40

To help identify the desorption of different species, derivative curves were also produced. The results obtained from a sample of silica gel taken directly from the DVS instrument are shown in figures.4.5 and 4.6.

4.4 CFD model

In this study a CFD model was developed to simulate the adsorption dynamics of water vapour of silica gel granules in an adsorption tube by using the Solidworks® Flow Simulation module. The model consisted of two modes of operation, the water vapour adsorption and the desorption mode.

In each mode, the water vapour flow profile surrounding a single silica gel granule was determined by solving the Navier-Stokes equations and the resulting velocity profile was regarded time-invariant and stored for later use. Also, the time dependent mass transfer both outside and inside the porous silica gel due to its adsorpitivity was simulated through a user defined function developed to solve the Brunauer, Emmett and Teller (BET) equation [85] for both adsorption and desorption processes. The developed Simulation model was used to determine the adsorption capacity of two different sizes of silica gel granules namely; 3.5mm

and 5mm as a function of time at different operating temperatures. The simulation results were compared with experimental data and found to agree.

4.4.1 Geometry and Analysis

Geometrical modelling was one of the most critical stages in the CFD simulation; correct definition of the geometry provides a more practical state for the simulation, and the technique used for constructing the geometry will ensure the feasibility of generating a mesh good enough to capture all of the phenomena involved in the problem.

4.4.2 Thermal Variables

The boundary conditions determine the flow and thermal variables on the boundaries of the physical model. There are a number of classifications of boundary conditions:

1. Flow inlet and exit boundaries: pressure inlet, velocity inlet, pressure outlet.
2. Wall, repeating, and limit boundaries: wall, symmetry.
3. Internal fluid, solid
4. Internal face boundaries: porous, wall, interior

In the model velocity was applied at the flow inlet of the adsorption bed. This boundary condition defines a flow velocity at the inlet of the bed. The flow exit boundary is defined as a pressure outlet; the outlet pressure is defined as atmospheric pressure. The bed and packing interior are defined as boundaries. The wall boundaries separate the fluid zone, vapour, in between the silica gel particles from the wall zones [68-86]. With the determination of the boundary conditions the physical model was defined and a numerical solution provided. It was then necessary to determine how the solution will be established. This was done by setting the iteration parameters. With all boundary conditions defined, a number of additional parameters and solving schemes where selected. An initial condition was assigned to the model and was used to help speed the convergence of the computation. The computation is an

iterative process that solves the governing equations for flow and energy in each simulated cell.

4.4.3 Modelling of Vapour Flow in a Single Silica Gel Particle

The diffusion equation in the silica gel particle is as a first introduction to CFD. A simple model was created; the model represented one silica granule in a tube as shown in (Figure.4.7) the flow inlet and flow outlet.

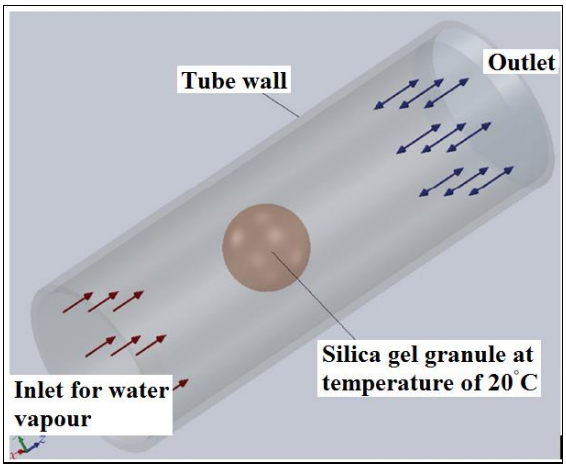

Figure 4.7 One silica gel in a tube geometry used for validation of CFD against experimental work.

4.4.4 Porous Media Simulations

A porous material had to be defined for the adsorbent used in the simulation. This data was taken from the experiment Type B size 3.5mm data was created with a density of 730 kg/m^3, and for type B size 5mm a density of 730 kg/m^3 and a heat capacity of 0.921 J/kg K and a thermal conductivity of 0.174 W/ m K (See Table.4 .1).

4.4.5 CFD Porous Medium Methodology

For the porous medium approach the CFD model has a mass of cells representing the fluid inlet. This is followed by the porous medium cells, which are used to model fluid flow through porous medium. Full flow field predictions are possible with the porous medium approach because the resistance of the porous medium to flow is described by the expression:

$$\frac{\Delta P}{L} = -\alpha U_s^2 - \beta U_s, \qquad (1)$$

Where the permeability coefficient values $\boldsymbol{\alpha}$ and $\boldsymbol{\beta}$ are assigned temperature dependent values that describe the behaviour of a porous medium. High values of $\boldsymbol{\alpha}$ and $\boldsymbol{\beta}$ preclude flow at right angles to the porous medium. Upstream and downstream of the water vapour flow field is solved using the usual Reynolds averaged Navier-Stokes methodology.

Table.4.2 **Thermophysical Properties Used in CFD simulation**

Material	**Water**
Density, ρ (kg/m3)	**1000**
Specific heat capacity, C_p (J/kg K)	**4200**
Thermal conductivity, k (W/mK)	**0.61**
Dynamic viscosity, μ (kg/ms) x 10^{-3}	0.96172

4.4.6 Model Mesh

One of the most important parts of this CFD simulation was the module mesh creation. The mesh which establishes the accuracy of the simulation has to be chosen with enough detail to describe the simulation processes accurately and with a degree of coarseness that enables solution within an acceptable amount of time. When an optimal density has been found refining this will increase the model size without displaying more flow detail. When it is coarsened the mesh will obscure, possibly essential part of the flow detail. The mesh determines a large part of creating an acceptable simulation.

4.4.7 The CFD Mesh Density

For this study we focused mainly on maintaining a 3D simulation that described the physical model accurately and was able to handle the flow specifics of the silica gel geometry. The mesh densities were varied to establish the optimal mesh density, describing the flow characteristics and limiting the calculation times. The initial mesh was specified in the following stages:

Specifying an initial mesh, so all the following specifications consist in changing the default values of its parameters.

1. Specifying a basic mesh consisting of nearly uniform cells.
2. Refinement of the basic mesh to capture the relatively small silica gel porous features, to resolve the small porous features in contact with fluid.
3. Refinement of the basic mesh to resolve the solid/fluid interface (as well as porous/ solid, fluid/ porous interfaces.
4. Specifying other initial meshes in local regions (solid and/or fluid) to better resolve the model specific geometry and/or flow (and/or heat transfer in solids) peculiarities in these regions.

4.4.8 Simulation Data

When the simulation has converged the last data set is stored as a final solution. This data set has a record of the status of all elements in the model, temperature, densities, pressures, flow aspects etc. To be able to interpret the data it needs to be ordered and reduced to comprehensible sizes. [82] This displaying of the data is called post-processing and makes it possible to compare the different simulations with each other and with external data. There were as many ways of displaying the data as there were data points so it was important to select the data representation that was required for the desired data comparison. Some of the

standard options available are contour plots and velocity vector plots. Contour plots will give a plot in the defined data point collection; this can be a plane or a volume, of contours of another variable.

For example a plane can be defined as a constant x coordinate plane (y-z plane) we can then make a contour plot showing temperature contours in this plane. In the same plane a velocity contour plot can be made showing absolute velocities of the fluid in the defined plane. Other variables that can be used for contour plots are magnitude of velocity components, turbulence components, pressure etc. Velocity vector plots can be made to get an insight into the flow patterns in the overall geometry or detailed at specific locations [85,89-90].

4.4.9 Fluid Flow Fundamentals

For iteration, CFD solvers use generalized fluid flow and energy balances based on the Navier Stokes equations. The balances are generalized so the user can influence which elements are added in the balance and which are not. The number of balances to be solved is also user defined; it can be advantage not solve all balances initially. The generalized balances that are used by the Flow simulation commercial CFD package are the Navier Stokes equations for conservation of mass, momentum and energy in the flow geometry of concern, together with additional sets of equations reflecting the problem needed to be solved [82,83,90].

4.5. CFD Results and Discussion

Figure 4.8 shows the adsorption curves for water adsorption on one granular size of silica gel there curves were compared to Fuji data for smaller silica gel granules.

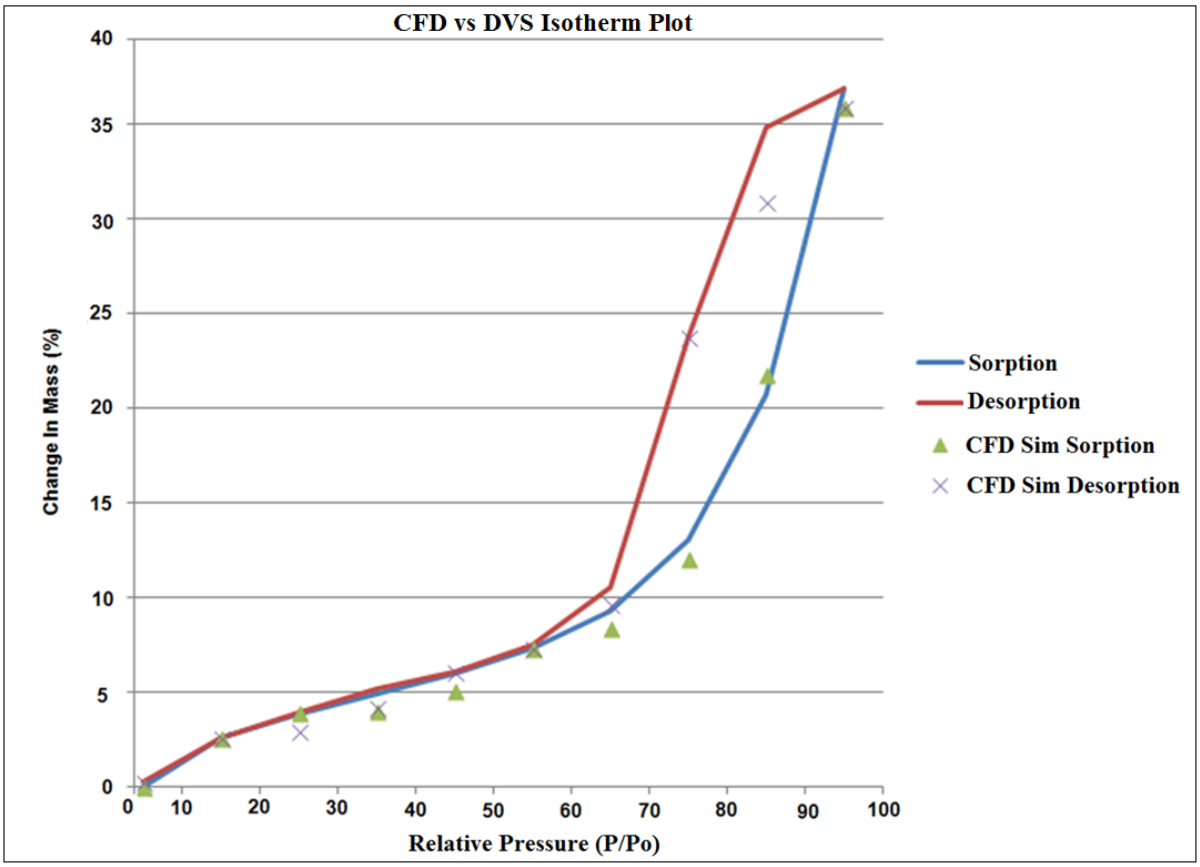

Figure 4.8 Adsorption and desorption curves for silica gel granules size 3.5mm.

Figure.4.8 is a adsorption isotherm plot comparison between CFD simulation and the experimental results on silica gel size 3.5mm.

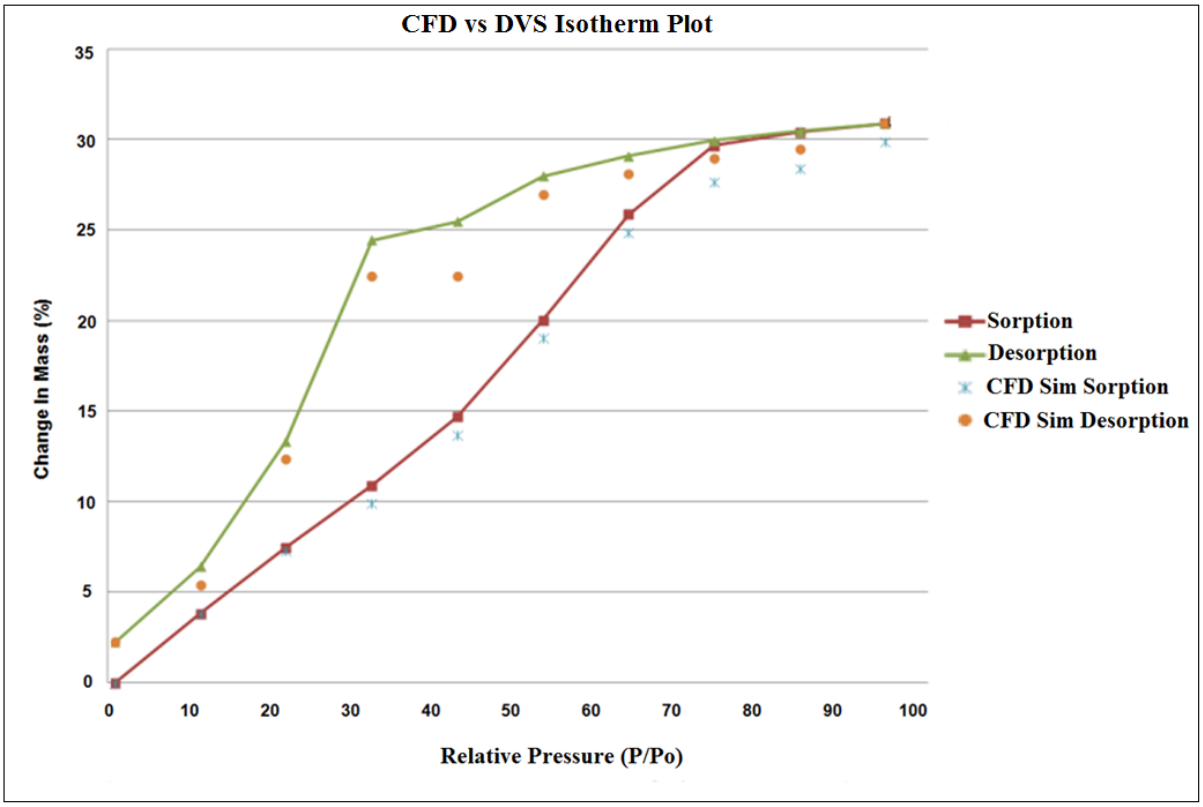

Figure.4.9: Adsorption and desorption curves for silica gel granules size 5mm.

Figure.4.9 is a adsorption isotherm plot comparison between CFD simulation and the experimental results on silica gel size 5mm.

4.5.1 Water Vapour Adsorption CFD Simulation

The CFD simulation determines the distribution of water vapour molecules in the flow vapour phase and the adsorption of adsorbed vapour molecules on the silica gel surfaces. (Fig.4.10) shows a silica gel porous media with a typical adsorption of water vapour molecules. This simulation was develop through a user defined function developed to solve the Brunauer, Emmett and Teller (BET) equation for both adsorption and desorption processes. The developed model was used to determine the adsorption capacity of two different sizes of silica gel granules namely; 3.5mm and 5mm as a function of time at different operating temperatures.

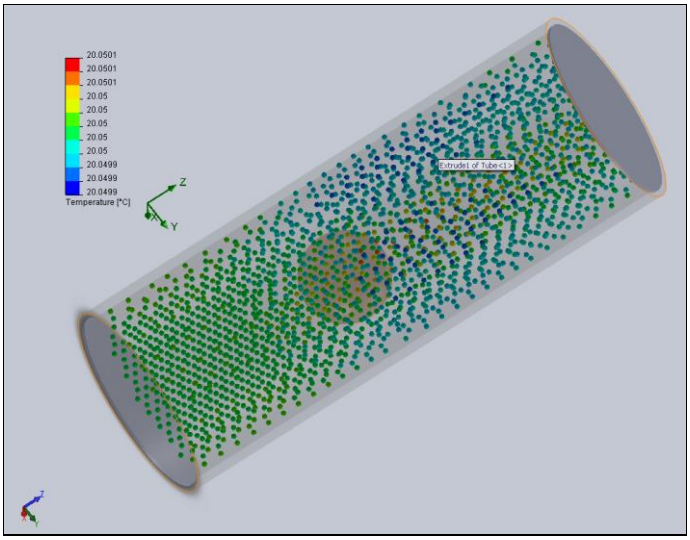

Figure 4.10 Simulation of water vapour adsorption on porous silica gel.

Figure 4.10 shows the water vapour being adsorbed on to the single silica gel particle. The porous media capabilities of CFD model determine the distribution of water vapour molecules in the flow vapour phase and the adsorption of adsorbed vapour molecules on the silica gel surfaces.

4.5.2 CFD Simulation of Desorption of Water Vapour from Silica Gel

When attempting to simulate the desorption of water vapour from silica gel it was necessary to create a user defined function (UDF). The major challenge in the use of CFD simulation of the desorption of water vapour from silica gel is the complex interconnected void space silica gel has. In traditional 2D mathematical approaches the engineers use to largely ignoring this fact. In CFD simulation this is not ignored, it is modelled into the 3D model of the porous media. In order to simulate desorption we had to create a function called desorption that would take several inputs (material, fluid, pressure, flow rate, and whatever factors affect the silica gel Calculations see figure.4.12 this is a simulation of the water vapor desorption).

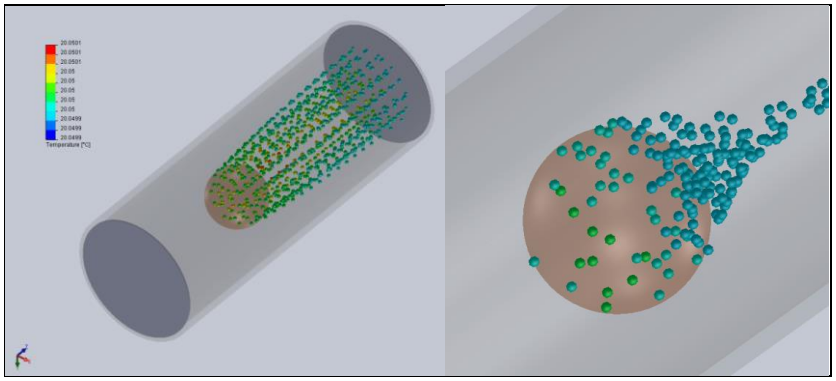

Figure 4.11 Simulation of water vapour desorption on porous silica gel.

4.5.3 Velocity Profiles

To study the velocity distribution in an adsorption silica gel packed bed section cuts were made along the packed bed to generate velocity vector plots. Velocity profiles were also observed in the *near-wall* region of the modelled arrangements. As expected, in all of the cases analysed, flow channelling took place near the wall and inside the bed, due to the presence of constrained flow areas. Strong radial flow from the middle to the wall was also noticeable. Due to the channelling of the flow (strong axial flow and reduced radial flow) at the wall, the local radial heat transfer rate decreases.

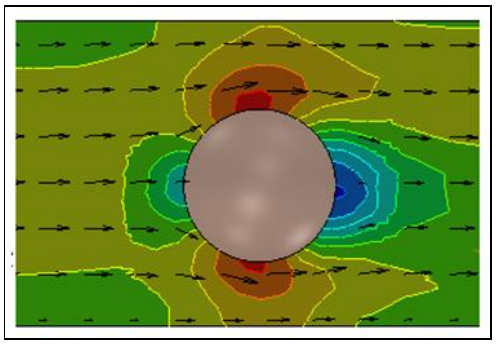

Figure 4.12 Velocity vectors profile vector plot of the water vapour velocity field around a single silica gel.

The inlet velocity is 0.5 m/s and the velocity field plotted in the plane passing through the centre of the particle see figure. 4.12.

4.6. Conclusions

A CFD model was developed for simulating the adsorption of water vapour on silica gel granules and used to study the effect of granule sizes indicating that reducing the granule size increases the adsorption. The thermo gravimetric (DVS) results were used to make the CFD module and compare our measurements with the CFD simulation. A good comparison was found with CFD and experimental data. In conclusion to this study it is thought by using CFD could provide useful information for the design of adsorption cooling systems and to better predict the system performance.

CHAPTER 5

A CFD SIMULATION ON HOW THE DIFFERENT SIZES OF SILICA GEL USED IN AN ADSORBENT BED WILL AFFECT THE ADSORPTION PERFORMANCE OF SILICA GEL

Abstract

The last chapter has provided analyses of a (DVS) method used for measuring adsorption uptake of a single adsorbent. A CFD simulation was also carried out to compare the results. This chapter investigates the effect of silica gel granular size on the water adsorption rate using computational fluid dynamics.

5.1 INTRODUCTION

The adsorption properties of silica gel have been studied for many years as silica gel is used in many industries including adsorption cooling systems. Past research has shown experimentally that the adsorption of silica gel granules depends on their size. The purpose of this work was to study the effect of granule size on the adsorption properties of silica gel by using CFD and comparing the simulation results to those obtained experimentally. To design an efficient adsorbent bed, flow and temperature, adsorption information is essential. Studies of fluid dynamics and heat transfer in adsorbent beds date back to the early twentieth century [82, 83]. The early investigation of flow in porous media packed beds provided mainly such bulk information as pressure drop correlations [82, 83- 85]. Predict the pressure loss for flow in adsorbent beds. [85, 89-90]. Computational fluid dynamics (CFD) provides an innovative approach to model and analyse the local flow and the effect of silica gel size on adsorption performance of a packed bed. CFD simulation of porous media local flow and heat transfer based on CFD technique has increasingly been reported in recent years in fields of packed bed flow and heat transfer modelling [90,]. CFD simulation was based on fundamental

principles of diffusion and adsorption/desorption of porous materials. In this study an integrated CFD model was developed to model and simulate the adsorption dynamics of water vapour in three different sizes of silica gel in a fixed bed adsorption column.

The developed integrated model was used to determine the adsorption capacity of the three silica gel size type over a function of time, based on different operating conditions. The simulated results were compared with past research papers experimental data and found to give a good agreement. The effect of various influencing parameters such as velocity and silica gel porosity were studied to investigate their influences on the adsorption capacity.

5.2 Methods

5.2.1 3D Geometry of silica gel packing

Geometric models of the silica gel adsorbent bed systems are generated for a tube of 25mm length of 100 mm diameter.

The size of silica gel that is used in this CFD simulation is:

Silica gel granular size 1 mm

Silica gel granular size 2 mm

Silica gel granular size 3 mm

Adsorbent particle size affects how the water vapour flows through the adsorbent bed. Smaller particles (higher mesh values) larger particles (lower mesh values).

First we selected the silica gel to particle sizes the silica gel were selected in the ranges of 40–60 mesh, 60–100 mesh, and 100–200 mesh.

5.2.2 Modelling Approaches for Silica Gel Adsorbent Beds

In this study an integrated CFD model was developed to simulate the adsorption dynamics of water vapour of silica gel granules in a fixed bed adsorption column using the SolidWorks Flow Simulation module. The model consists of two modes of operation, the water vapour adsorption and the desorption mode. In each mode, the water vapour flow profile surrounding the granules was determined by solving the Navier- Stokes equations and the resulting velocity profile was regarded time-invariant and stored for later use. Also, the time dependent mass transfer both outside and inside the porous silica gel due to its adsorption was simulated through a user defined function developed to solve the Brunauer, Emmett and Teller (BET) equation [70] for both adsorption and desorption processes. The developed model was used to determine the adsorption capacity of three different sizes of silica gel granules namely; 1mm, 2mm and 3mm as a function of time at different operating temperatures.

The simulation results were compared with past experimental data and found to give a good agreement about 3%.

5.2.3 Modelling of Vapour Flow in Silica Gel Particle

The porous media capabilities of Flow Simulation are used to simulate porous media silica gel which allows you to model the volume that the silica gel occupies as a distributed resistance instead of discretely modelling all of the individual passages within the silica gel, which would be impractical or even impossible. We consider the influence of the porous medium permeability type (isotropic and unidirectional media of the same resistance to flow) on the water vapour mass flow rate distribution over the silica gel. We will observe the latter through the behaviour of the water vapour flow trajectories distributed uniformly over the model's inlet and passing through the porous silica gel.

Additionally, by cooling the flow trajectories by the flow velocity the vapour residence time in the porous media can be estimated, which is also important from the silica gel adsorption of water vapour effectiveness viewpoint. As a first introduction to CFD a simple model was created. The model represented one silica granule in a tube as shown in (Figure.5.1) the flow inlet and flow outlet [94].

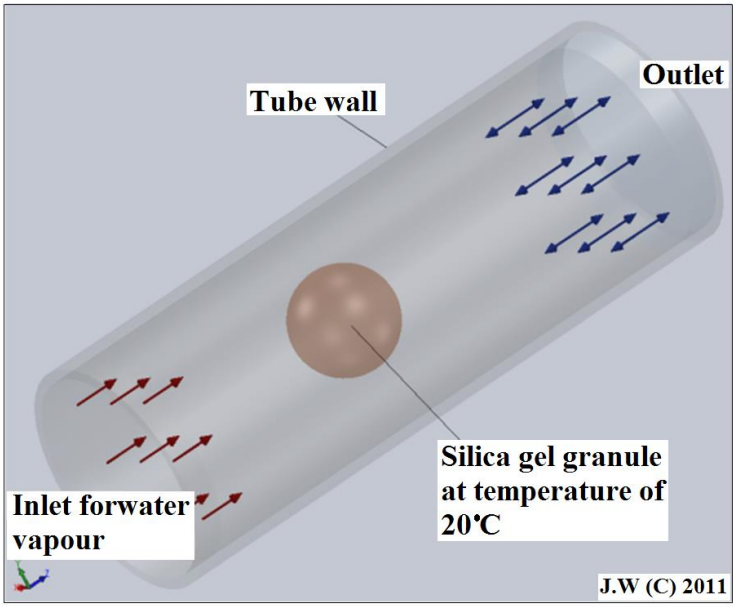

Figure.5.1. One silica gel in a tube geometry used for validation of CFD against theoretical models.

The silica gel granule in the tube was designed with the dimensions of 1mm, 2mm and 3mm this was then used in the validation model. With this model it was tried to fit CFD data to generally accepted experimental data. This one granule was then cloned to 40 granules 60 and 120. These cloned granules were then simulated in a tube bed (see figure.5.2).

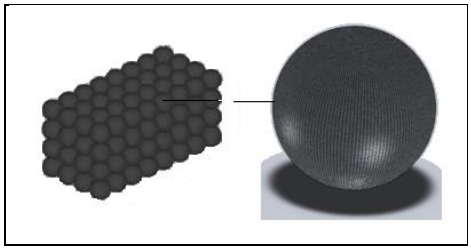

Figure 5.2 This one granule was then cloned to 36 granules 65 and 114 granules.

This limitation of granules was necessary to keep the model reasonable in size with a mesh density comparable to the validation model. A series of runs was conducted at a number of flow velocities see Table 5.3. In all these runs the centrally located granules had a defined temperature of 20°C. The tube wall temperature was set at 20.5°C to create a 0.5°C temperature difference between the granule and the fluid at infinite distance. The water vapour that flowed through the tube was defined at 20°C at the entrance. The temperature of the granules was simulated and recorded.

A constant diffusion coefficient D_e was assumed according to the reference of Sakoda et al. [13]. The spherical silica gel particle with initial conditions of water content m(r) = 0 and a temperature T_{in} is instantaneously exposed to vapour flow. The diffusion equation in the silica gel particle is

$$\frac{\partial m_r}{\partial t} = \frac{1}{r^2}\frac{\partial}{\partial r}\left(D_e\, r^2\, \frac{\partial m_r}{\partial r}\right) \qquad (5.1)$$

The initial condition and boundary conditions for equation (5.1) are

$$m_r(r; t = 0) = 0$$

$$\frac{\partial m_r}{\partial r} \backslash r = 0$$

$$\mathrm{m_r}\left(r = d_p/2, t\right) = m_s\,(T, x, P) \qquad (5.2)$$

The m_r is local water content of a silica gel particle in the radial direction and the m_e is the equilibrium water content on the particle surface. The water content averaged in a silica gel particle is given by

$$m = \frac{24}{d_p^3}\int_0^{\frac{d_p}{2}}(1 - e_p) r^2 m_r dr \qquad (5.3)$$

Where the porosity in a silica gel particle was fixed at e_p = 0.38 for 1mm silica gel, 0.38 for 2mm silica gel and 0.34 for the 3mm silica gel.

5.3 CFD Governing Equations

The transport phenomena can be divided into adsorption and water vapour flow in the adsorber bed, silica gel granules surfaces Navier-Stokes equations for flow are used to solve the water vapour flow phase:[1,91,94]

$$\frac{\partial \vec{u}}{\partial t} = -\frac{1}{\rho}\nabla p + n\Delta\vec{u}$$

$$\nabla.\vec{u} = 0 \qquad (5.4)$$

The *p* represents pressure, η dynamic viscosity and ρ density of the fluid the flow velocity can be simulated in first. This simulated data is then stored and used for solving the convection-diffusion equation.[1]

$$\frac{\partial c}{\partial t} = -\vec{u}.\ \nabla c + D.\Delta c \qquad (5.5)$$

The *c* represents the water vapour molecule adsorbed into the silica gel, and *D* the diffusion flow coefficient in the silica gel. In contrast to diffusion, an effective diffusivity D_e must be applied [1,91,94]:

$$\frac{\partial c_p}{\partial t} = D_e.\Delta c_p - \frac{1-\varepsilon_e}{\varepsilon_e}\frac{\partial q}{\partial t}$$

$$D_e = \frac{\varepsilon_i D}{\theta} \qquad (5.6)$$

The c_p represents the water vapour molecule adsorbed within the silica gel particle. The mass transfer resistance between the silica gel surface is also modelled.[1]

$$\vec{n}.\ (-D\nabla c + \vec{c_u}) = k_f\ (c - c_p)$$

$$-\vec{n}.\ (-D\nabla c + \vec{c_u}) = k_f\ (c_p - c) \qquad (5.7)$$

The $\vec{n}$ represents the normal vector of the outer silica surface. The driving force of transport over the particle boundary is relative to the adsorption difference, and k_f is the corresponding mass transfer coefficient. The adsorbent beds in the CFD simulation are simulated with far less

silica gel granules than in a real adsorbent bed. In order to simulate similar systems, the effective diffusivity D_e is increased. The adsorption of the water vapour molecules at the silica surfaces is described by a classical Langmuir-type kinetic:[1,91-93].

$$\frac{\partial q}{\partial t} = k_a\,.c.(q_{max} - q) - k_d.q \qquad (5.8)$$

The k_a and k_d represents adsorption and desorption rates, q_{max} maximum capacity, and q the current occupation of binding sites at the surface.

5.3.1 Desorption of Vapour in Porous Materials

When considering desorption in a porous material one must considers vapour transport the Lattice Boltzmann equation can be expressed as:

$$\frac{\partial s}{\partial t} = r\left(k_p c^p - s^q\right) \qquad \textbf{(5.9)}$$

This can be done with Lattice Boltzmann multi physics extension by applying a local rule describing the change of the adsorption rate $\partial s/\partial t$ on the water vapour concentration C and the adsorbed mass S deposited per unit volume of the porous media matrix.

With parameters $k_p > 0$ and exponents p, q fulfilling $p/q \leq 1.$ At equilibrium, i.e. for $\partial s/\partial t = 0,$ this model reduces to a Freundlich isotherm:[91,93-94].

$$s = kc^n$$

$$with\ k = k_{p^{1/q}\ and\ n= P/q.} \quad (5.10)$$

5.4. CFD Modelling Method

In all types of CFD modelling there are some factors that determine the difficulty of modelling granules packed adsorption beds. In a silica gel packed bed the amount of packing and the narrow region between them makes its modelling more complicated. One way of solving this problem is to model a single granule of silica gel in CAD software. This single granule can then be clone into thousands of granule then pack into a 3D adsorption bed (see figure.5.3). The clone pack silica gel can then be inserted as a parasolid CAD file then one could applied a porous media material using a CFD software called flow simulation. Then this porous media could be solved by using a finite control-volume method.

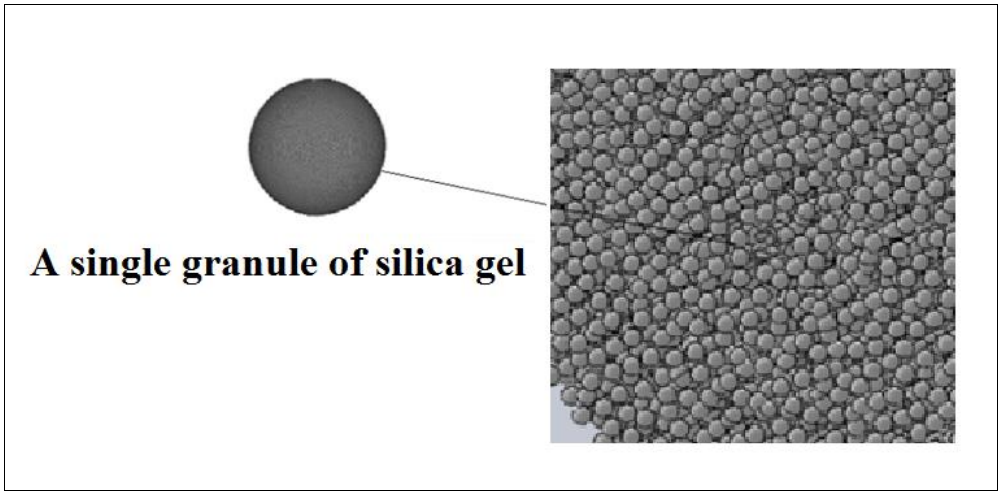

Figure.5.3 Thousands of granule pack the silica gel into a 3D adsorption bed.

5.4.1 Smaller Arrangements of Silica Gel Granules

The amount of silica gel granules in a real adsorbent bed cannot be reproduced in a three dimensional model using CFD-tools. However to simplify the numerical calculations you can

simulate smaller arrangements of silica gel granules. In this study there are three silica gel sizes in the adsorbent beds these beds contain 36, 65 and 114 particles, respectively (see figure.5.4).

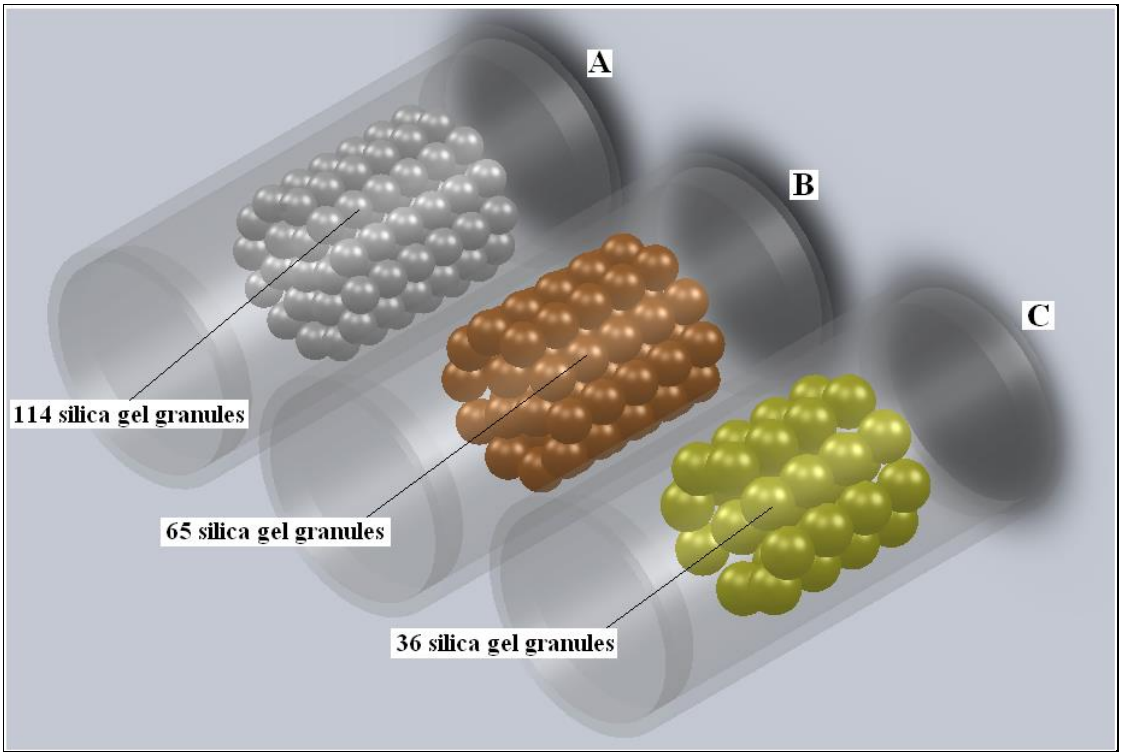

Figure.5.4. The three adsorption bed tube containing the numerically created example packing with (a) 114 granules, (b) 65, granules (c) 36 granules.

Different porosities were obtained by changing the particle sizes and arrangements. Constant thermo physical properties at 20ºC were assumed for the water vapour. Periodic boundary conditions were imposed on the boundaries of the computational domain. The inflow into the domain was set as a velocity inlet with the outflow set as the pressure outlet boundary condition. The dimensions and porosities of the porous media used in the simulation were based on the experimental research, are listed in Table.5.1. The constant contact areas between the particles were calculated based on the desired porosity.

Table.5. 1 Geometry and mesh parameters

Test section	Porous media sizes (mm)	Porosity ε	Total number of elements
No. 1	1 mm	0.38	1065623
No. 2	2 mm	0.38	1122425
No. 3	3 mm	0.34	1097191

5.4.2. Computational Mesh Domain

In this work the mesh creation was done using flow simulation, a general-purpose program providing a variety of automatic meshing strategies. All the simulation in this exercise were conducted first with automatic meshing and then secondly modified manually to help determine the influence of mesh density on the outcome of the simulation.

5.4.3 A Porous Sample with Non-uniform Porosity

The mesh domain was split into 1065623 cells containing 1122425 faces and 1097191 nodes. The grid was then partitioned along the principal axis into 3 segments to allow the domain to reduce simulation time on computer, see figure.5.5

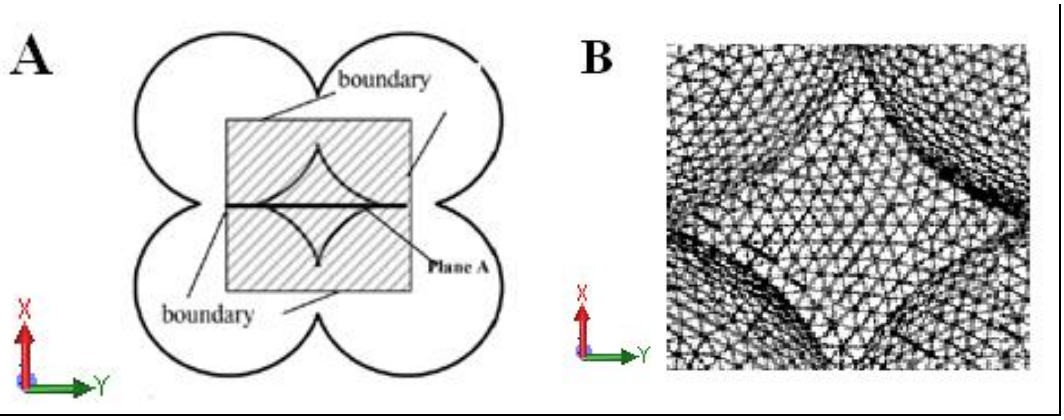

Figure 5.5. Schematic diagram of the computational domain [81].

5.4.4 3D Silica Gel Granules Packing Arrangements

When simulating the adsorption of water vapour on porous silica gel the volume of silica gel packing and pore spacing will depend upon the size of silica gel. But in some sense the relationship between size and pore spacing can be more complex because of the influence of packing arrangements.

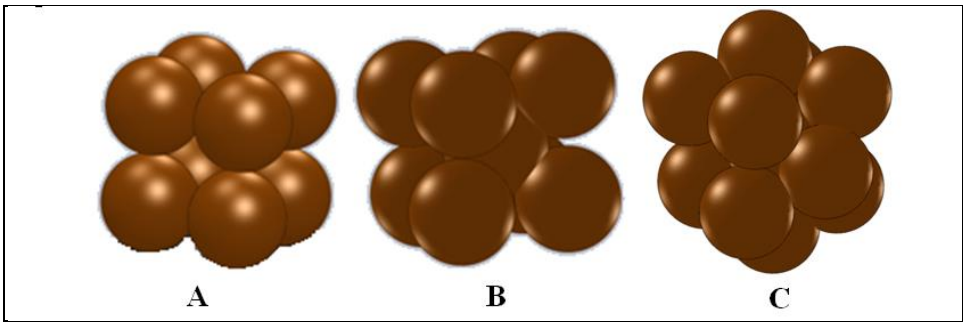

Figure 5.6 Arrangements of the silica gel particles for CFD simulation [81].

For example, the packing of spherical porous media of 1mm uniform size in (Figure.5.6 arrangement A) when a simulation was completed on this type of packing arrangement the porosity was 0.45. But when the simulation was simulated in (Figure.5.6 arrangement B) the porosity was 0.26 and when a simulation was completed in the (Figure.5.6 arrangement C) it was 0.38 this arrangement was a more realistic packing arrangement this was a random arrangement. In a real world scenario adsorption bed would have randomly packing of silica gel and not uniform arrangement. So it was determined that this was the packing arrangement to be used in all CFD simulation.

5.4.5 CFD Mesh Generation

For all types of geometries the creation of the mesh has different obstacles. In the meshing of silica gel packed bed geometry the major issue is resolving the areas where two solid surfaces touch the contact points. Because of this fact the silica gel radii were reduced by about 2 % in order to avoid mesh failures in the area of the silica gel contact points (see figure.5.7).

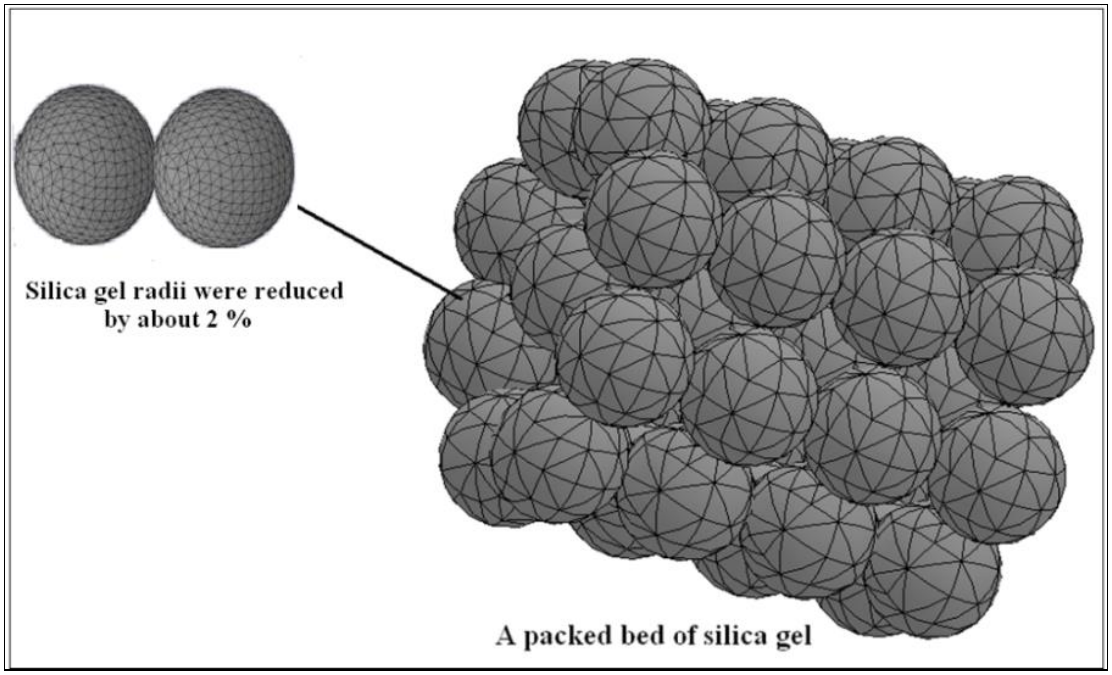

Figure.5.7 3D Dimensional display and detail of the control volumes in the fluid region near particle-to particle contact points.

5.4.6. Porous Media Simulations

A porous material had to be defined for the adsorbent used in the simulation. Material were found in different sources one of the source was from the experimental data of [93] Akisawa, Saha (2001) and experimental data from [91] Akira Akahira, K.C. Amanul Alam (2005). Type A and Type RD was created with a density of 730 kg/m^3, for type A and a density of 800 kg/m^3, for type RD and a heat capacity of 0.921 J/kgK and a thermal conductivity of 0.174 W/mK (See Table.5.2).

Table.5.2 Thermophysical properties of silica gel

Thermophysical properties of silica gel

	Type A	Type 3A	Type RD
Specific surface area (m^2/g)	650	606	650
Porous volume (ml/g)	0.36	0.45	0.35
Average pore diameter (A)	22	30	21
Apparent density (kg/m^3)	730	770	800
pH value	5.0	3.9	4.0
Water content (wt.%)	<2.0	0.87	–
Specific heat capacity (kJ/kg K)	0.921	0.921	0.921
Thermal conductivity (W/m K)	0.174	0.174	0.198
Mesh size	10–40	60–200	10–20

By studying the table above you can see that Type A silica gel and Type RD have similar physical properties which give them similar adsorption/desorption characteristics at different regeneration temperatures [93].

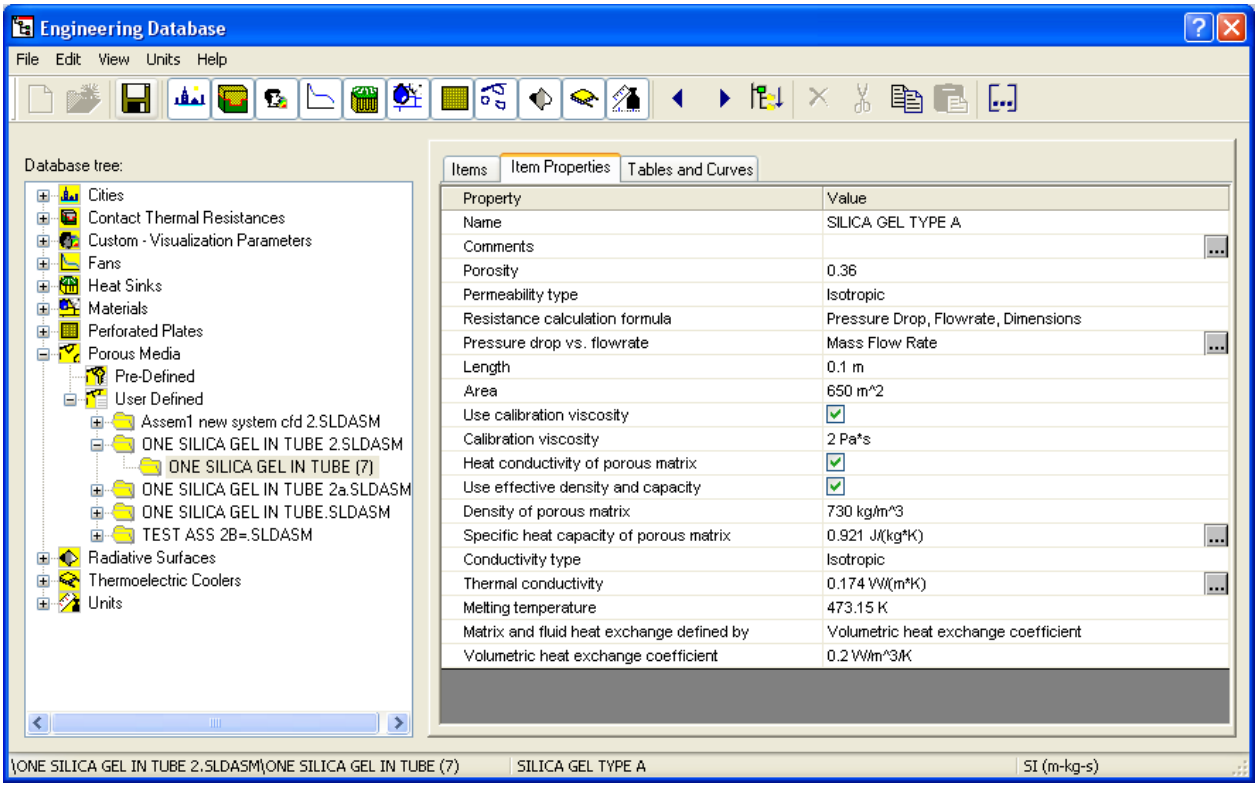

Figure.5.8. CFD Engineering Database

to define a porous medium in this simulation you need to specify the porous medium's properties (porosity, permeability type, etc.) in the Engineering Database and then apply the porous medium to a silica gel in the assembly see figure.5.8.

5.4.7. Porosity of Silica Gel Used in CFD Simulation

Porosity is the effective porosity of the porous medium, defined as the volume fraction of the interconnected pores with respect to the total porous medium volume; here, the porosity is equal to 0.36. The porosity will govern the water vapour flow velocity in the porous medium channels, which, in turn, governs porous medium efficiency. The porosity of the granules is defined as the ratio of the volume of the total pore space filled by the fluid to the total volume of the porous medium, all within the domain of interest. Since mesh cells in the domain have been tagged as solid or fluid, the volume of total pore space can easily be obtained numerically by finding the sum of volumes of the cells tagged as fluid. Similarly, the volume of the solid matrix is the sum of volumes of the cells tagged as solid. Finally, the total medium volume is simply the sum of the volumes of all cells, see also Figure.5.9. Then the porosity is defined by the following equation.

$$\frac{\Delta P}{L} = -\alpha\, U_s^2 - \beta U_s \qquad (5.11)$$

For some materials which have non-constant porosity there are various techniques available to generate numerical porous media with the same non-uniform characteristics.

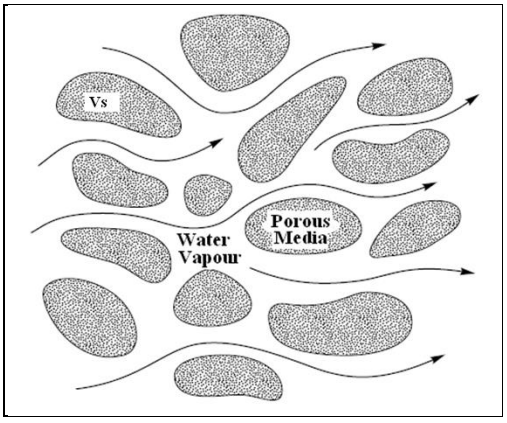

Figure 5.9 Typical domain of a porous medium two phase problem.

5.4.8 Pressure Drop and Mass Transfer

The pressure drop and water vapour flow rate caused by the different size of silica gel perpendicular to the flow direction together with the mass transfer coefficient are very important in determining optimal packing design.

Table 5.3 Shows the pressure drop for different simulated silica gel size and arrangement.

Inlet velocity (m/s)	Pressure drop size 1mm (kPa/cm)	Pressure drop size 2mm (kPa/cm)	Pressure drop size 3mm (kPa/cm)
0.5	0.27	0.32	0.35
1.0	0.92	1.05	1.13
2.0	2.19	2.60	3.02

It can be seen that the pressure drop in the different size of silica gel arrangements in the adsorption tube increased significantly with inlet velocity. The silica gel size 1mm has the lowest pressure drop values are observed. This may be partly due to the fact that the diameter of these silica gel arrangements is smaller than the two silica gel 2mm and 3mm arrangement in the adsorption tubes. The pressure drops for silica gel size 2mm is slightly higher than 3mm silica gel this is also because of the different size effect on flow of vapour figure 5.10.

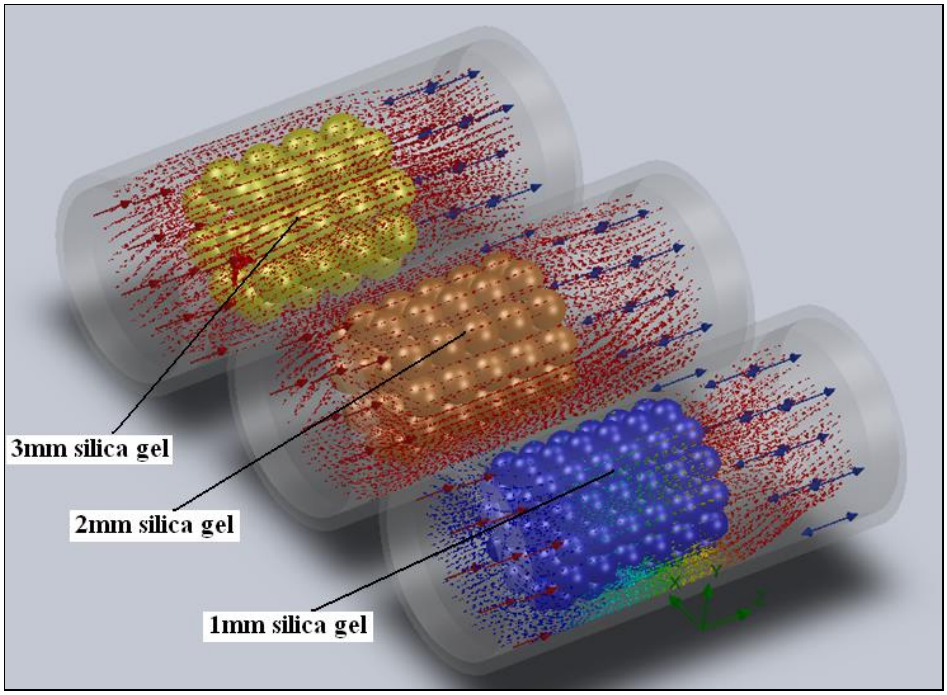

Figure 5.10 Flow profile in an adsorbent test beds.

5.4.9. Conditions Used in Simulation

The boundary conditions determine the flow and thermal variables on the boundaries of the physical model. There are a number of boundary conditions:

- Flow inlet and exit boundaries: pressure inlet, velocity inlet, pressure outlet.
- Wall, repeating, and limit boundaries: wall, symmetry
- Internal fluid, solid
- Internal face boundaries: porous, wall, interior

In our model we use a velocity inlet at the flow inlet of the adsorption bed this boundary condition defines a flow velocity at the inlet of the bed. The flow exit boundary is defined as a pressure outlet; the outlet pressure is defined as atmospheric pressure. The bed and packing interior are defined as boundaries. The wall boundaries separate the fluid zone, vapour, in between the silica gel particles from the wall zones [3, 92, 95-97].

With the determination of the boundary conditions the physical model has been defined and a numerical solution can be provided. It was then necessary to determine how the solution will be established. This was be done by setting the iteration parameters. With all boundary conditions defined, a number of additional parameters and solving schemes where selected. An initial condition was assigned to the model and was used to help speed the convergence of the computation. The computation is an iterative process that solves the governing equations for flow and energy in each simulated cell. Depending on the complexity of the model and the computer resources available, CFD simulation can take anywhere from minutes to days [10]. The results of the simulation can be viewed and manipulated with post-processing software once the simulation has converted to a solution [98-100].

5.4.10. Fluid Flow Fundamentals

For iteration CFD solvers use generalized fluid flow and energy balances based on the Navier- Stokes equations. The balances are generalized so the user can influence which elements are added in the balance and which are not. The number of balances to be solved is also user defined; it can be advantageous to not solve all balances initially. The generalized balances that are used by the Flow simulation commercial CFD package are the Navier-Stokes equations for conservation of mass and momentum, when it is set to calculate laminar flow without heat transfer. Additional equations are solved for heat transfer, species mixing or reaction or κ and ε for turbulent cases [99].

5.5. Results and Discussion

The present CFD simulation attempt to clarify the adsorption characteristics of the adsorption bed packed with spherical silica gel type A under the boundary condition of parameters such as a width of packed bed, the inlet water vapour velocity and granule size of silica gel[89].

5.5.1. Granules Packing Gap Between Walls

To be able to solve for turbulent flow in a CFD simulation it was necessary to introduce a small gap between the wall and the silica gel granules. It was shown from comparisons of flow profiles at several gap sizes that the small gaps used in the final model did not affect the stagnant flow area around the contact points. Rahimi, M. and Mohseni, M (2008) [3].

5.6. CFD Validation against DVS Experimental Results

The CFD simulation model has been used to simulate the water vapour adsorption and desorption onto silica gel porous media, heat transfer and velocity. The results simulated using the CFD model, were compared with the experimental DVS results. Based on the simulation results, the data demonstrated a good agreement with the experimental data. Based on the comparison of the experimental results and CFD simulation several important operating parameters were verified.

5.6.1 Velocity Profiles

In all CFD simulation it was notice that the water vapour flow in the middle of the porous media granules and the wall channel as expected Rahimi, M. and Mohseni, M (2008) [3]. It was also noticed that velocity increased by the inlet and velocity in some constrained areas of the adsorption bed. Stagnation points and secondary flows were also noticed near the contact points Figure.5.11.

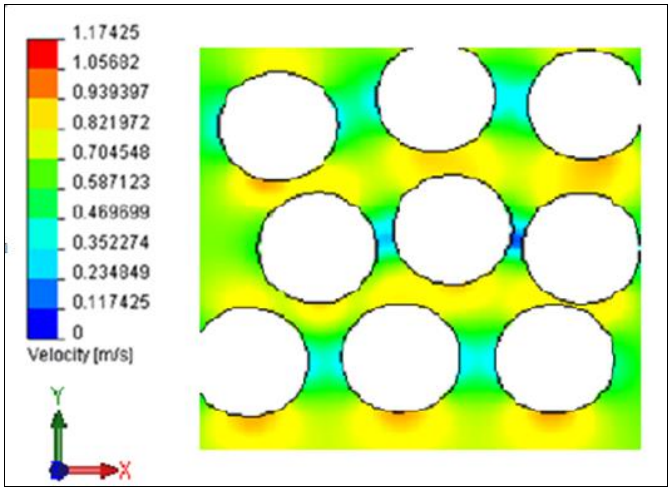

Figure.5.11 Velocity vectors profile in an axial cut model velocity profile expressed in m/s.

It can be noticed that all simulation shows a good correlation with Ergun's equation, turbulence and velocity model. The packing of the Silica gel granules is clearly visible; also note the practical difference between the interior of the bed and the near-wall region where the packing of the spheres is constrained by the presence of the wall [2, 3].

This lowers the porosity in these regions and a significant fraction of the flow is being channelled through this region. One advantage of computational simulation of the flow is the sheer volume of data available for analysis; in particular here, flow velocities at every point in the bed, which are available for statistical analysis.

5.6.2. Effect of Flow Velocity

Flow velocity has a directly proportional effect over heat transfer when forced convection takes place. An increase on flow velocity leads to an increase on kinetic energy. This fact generates a better heat transfer coefficient [1,-3].

The velocity variation within the porous medium depends on the structure of the porous media, as manifested via the pressure drop. The pressure drops occurring across the porous medium is attributed to several factors, including form drag, viscous drag from bounding wall

and inertia force. The obtained results confirm that the pressure drop is a linear function of flow velocity [1,89,91- 100].

5.6.3 The Performance of the Silica Gel

The performance of the silica gel is commonly illustrated and evaluated on the basis of adsorption of the water vapour molecules in the adsorbent bed over time. These simulations reveal the impact of silica gel granule adsorption rates.

$$\bar{c} = \frac{1}{A} \cdot \int_A^{\cdot} c dA \qquad (5.12)$$

Figure 5.12 shows the CFD simulation and experimental results of a 114 silica gel granules size 3mm obtained from the adsorption DVS test rig located in the School of Chemical Engineering at the University of Birmingham.

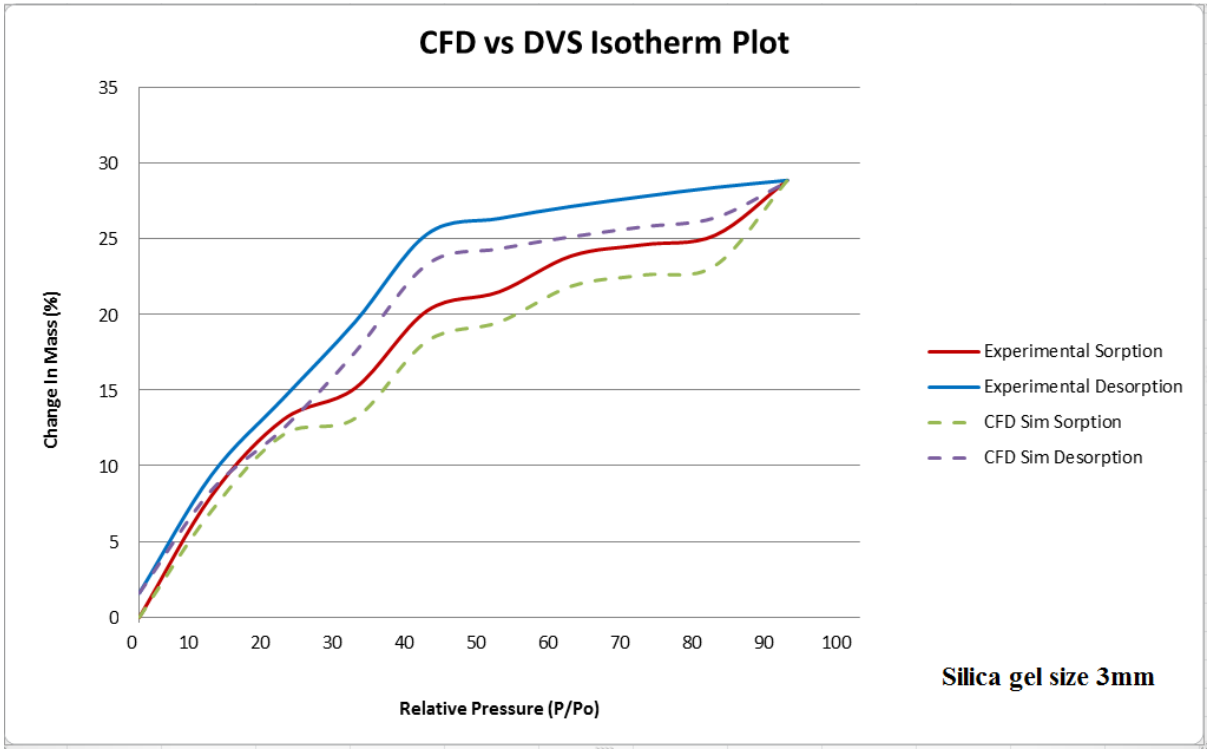

Figure 5.12 Influence of the silica gel size and number on the isotherm plot.

The size of the adsorbent used in an adsorbent bed will have effect on the adsorption and desorption of water vapour. The size of the adsorbent will also have an influence on the vapour pressure in an adsorbent bed. Consequently when designing a adsorbent bed these two important design parameters need to be consider carefully.

5.6.4 Water Vapour Flow profile

The water vapour molecules adsorption accumulation on the silica gel is shown in (figure.5.13). In this study an CFD model was developed to simulate the adsorption dynamics of water vapour of silica gel granules in a fixed bed adsorption column using the Solidworks Flow Simulation module the model consists of two modes of operation, the water vapour adsorption and the desorption mode. In each mode, the vapour flow contour surrounding the porous adsorbent was determined by using the Navier- Stokes equations.

The time dependent mass transfer both outside and inside the porous adsorbent due to its adsorption and desorption rate was program through the user defined function established to solve the Brunauer, Emmett and Teller (BET) equation [1] for both adsorption and desorption of water vapour. The developed model was used to determine the adsorption capacity of two different sizes of silica gel granules namely; 3.5mm and 5mm as a function of time at different operating temperatures.

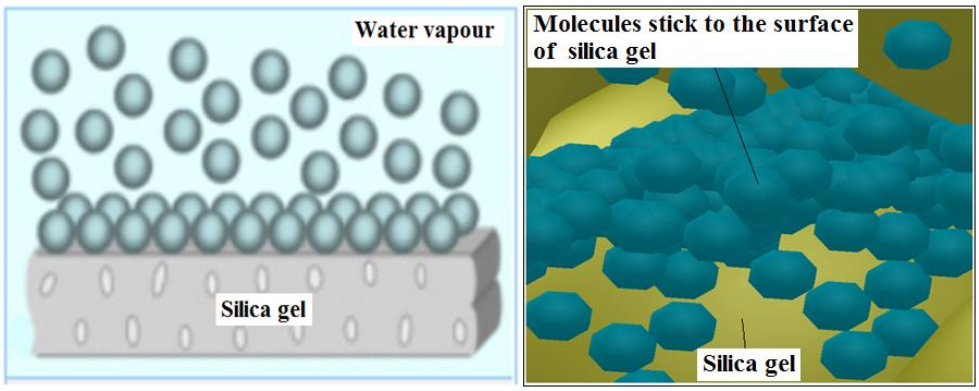

Figure 5.13 The adsorption starting to take place with the formation of multilayer of adsorbate on adsorbent.

In figure.5.13 the water molecules stick to the surface of the silica gel the same as the Brunauer, Emmett and Teller's model of multilayer adsorption method [95,96] in the CFD simulation the water vapour molecules is a randomly distributed on to the porous silica gel material surface.

5.6.5. Water Vapour Adsorption profile

The CFD simulation determines the distribution of water vapour molecules in the flow vapour phase and the adsorption of adsorbed vapour molecules on the silica gel surfaces. **(Figure.14)** shows some views of typical adsorption of water vapour molecules (a), (b) and (c) at different times of the adsorption of the beds t = 129 sec, t = 350 sec and *t* = 700 sec. [1,13, 93].

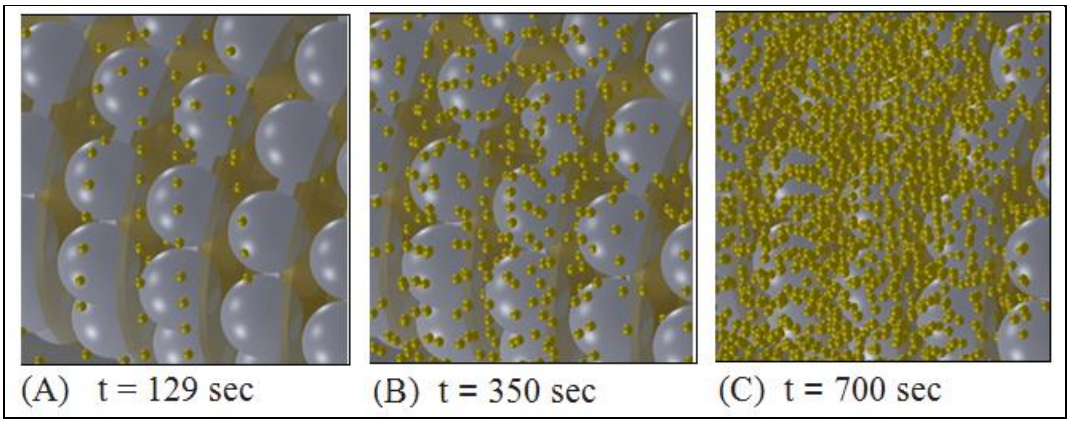

Figure 5.15 Concentration profiles for *c* and *q* at different times in a column filled with 100 silica gel beads.

5.6.6. CFD Simulation Of Desorption of Water Vapour from Silica Gel

As mentioned before when attempting to simulate the desorption of water vapour from a porous adsorbent it was necessary to create a user defined function (UDF) the major challenge in the use of CFD simulation of the desorption of water vapour from silica gel is the complex interconnected void space silica gel has. In traditional 2D simulation methods the engineers use to overlooking this problem. In CFD simulation this is not overlooked it is

model into the 3D model of the porous adsorbent see figure.5.16. In order to simulate desorption we had to create a function called desorption that would take several inputs (material, fluid, pressure, flow rate, and whatever factors affect the silica gel calculations).

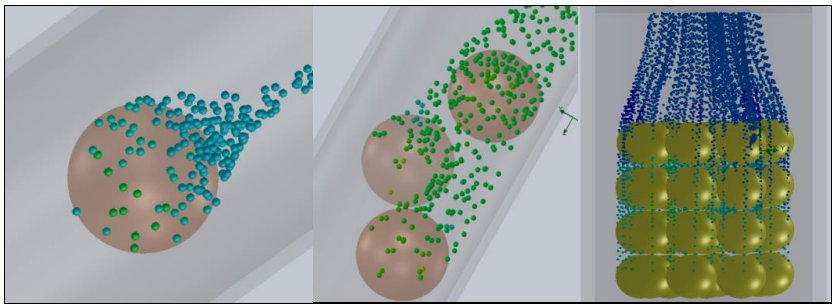

a **b** **c**

Figures 5.16 Desorption of water vapour in porous materials.

In the simulation of the desorption of water vapour for silica gel was simulated on a 3D test with one silica then was tested on a 3 silica gel then ultimately on a 40 silica gel simulation.

5.6.7. The Heat Transfer Performance

The CFD simulation showed that the heat transfer performance of the silica gel adsorption bed is one of the important factors to affect the adsorption efficiency of the bed. The surface temperature of the silica gel was measured in the simulation to get a better understand of the heat transfer performance of the silica gel. The water temperatures of 70 ºC, 80 ºC and 90 ºC were used to heat the silica gel different surface temperatures to help one to understand the heat transfer performance of the adsorbent bed with silica gel. Figure 5.17 shows that the silica gel surface temperature increased steadily in the bigger silica gel sizes as compared to the smaller sizes and its surface temperature was lower than that of the smaller sizes of silica gel. As was expected the heat transfer performance in the smaller sizes was better than that of the bigger silica gel sizes.

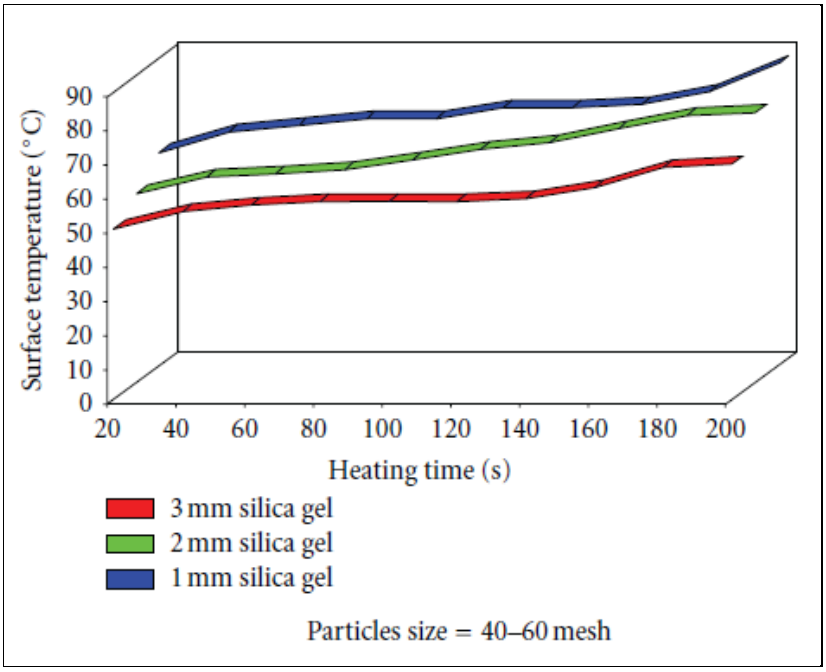

Figure 5.17 The variation of the surface temperature of silica gel size with the heating time.

5.7 Conclusions

A CFD model was developed for simulating the adsorption of water vapour on silica gel granules and used to study the effect of granule sizes indicating that reducing the granule size increases the adsorption. It can be concluded that CFD is a promising tool in evaluating heat transfer behaviour in an adsorption bed. Further CFD studies, with a larger silica gel and porous media, are required in the future simulation to show whether they will produce the same results.

CHAPTER 6

CFD SIMULATION OF TWO DIFFERENT DESIGN CONFIGURATIONS OF HEAT EXCHANGER USED IN ADSORBENT BED AS PART OF AN ADSORPTION COOLING SYSTEM

Abstract

The performance of the adsorption cooling system is assessed in terms of the heat transfer coefficients of adsorbent bed heat exchanger. These parameters in-turn determine the specific cooling capacity (SCC) and the coefficient of the performance (COP) of the adsorption cooling system. It was observed that the overall heat transfer coefficients of the heat exchanger have a direct linear relation with the hot water output temperatures.

6.1. Introduction

An Adsorption cooling system is promising technology since it incorporates environmentally benign refrigerants and the industrial waste heat or low grade solar energy instead of mechanical power. However the low value of performance parameters (COP and SCP), high initial cost and the operating pressure, which is quite low these are the main issues that hold back the widespread application of the adsorption cooling systems. One of the efficient ways to improve the low SCP and COP of this system is the appropriate selection of the design and operating parameters of an adsorbent bed. The heat exchanger used as part of the adsorption system is one of the influential parameter in the heat transfer performance of an adsorption cooling system.

Studies relevant to this research span the last few decades. Chang et.al (2005) [25] experimental study that investigated the heat transfer efficiency of flat tube heat exchanger concluded that the flat tube heat exchanger thinner improves the mass transfer performance

In 2007, Riffel et.al [56] investigated the heat transfer effects of shell and tube heat exchanger for a solar adsorption cooling with an aim to improve the optimum performance of the system. Twenty years prior to this, Beecher and Fagan (1987)[128] designed and tested a heat exchanger for a surface temperature condition and in 1977, Ito et al. [129] applied the constant heat flux condition. They measured the heat transfer coefficient (h) since the fin efficiency (η) could be assumed as 100%.

6.1.1 The Motivation for Heat Transfer Enhancement of the Adsorbent Bed Heat Exchanger

The study of improving heat exchanger heat transfer efficiency has gained serious momentum over recent years due to increased demands by adsorption cooling industry for heat exchange equipment that is less expensive to build, and that operates better than standard heat exchange devices savings in heat exchanger materials. There is demand too, for adsorption cooling design with heat exchangers that are more compact and lightweight.

One way to increase the heat transfer of the heat exchanger and accomplish a lightweight design could be by changing the design configuration to increase the surface area, without increasing the size of the heat exchangers.

There are three basic ways of accomplishing this [101]:

1. Increase the operational heat transfer surface area by using wire type copper finned compact heat exchanger. This change of design configuration and materials could considerably change the heat transfer coefficient see table 6.1 for thermal conductivity of copper [101].

2. Increase heat transfer without significantly changing area. This can be accomplished by using a special channel shape, such as a wavy or corrugated channel,

which would provide mixing due to secondary flows and boundary-layer separation within the channel. Vortex generators also increase heat transfer coefficient without a significant area increase by creating longitudinally spiralling vortices exchange fluid between the wall and core regions of the flow, resulting in increased heat transfer [101].

3. Increase both heat transfer coefficient and surface area of a heat exchanger by. Interrupted fins (i.e., offset strip and louvered fins) act in this way. These surfaces increase the effective surface area, and enhance heat transfer through repeated growth and destruction of the boundary layers [101].

The use of any one of these heat transfer method mentioned could substantially increase the heat transfer fin efficiency and the motivation behind the design of new a adsorbent bed compact copper wire woven heat exchanger.

6.1.2 The heat exchanger fin performance

Heat exchanger fin performance can be explained by two different methods. The first is fin effectiveness this is the ratio of the heat exchanger fin heat transfer to the heat transfer of the tube without fin [101]. The second is the fin efficiency and is defined as the ratio of the heat transferred through the actual fin to that transferred through a perfect fin.

A perfect fin is thought to be one made of a perfect or infinite conductor material. A perfect conductor has an infinite thermal conductivity, so in theory, the entire fin is at the base material heat transfer temperature [54,101].

The equation for this is

$$\epsilon_f = \frac{q_f}{hA_{c,b}\theta_b}, \qquad (6.1)$$

where $A_{c,b}$ is the heat exchanger fin cross-sectional area at the root. Fin performance can also be considered by heat exchanger fin efficiency this is the ratio of the heat exchanger fin heat transfer to the heat transfer of the fin if the entire fin were at the root heat [101].

$$\eta_f \equiv \frac{\text{actual heat transferred by a fin}}{\text{heat that would be transferred if the entire fin were at } T = T_0}$$

The fin efficiency as

$$\eta_f = \frac{q_f}{hA_f\theta_b} \tag{6.2}$$

A_f this equation is equivalent to the surface area of the heat exchanger fin.

The third method of heat exchanger fin performance can be explained as its entire surface efficiency.

$$\eta_o = \frac{q_t}{hA_t\theta_b,} \tag{6.3}$$

where A_t is the overall area and q_t is the sum of the heat transfer of the overall heat exchanger fins[67,101].

6.1.3 Common flat plat fin heat exchanger used in a adsorbent bed

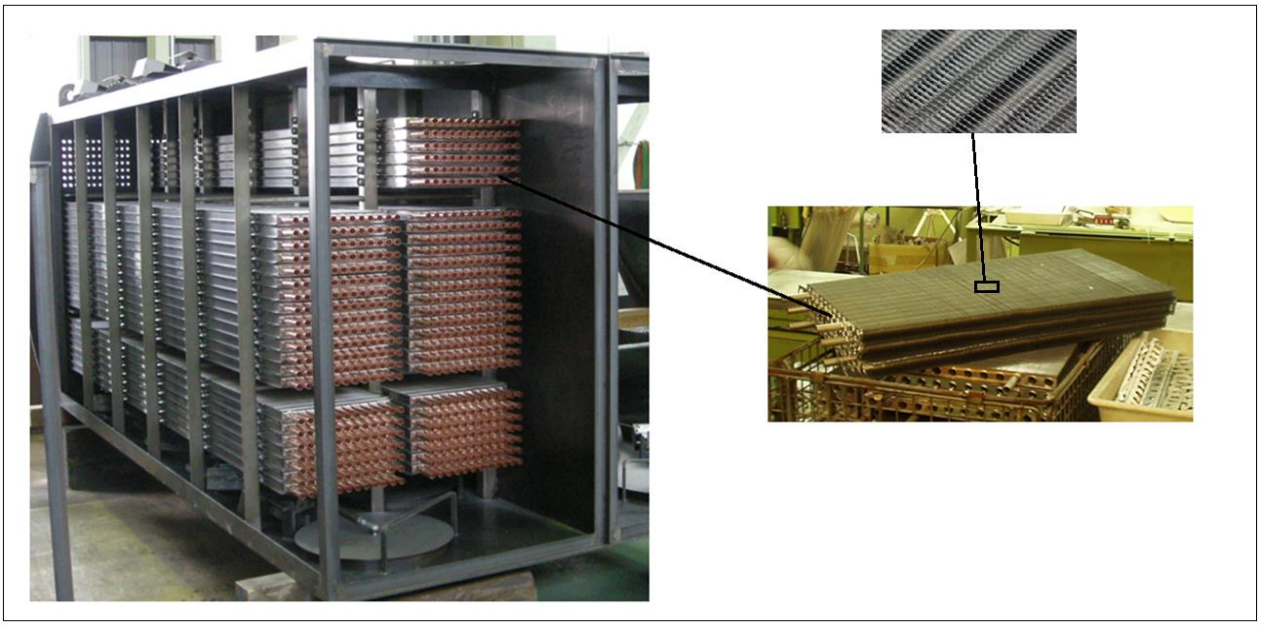

Figure 6.1 Common type of flat fin heat exchanger used in adsorption cooling system.

6.1.4 Different type of heat exchanger fin configuration that could be used in adsorbent beds

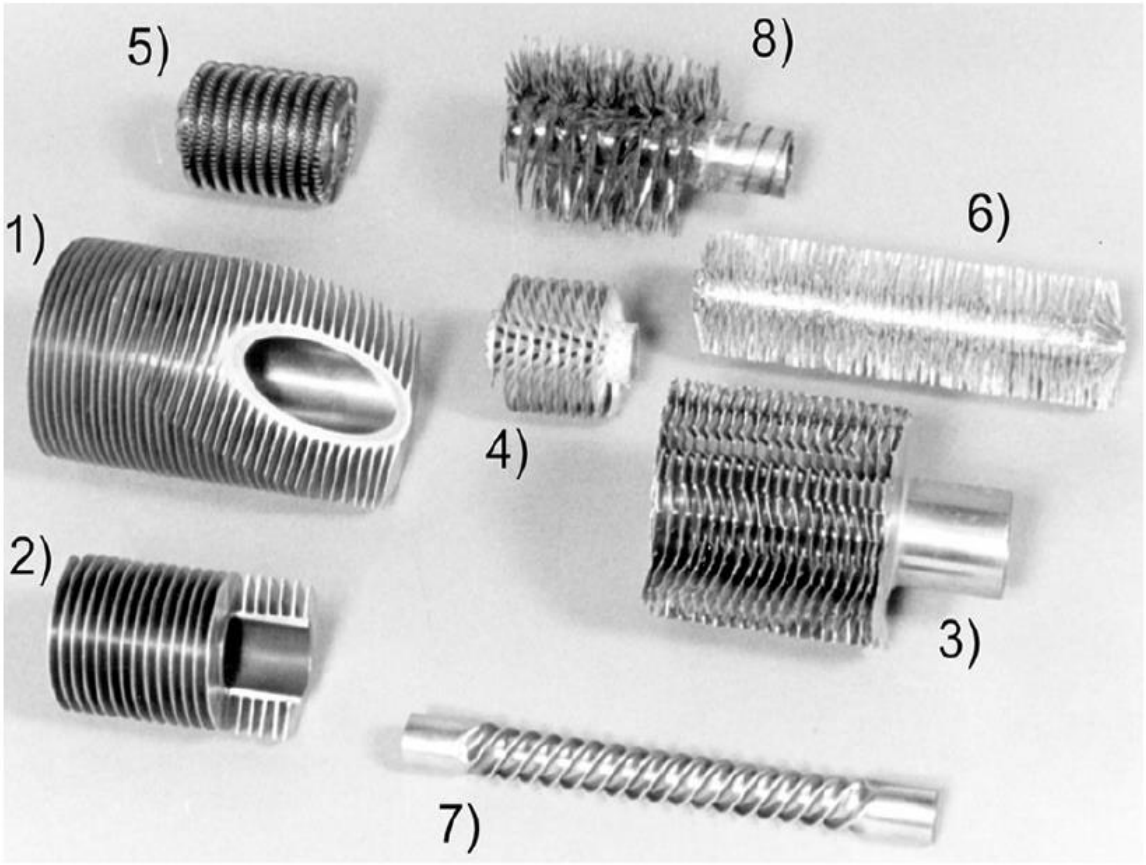

Figure 6.2 Some of the many varieties of finned tubes [101] Lienhard IV, et al., 2005 A Heat Transfer Textbook Third Edition.

figure 6.2 has eight different types of heat exchanger that could be used in an adsorbent bed to improve heat transfer and reduced the size of the heat exchangers (1) and (2) are typical circular fins. (3) and (4) serrated circular fins and dimpled spirally wound circular fins, both are design to improve convection (5) wire wound copper coil fin design to improve convection and increase surface area. (6) bristle fins, (7) spirally wound and (8) machined from base metal are also design to improve convection and increasing surface area.

6.1.5 Comparison of aluminum flat fins heat exchangers to copper wire woven fins heat exchanger

An important design aspect of adsorbent bed heat exchanger technology is deciding what materials are appropriate for the design of adsorbent bed heat exchanger. The common choice is aluminum alloy 1050A or 6063A flat fins. These types of aluminum have one of the highest thermal conductivity values, see table 6.1. Thus is a good material for removing heat from a system to an external environment. In the case of an adsorbent bed, the heat exchanger is packed with porous adsorbent material and so the extended fins are used to increase and decrease the heat transfer rate from the fluid inside the heat exchanger to the surface of the porous adsorbent.

The porous adsorbent affects thermal conductivity of flat fins heat exchange. To overcome this problem, the heat exchanger designers design the heat exchanger fins larger to improve the heat transfer. This is one of the causes for the bulky size adsorption cooling system. One way designers could solve this problem is by changing the material and design configuration of the heat exchanger of the adsorbent bed.

In this chapter a copper wire woven fins heat exchanger is used for the adsorbent bed. Copper has around twice the thermal conductivity of aluminium see table 6.1 for the properties of copper heat exchangers materials [101].

Table 6.1 thermal conductivity

Material	Thermal conductivity (W/m°C)		
	At 25°C	At 125°C	At 225°C
Iron	80	68	60
Low carbon steel	54	51	47
Stainless steel	16	17.5	19
Tungsten	180	160	150
Platinum	70	71	72
Aluminium	250	255	250
Gold	310	312	310
Silver	420	418	415
Copper	401	400	398

[101,105]

Copper wire fins heat exchanger is a small diameter wire fins. It has better rates of heat transfer than aluminum flat plate fins heat exchanger. The performance advantages of copper over aluminum as a heat transfer material include greater heat exchange, better long-term durability and resistance to corrosion.

Wire wound fins heat exchangers are made from one continuous piece of wire wound helically and root soldering onto a copper tube. The root soldering eliminates air gaps between the fins and the copper tube [101,105].

6.2 Equations [92]

$$\frac{1}{v[\left(\frac{P_0}{P}\right)-1]} = \frac{c-1}{v_m c}\left(\frac{P}{P_0}\right) + \frac{1}{v_m c} \qquad (6.4)$$

P and P_0 are the balance and the diffusion force of adsorbents temperature of the adsorption, v is the adsorbed [92]. Vapour capacity and v_m is the monolayer adsorbed vapour amount.

c is expressed by

$$c = \exp(\frac{E_1 - E_L}{RT}) \qquad (6.5)$$

E_1 is the adsorption for the first layer, and E_L is that for the second layers. [110].

6.3 Heat Transfer in the Adsorbent Bed Heat Exchangers

There are many factors that could affect the design of a heat exchanger used in an adsorbent bed but the most important one is the heat transfer rate. This is because the heat exchanger has to transfer heat from the fin to porous adsorbents this is done by the three basic forms of conduction, convection and radiation simultaneously as shown in figure 6.3. The amount of heat conduction can be controlled by the material chosen to build the heat exchanger. Further, radiation is of less concern for heat exchangers operating under moderate temperatures between 15ºC to 85ºC whereas the concentration of the heat transferred is by the convection. Therefore in order to achieve a high heat transfer rate, one can increase the heat transfer surface area or the heat transfer coefficient, or both of them simultaneously.

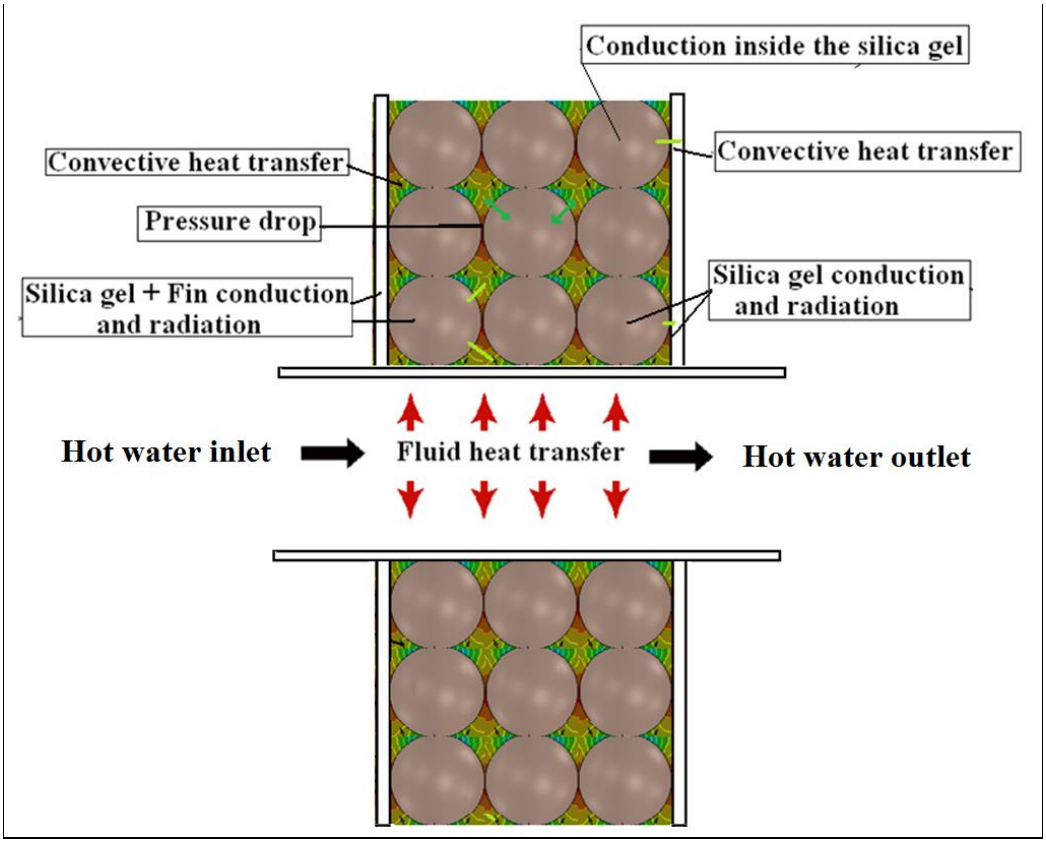

Figure 6.3 Different heat transfer taken into account in the packed bed modelling approach.

6.3.1 The thermal heat transfer of packed beds

Modelling the thermal heat transfer in a porous adsorbent bed includes two main studies (i) conduction between porous adsorbents and (ii) heat transfer through adsorbed water vapour and between porous adsorbent. The geometry of a common joint is shown in Figure 6.3 where spherical porous adsorbent are placed in contact. The gap between the contacting bodies is filled with a water vapour heat is transferred from one sphere adsorbent to another.

The heat transfer through a porous adsorbent bed can be affected by various variables. The type of porous adsorbent, the packing size, the packing ratio, the inlet water and vapour temperature, the velocity of the vapour fluid, also the type of refrigerant fluid used in the evaporator. These various variables will have an significant effect on the heat transfer phenomenon occurring in the porous adsorbent bed. [1-3].

Another area of particular difficulty in the modelling of heat transfer in a porous adsorbent bed is the heat transfer near the heat exchanger fins wall. Experimental data used in CFD simulation modelling are taken from thermocouples fixed to the surface of the heat exchanger fins. However, due to physical limitations the thermocouples near to the fins it can sometime be difficult to obtain accurate experimental recordings because of the adsorbent packing near the fins wall.

6.3.2 Near- Heat Exchanger Fins Wall Small Section Geometries

As mentioned before, computational fluid dynamics modelling is constrained by the available computational power and the required accuracy. In all modelling cases an appropriate balance between the two has to be found. For more accurate modelling a more detailed computational model has to be used, which increases the strain on the simulations. To be able to get more detailed views of certain areas in the simulation model, or to be able to simulate a specific section quicker, geometry can be created of a segment of the overall simulation model.

Since the major concern in this study is to find the performance of heat transfer from the heat exchanger fins to the porous adsorbent granules for two different types of heat exchangers, i.e., copper wire woven fins and aluminium flat plate, segment geometry can be used to generate simulation results more quickly, due to its limited size. One segment of fins with porous adsorbent spheres was simulated in order to predict the heat transfer from fin to porous adsorbents granules. Three dimensional model of a fins and silica gel adsorbent model can predict the distribution of the thermal heat transfer between fins and porous silica gel during heating desorption heat phases.

6.4 Heat Transfer Equations

The heat transfer equation is given as

$$\rho c_P \frac{\partial T}{\partial t} = \frac{\partial}{\partial x}\left(\lambda \frac{\partial T}{\partial x}\right) + \frac{\partial}{\partial y}\left(\lambda \frac{\partial T}{\partial y}\right) + \frac{\partial}{\partial z}\left(\lambda \frac{\partial T}{\partial z}\right) + S_V \quad (6.6)$$

The initial condition is

$$t = 0, T = T_0 \quad (6.7)$$

and the boundary conditions are as follows: on the x, y and z symmetries,

$$-\lambda \frac{\partial T}{\partial n} = 0 \quad (6.8)$$

on the surfaces of silica gel

$$-\lambda \frac{\partial T}{\partial n} = q_{evap,sur} + q_r \quad (6.9)$$

where q_r is heat loss by radiation on the surface of the fins of the heat exchanger which is calculated based on the Stefan–Boltzmann law:

$$q_r = \frac{Q_r}{A} = \sigma \varepsilon_r (T_{sur}^4 - T_w^4) \quad (6.10)$$

The water vapour rate s_v is,

$$S_V = h_{\mathrm{fg}} f_V \tag{6.11}$$

where f_v is the water vapour generation rate for the control volume.

The latent heat of vaporisation of water h_{fg} which can be calculated by the following formula [101,130].

$$h_{\mathrm{fg}} = 2500.8 - (T - 273.15)\mathrm{x}\ 2.422449 \tag{6.12}$$

The Fick's second law of diffusion can be used to describe mass transfer phenomenon

$$\frac{\partial C}{\partial t} = \frac{\partial}{\partial n}\left(D \frac{\partial C}{\partial n}\right) \tag{6.13}$$

For mass transfer through the silica gel porous medium, Eq. (6.10) can be rewritten as

$$\frac{\partial C}{\partial t} = \frac{\partial}{\partial n}\left(D_{eff} \frac{\partial C}{\partial n}\right) = \frac{\varepsilon}{\tau} \frac{\partial}{\partial n} \left(D \frac{\partial C}{\partial n}\right) \tag{6.14}$$

Since concentration is proportional to the partial pressure, when considering water vapour through a porous medium, concentration can be normally expressed as the equilibrium relationship in terms of partial pressure [89-110]. Noting that for an ideal gas the concentration units can be converted to partial pressure units as follows:

$$C = \frac{P}{R_0 T} \tag{7.15}$$

Then the inner mass transfer rate is

$$f\mathrm{v} = -\frac{\varepsilon}{\tau} \frac{M}{Ro\ T} \left(D\mathrm{vx} \frac{\partial^2 p_x}{\partial x^2} + D_{VY} \frac{\partial^2 P_y}{\partial y^2} + D_{\mathrm{vz}} \frac{\partial^2 p_z}{\partial z^2}\right) \tag{6.16}$$

The mass transfer happens in the area within the adsorbent bed where water vapour is actually being adsorbed on the silica gel. The mass transfer moves from the input end toward

the output end of the adsorbent bed during operation. That is, as the silica gel near the input becomes saturated with water vapour, the vapour moves toward the output end of the bed where the silica gel is not yet saturated.

$$P = P_{sat,0,}\, T = T_0 \tag{6.17}$$

And the boundary conditions are as follows: on the x, y and z symmetries,

$$\frac{\partial p}{\partial n} = 0 \tag{6.18}$$

on the surfaces,

$$P = P_{VC} \tag{6.19}$$

The vapour transport within the silica gel surface can be treated as vapour movement through the porous medium [4], which can be expressed as a transfer of vapour in the pores with inner vapour generation rate.

$$f\mathrm{v} = -\frac{\epsilon}{\tau}$$

$$\mathrm{X}\ \left(\frac{\partial}{\partial \mathrm{x}}\left(K_{\mathrm{VX}}\ \frac{\partial p}{\partial x}\right) + \frac{\partial}{\partial \mathrm{y}}\left(K_{\mathrm{Vy}}\ \frac{\partial p}{\partial y}\right) + \frac{\partial}{\partial \mathrm{z}}\left(K_{\mathrm{Vz}}\ \frac{\partial p}{\partial z}\right)\right) \tag{6.20}$$

where $\boldsymbol{k_v}$ is the mass transfer coefficient of vapour in the vapour-filled pores, which is given by

$$k_V = \rho_{V\,\frac{d_a^2}{32u}} \tag{6.21}$$

6.5 Results

6.5.1 Comparative study

In heat exchangers there may be different thermal heat transfer owing to different type of heat exchanger design, creating different behaviour in the heat exchanger. Therefore, CFD thermal heat transfer simulation analysis will help the design engineer to predict the behaviour of the different types of heat exchanger performance. The thermal heat transfer CFD simulation performance results from a 3D CFD simulation model of a wire woven finned heat exchanger and 3D CFD simulation model of flat fin heat exchanger shown in figure 6.5 and 6.6 were compared. The heat exchanger with the capability of transferring more heat to its tip will have greater heat transfer efficiency.

6.6 Experimental Setup and Procedure

The experiment apparatus used to measure the different types of heat exchanger fin efficiency consists of adsorbent bed hot water tank and a water pump as shown in figure 6.4. This experimental apparatus was design to perform heat transfer testing of heat exchangers.

The adsorbent bed section is removable this is to allow changing of the different heat exchanger.

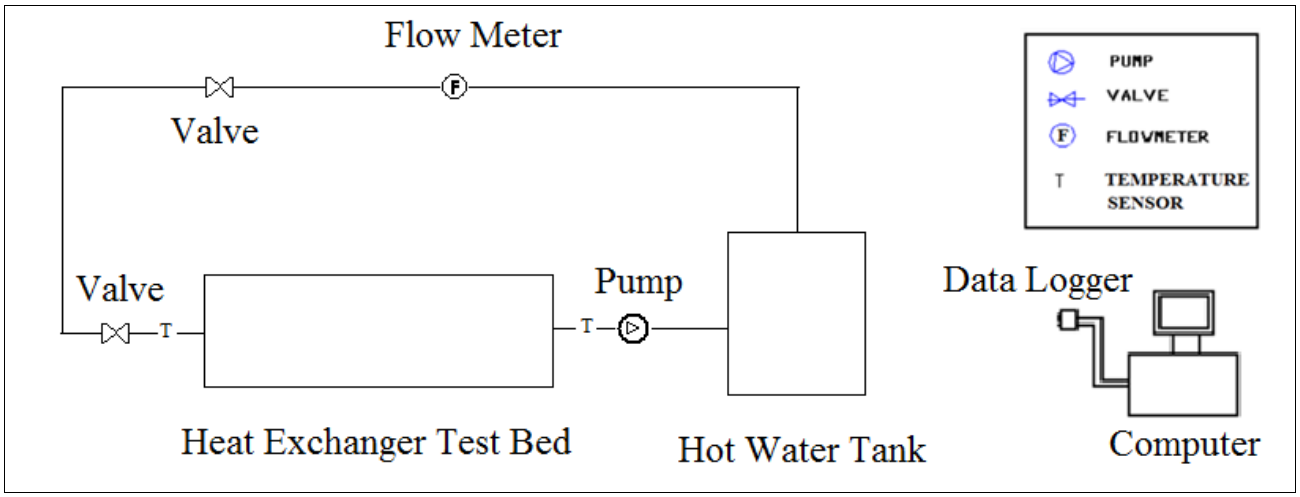

Figure 6.4 Heat exchanger test rig.

There is one adsorbent bed in the test apparatus and the function of the bed is to house the heat exchanger. In the apparatus of the experiment the heat exchanger is attached to the hot water tank so as to allow the hot water to be pump into the bed. The heat is conducted along each fin and is transferred by natural convection to the adsorbent packing.

Thermocouples are embedded at intervals along each fin so that temperature is known at selected points as shown in figure 6.5. It is at these points where the convection coefficient will be determined. Temperature readings were monitored at 60 seconds intervals to determine the efficiency of the different heat exchanger fin as shown in table 6.2.

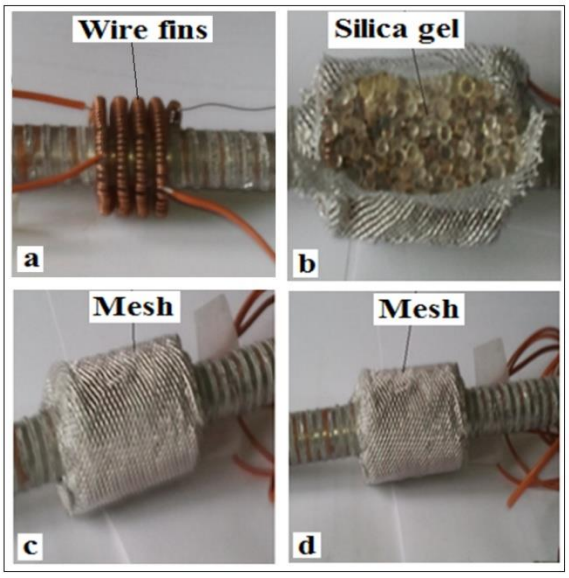

Figure 6.5 Setting up wire fin for heat transfer experiment.

The heat transfer coefficient and the effectiveness of the flat plate finned heat exchanger and wire woven heat exchanger are found based on different correlations from the experimental test rig results figure 6.6 show the flat finned heat exchanger.

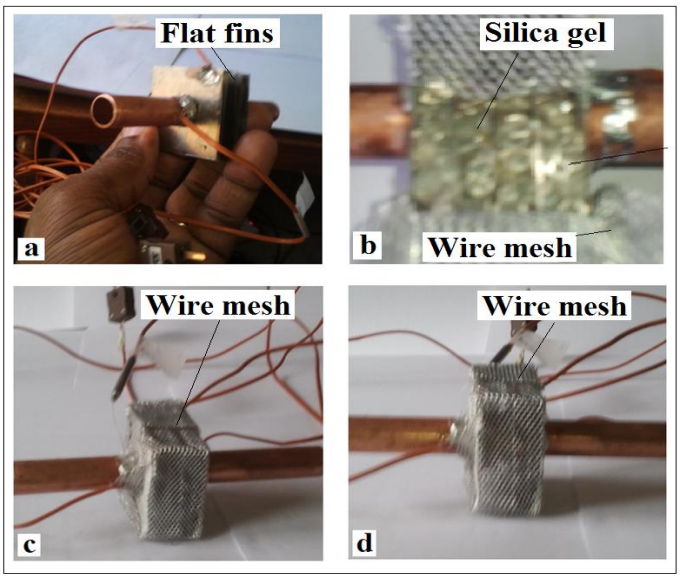

Figure 6.6 Setting up wire fin for heat transfer experiment.

Table 6.2 shows the heat exchanger heat transfer efficiency test at temperature of 85°C.

Table 6.2

Test	Wire Woven fin		Flat fin	
Time (Sec)	T-hot in	T-hot out	T-hot in	T-hot out
60	85	83.9	85	73.5
120	85	84.1	85	73.5
180	85	83.9	85	73.6
240	85	83.7	85	73.6
300	85	83.7	85	73.2
360	85	83.5	85	73.2
420	85	83.4	85	73.1
480	85	83.4	85	73.1
540	85	83.2	85	73.1
600	85	81.1	85	73.1
660	85	80.2	85	73.1
720	85	80.1	85	73.1
780	85	80.1	85	72.9

The highlighted column indicates the values used for CFD simulation of the hot water cycle.

6.7 Computational Fluid Dynamics Simulation of the two Different Heat Exchangers

6.7.1 The Physical Models

The flow and thermal variables on the boundaries of the physical model there are a number of classifications of boundary conditions:

1 Flow inlet and exit boundaries: Temperature inlet, velocity inlet, temperature outlet.

2 Heat exchanger fins wall, repeating, and limit boundaries: fins wall, symmetry.

3 Internal fluid, solid

4 Internal face boundaries: porous, fins wall, interior

In the model, velocity was assigned to the flow inlet of the adsorbent bed; this boundary condition defines a flow velocity at the inlet of the bed. The flow exit boundary is defined as a pressure outlet and the outlet pressure is defined as atmospheric pressure. The bed and packing interior are defined as boundaries. The fins wall boundaries separate the fluid zone and vapour in between the silica gel granules from the fins wall zones [109-110]. With the determination of the boundary conditions the physical model can be defined by a numerical solution. It was then necessary to determine how the solution will be established. This was be done by setting the iteration parameters. With all boundary conditions defined, a number of additional parameters and solving schemes where selected. An initial condition was assigned to the model and was used to help speed the convergence of the computation.

The computation is an iterative process that solves the governing equations for flow and energy in each simulated cell. Depending on the complexity of the model and the computer resources available, CFD simulation can take anywhere from minutes to days [98]. The results of the simulation can be viewed and manipulated with post-processing software once the simulation has converted to a solution.

One of the most important parts of CFD modelling is the construction of the mesh topology. It has to be chosen with enough detail to describe the processes accurately and with a degree of smoothness that enables solution within a satisfactory period of time. When an optimal density has been found, refining this will increase the model size without displaying more flow detail [110]. When it is coarsened the mesh will obscure, possibly essential, parts of the flow detail. The mesh determines a large part of creating an acceptable simulation see figures.6.7 and figures 6.8 illustrates the stages followed to achieve the results that was discussed in this section.

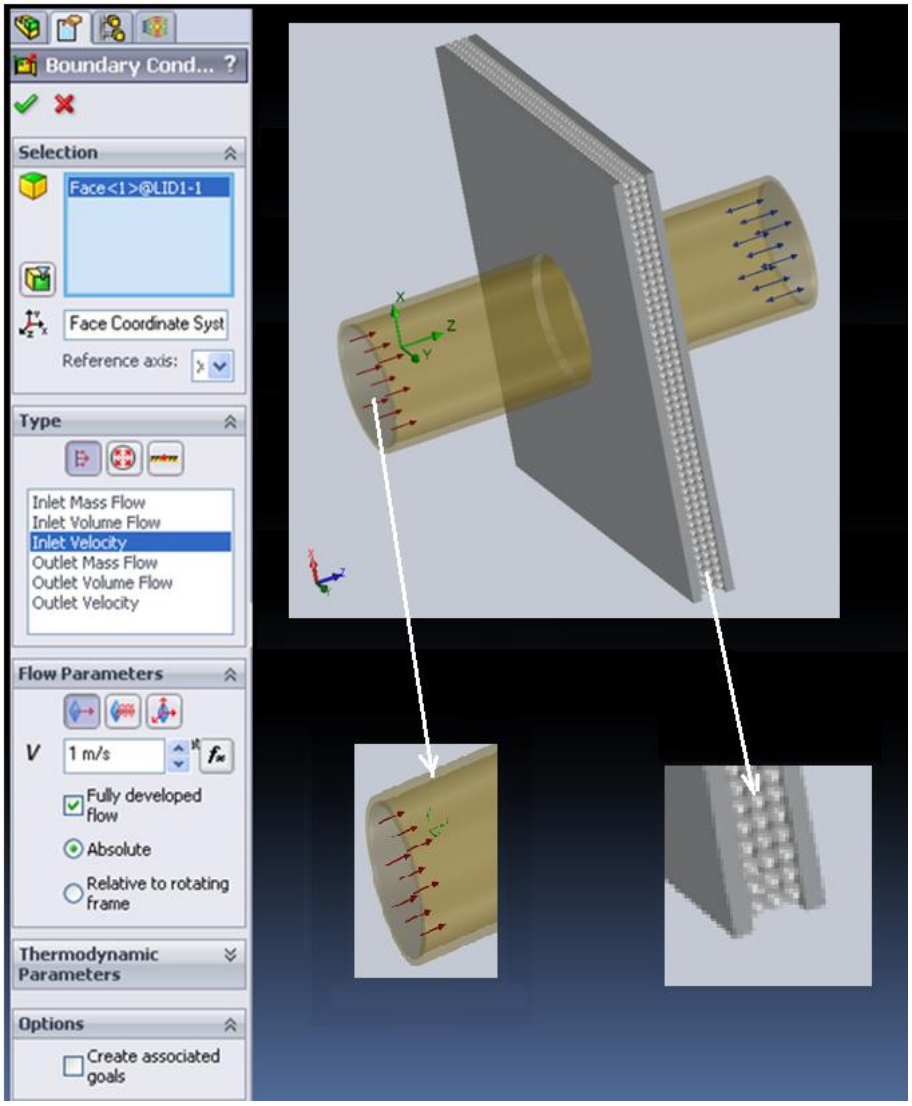

Boundary Conditions

A boundary condition is required anywhere fluid enters or exits the adsorption bed system and will be set as a Pressure, Mass Flow, Volume Flow and Velocity.

Figure.6.7 CFD porous adsorbent simulation methodology

Define the Engineering Goal

Engineering goals are the parameters which you need for the CFD simulation. Setting goals is one way of assigning to CFD Flow Simulation what you are trying to get out of the analysis, as well as a way to reduce the time CFD Flow Simulation needs to reach a solution.

Goals can be set throughout the entire domain (Global Goals), within a selected volume (Volume Goals), in a selected surface area (Surface Goals), or at given point (Point Goals).

Figure.6.8 Define the Engineering Goal

6.7.1 Creating the Silica Gel Porous Medium

To create a silica gel porous medium for the adsorption bed the need is to, first specify the porous medium's properties (porosity, permeability type, etc.) in the Engineering Database and then apply the porous medium to the spheres in the packed bed assembly. The data shown in figure 6.9 were those specified in this simulation.

Property	Value
Name	SILICA GEL TYPE A
Comments	
Porosity	0.36
Permeability type	Isotropic
Resistance calculation formula	Pressure Drop, Flowrate, Dimensions
Pressure drop vs. flowrate	Mass Flow Rate
Length	0.1 m
Area	650 m^2
Use calibration viscosity	☑
Calibration viscosity	2 Pa*s
Heat conductivity of porous matrix	☑
Use effective density and capacity	☑
Density of porous matrix	730 kg/m^3
Specific heat capacity of porous matrix	0.921 J/(kg*K)
Conductivity type	Isotropic
Thermal conductivity	0.174 W/(m*K)
Melting temperature	473.15 K
Matrix and fluid heat exchange defined by	Volumetric heat exchange coefficient
Volumetric heat exchange coefficient	0.2 W/m^3/K

Figure.6.9 Creating the Silica Gel Porous Medium in CFD Cosmos flow simulation.

For the porous medium simulation method the CFD model has a mass of cells representing the fluid inlet [92]. This is followed by the porous adsorbent units which are used to model fluid flow through porous adsorbent [101-110]. Full flow field predictions are possible with the porous adsorbent simulation method because the resistance of the porous adsorbent to flow is described by the equations:

$$\frac{\Delta P}{L} = -\alpha U_s^2 - \beta U_s, \tag{6.22}$$

where the coefficient values $\boldsymbol{\alpha}$ and $\boldsymbol{\beta}$ are assigned temperature dependent values that describe the performance of a porous adsorbent. High values of $\boldsymbol{\alpha}$ and $\boldsymbol{\beta}$ preclude flow at right angles to the porous adsorbent. Upstream and downstream of the water vapour flow field is solved using the usual Reynolds averaged Navier– Stokes methodology.

6.7.2 Thermophysical Properties

Once the model was modelled, boundary conditions were assigned to each section of the model and were used to simulate the actual conditions set by the adsorption cooling system. Examples of common boundary conditions include velocity inlet, pressure inlet, pressure outlet, temperature profile.

Table.6.3 Thermophysical properties of copper tube

Material	Water
Density, ρ (kg/m3)	1000
Specific heat capacity, C_p (J/kg K)	4200
Thermal conductivity, k (W/mK)	0.61
Dynamic viscosity, μ (kg/ms) x 10^{-3}	0.96172

Table.6. 4 Thermo-physical properties of silica gel.

Thermophysical properties of silica gel	
	Type A
Specific surface area (m^2/g)	650
Porous volume (ml/g)	0.36
Average pore diameter (A)	22
Apparent density (kg/m^3)	730
pH value	5.0
Water content (wt.%)	<2.0
Specific heat capacity (kJ/kg K)	0.921
Thermal conductivity (W/m K)	0.174
Mesh size	10–40

Table.6.5 Thermo-physical properties of alumina fins

Property	Value	Units
Elastic Modulus	1.1e+011	N/m^2
Poissons Ratio	0.37	N/A
Shear Modulus	4e+010	N/m^2
Density	8900	kg/m^3
Tensile Strength	394380000	N/m^2
Compressive Strength in X		N/m^2
Yield Strength	258646000	N/m^2
Thermal Expansion Coefficient	2.4e-005	/K
Thermal Conductivity	390	W/(m·K)
Specific Heat	390	J/(kg·K)
Material Damping Ratio		N/A

6.8 Surface area and Volume of Flat Fin Results Generated by CFD

For most finned heat exchangers heat transfers are determined by the materials thermal conductivity and the structures surface area to volume ratio. As mentioned, before increasing the surface of a heat exchanger wills also increases the heat transfer of the heat exchangers. To study the surface area to volume ratio and heat transfer of heat exchangers, two different types of heat exchangers ware selected and compared.

The length and the height of the aluminium flat fin are 32mm length and 32mm height as shown in figure 6.10.

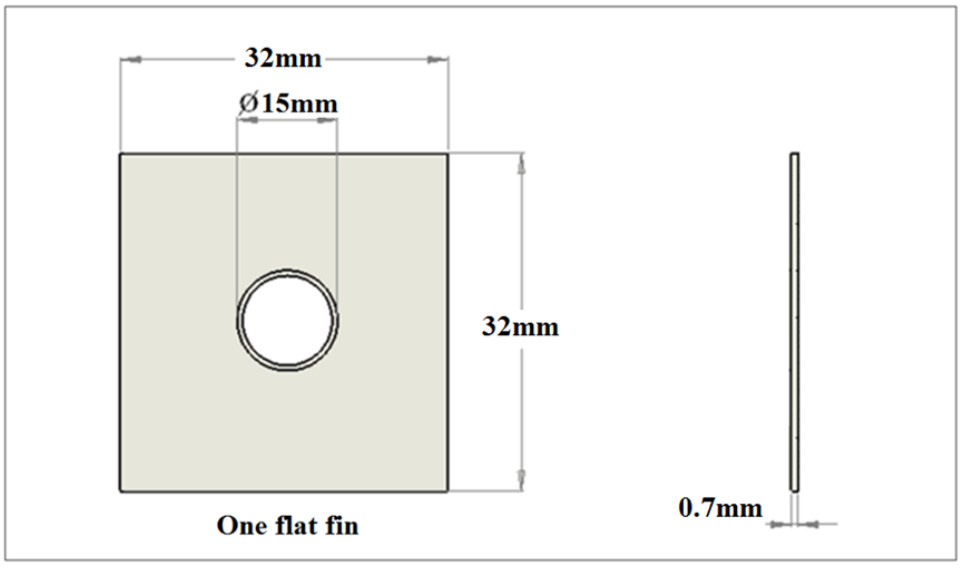

Figure.6.10 Drawings dimension for aluminium flat finned heat exchanger used to generate volume and surface area of fin.

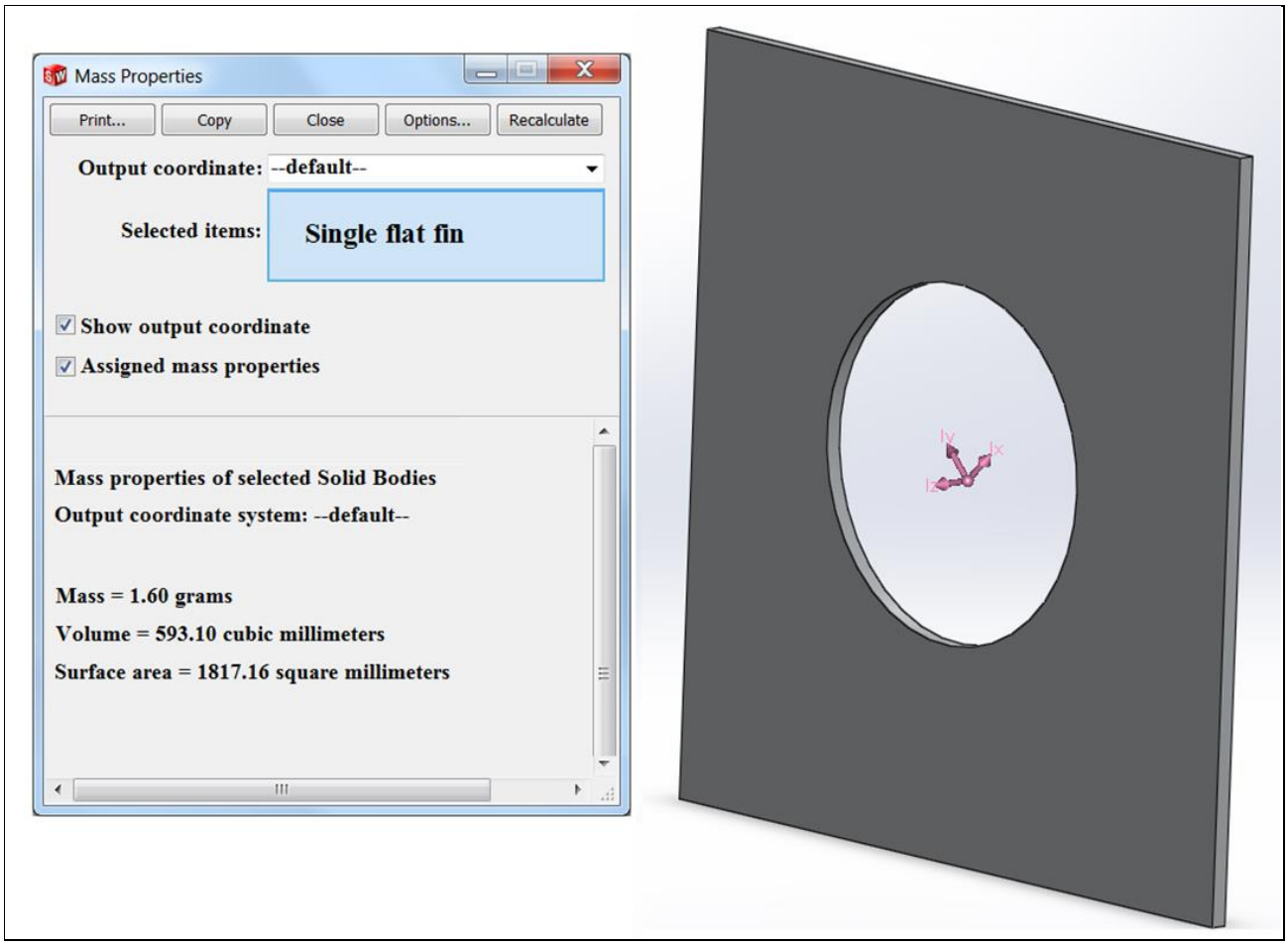

Figure.6.11 Single flat fin volume and surface area generated by assigning mass properties to 3D CAD model.

A mesh was created to focus on silica gel to silica gel contact points and silica gel heat exchanger fin wall contact points. The study of the silica gel geometry in Flow simulation was also made to compare the results from CFD codes. When actual contact points are created, both surfaces that are contacting have one common node [108]. In surface mesh creation this can be defined and does not pose any problems. The 3D mesh was created relatively easily by merging a number of nodes on the contacting surfaces. When, however, a solution is iterated convergence problems occur with the fluid elements around the contact point. In a laminar case, the solution parameters were adjusted to get a converging solution [109].

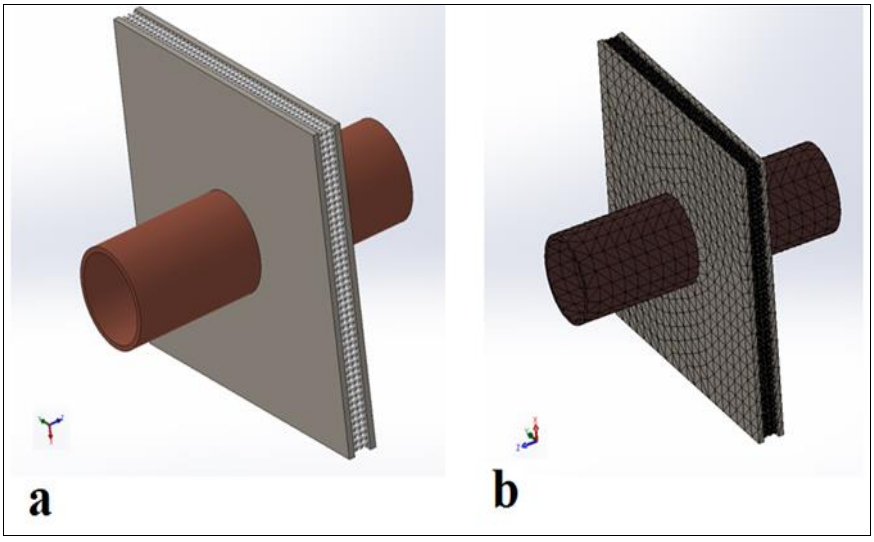

Figure 6.12 Aluminium flat plat finned heat exchanger figure (c) and (d) presents the flat fin mesh.

The fin root temperature was set from 85°C and the model was run until the solution approached the steady state behaviour after 750 seconds. The fin root temperature changed from 85°C to 73°C as heat was conducted to the top edge of the fin. This shows a reduction in temperature of the aluminium flat plat fin was by 12°C. This reduction in temperature is partly due to the heat transfer from the aluminium fin to porous adsorbent see figure 6.13 and 6.14.

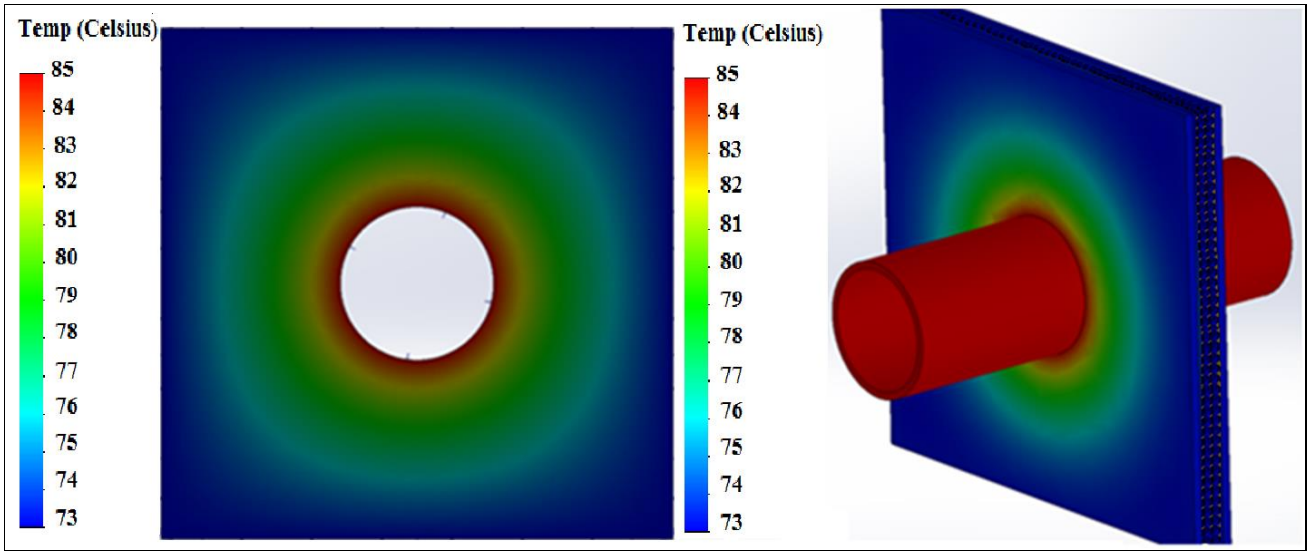

Figure 6.13 The contour thermal heat transfer temperature of the flat finned heat exchanger the centre of the fin is 85°C and fin edge is at 73°C.

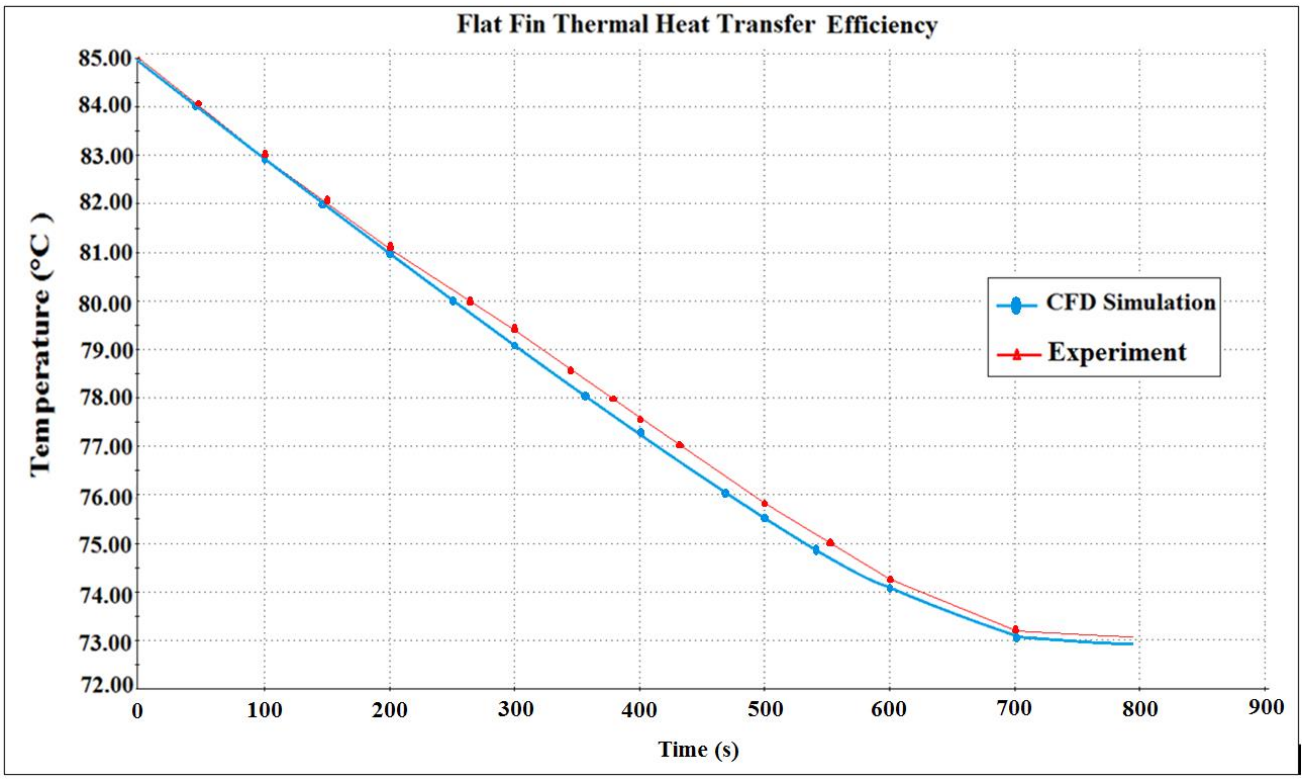

Figure 6.14 Changes of fin heat transfer efficiency over time due to the heat transfer of the heat exchanger the temperature decreases as it flows through the flat plate fin.

Temperature distribution figure 6.14 presents the temperature supplied along the length of the rectangular fin. A higher incline can be detected near the base of the fin due to the

concentrated temperature difference between fin surface and the surrounding porous adsorbents covering the fins.

6.8.1 Surface area and Volume of Wire Fin Results Generated by CFD

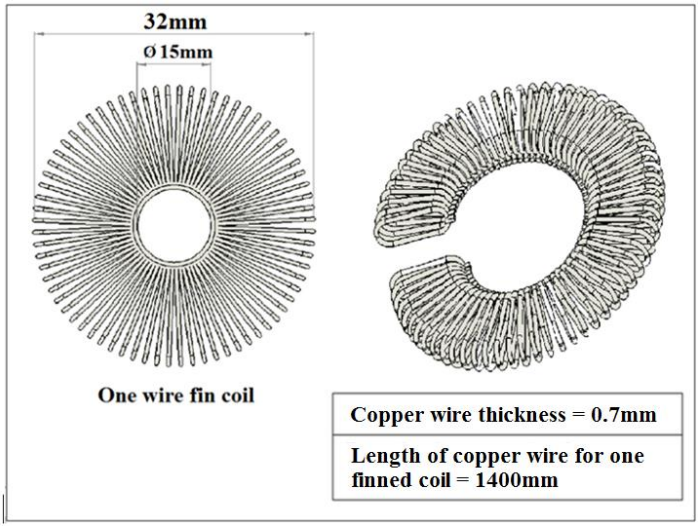

Figure 6.15 Drawing dimension for copper wire woven finned heat exchanger used to generate volume and surface area of fin.

6.8.2 Wire finned heat exchanger surface area and volume

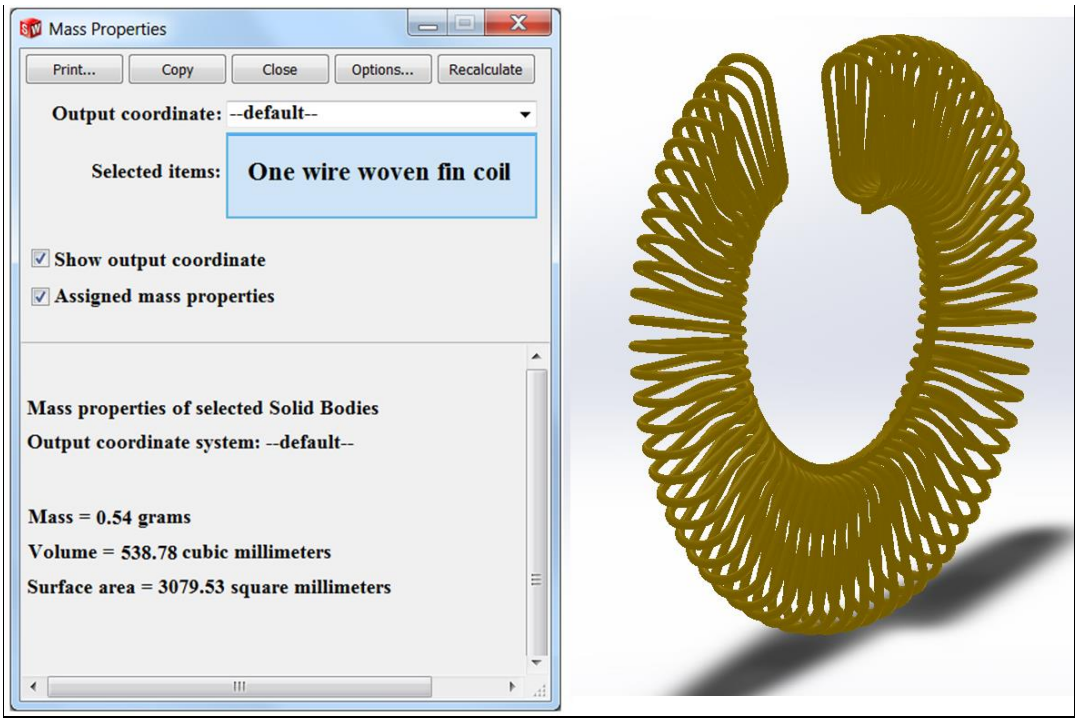

Figure.6.16 One wire woven fin volume and surface area generated 3D CAD model.

The surface area of one copper wire woven fin coil is 3079.53 square millimetres. This comprises 0.7mm copper wire of 1400mm length woven coiled into 70 loops as shown figure 6.15 and 6.16.

6.9 The Wire Woven Fin Adsorbent Bed

The method used to carry out the simulation of this type of adsorbent bed is the same as that described above. To reduce the time for CFD simulation a small geometries of the copper fin with adsorbent packed between one pitch was model for the CFD simulation.

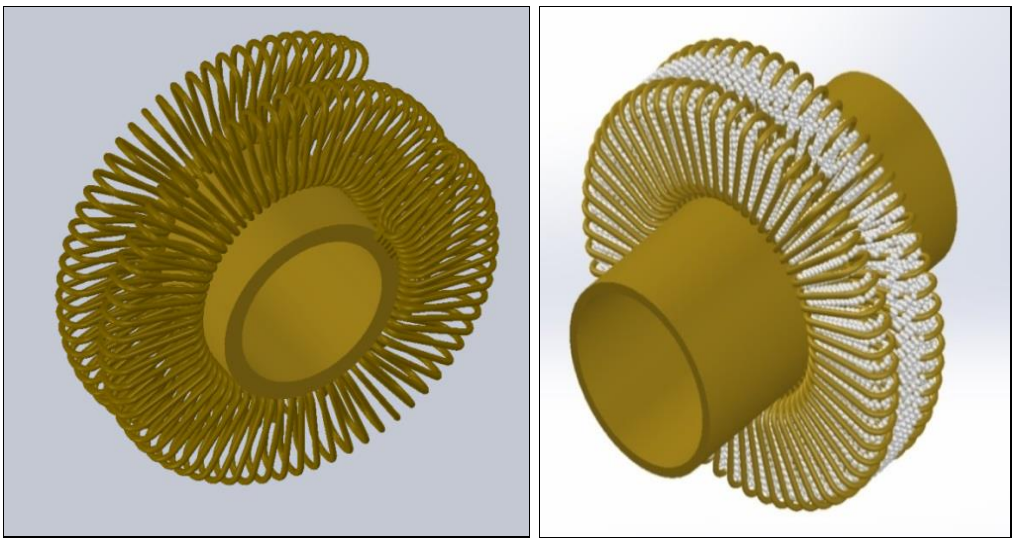

Figure 6.17 3D Model of the wire fin without silica gel and with silica gel.

6.9.1 One Pitch of Woven Wire Finned Heat Exchanger Mesh

The mesh for the one pitch of woven wire finned heat exchanger contains 187365 nodes and 84383 elements, see figure 6.18. The CFD programme creates the mesh based on the input parameters enter into the user define function menu. As can be seen in figure 6.18 the tetrahedral mesh is unstructured.

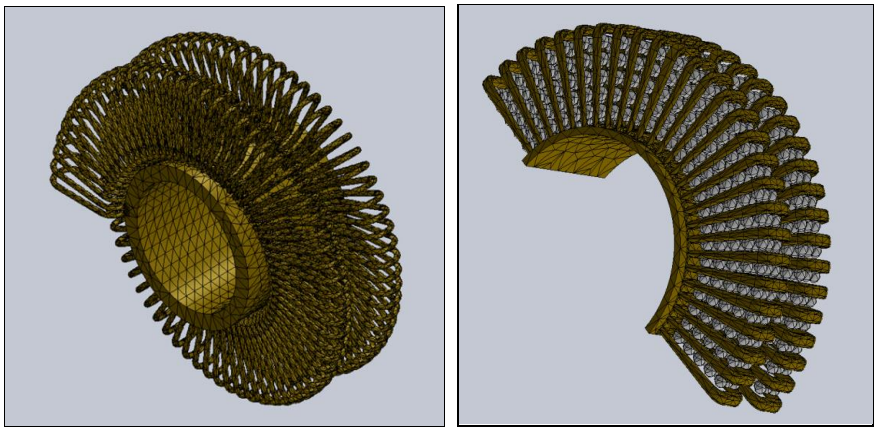

Figure 6.18 Nodes 187365 and elements 86483.

The first mesh to be simulated was a coarse mesh saving computations time on the CFD simulation. As the simulation was to be limited to a one pitch heat exchanger finned model it was determined that a fine mesh could be used as shown in figure.6.19

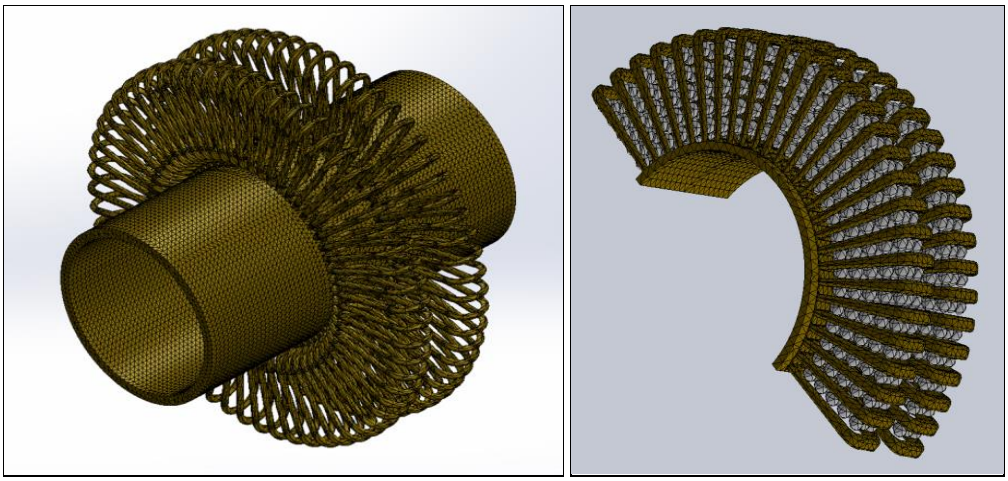

Figure 6.19 CFD Representations showing a mesh detail of the wire woven fin pack with adsorbent.

The CFD mesh quality can be identified through two main factors. The first factor is that the CFD simulation meshes must have a sufficient number of points in the internal of the computational domain to describe the physical domain correctly. The second factor requirement for CFD mesh quality is that a sufficient number of points must be specified on the boundary to represent it accurately. This requires the number of boundary points to adapt according to the model surface geometry.

6.9.2 One pitch of wire woven finned heat exchanger with adsorbent packing

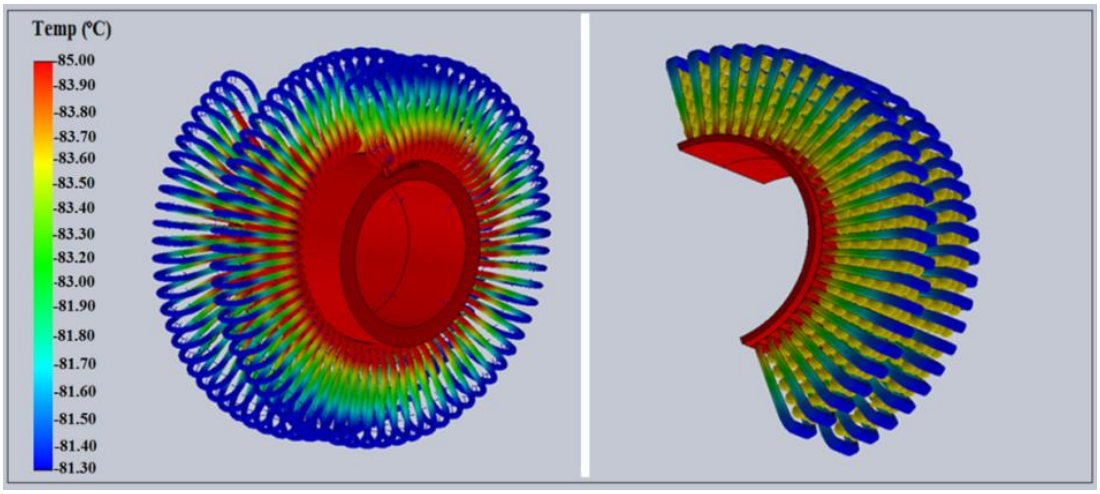

Figure 6.20 Displays the heat transfer efficiency of the wire fin heat exchanger root contour temperature is at 85°C and the fin tip temperature is at 81°C.

Figure 6.20 and 6.21 presents the temperature supplied along the length of the wire woven fin. A higher incline can be detected near the base of the fin due to the concentrated temperature difference between fin surface and the surrounding porous adsorbents covering the fins.

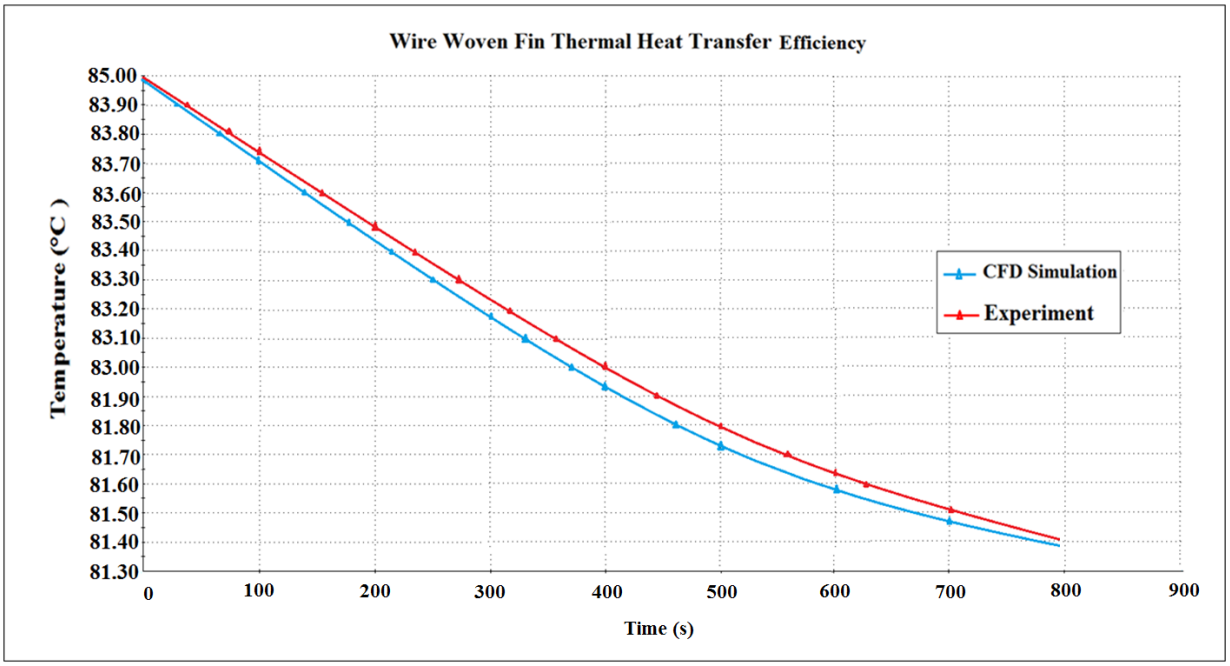

Figure 6.21 Changes of fin heat transfer efficiency over time due to the heat transfer of the heat exchanger the temperature decreases as it flows through the wire woven fin.

The CFD simulation method for the wire woven fin was as described for the flat fin heat exchanger. The fin root temperature of the wire fin was set from 85°C and the model was run until the solution approached the steady state behaviour (after 750 seconds), as shown in figure 6.21. The fin root temperature decreased to 81°C from 85°C as the heat transferred to the top edge of the wire fin. This shows the change in temperature of the wire woven fin was by 4°C. This low reduction in temperature is to some extent to do with the heat exchanger been design from a continuous wire copper coil, which contributes to the good heat transfer, also, being made of copper and not aluminium increase the heat transfer to the adsorbent. The thermal conductivity of copper compared to aluminium is shown in table 6.1.

6.10 Model validation

Several checks were performed in order to verify the generated results the adsorbent bed heat transfer performance was observed to ensure that the results satisfied the boundary conditions. The resulting file generated by Cosmos flow upon the completion of each run was carefully examined and analysed. The surface area to volume ratio of the heat exchangers was verified by comparing simulation result to surface area to volume simulation. The heat transfer results were compared to data from experiment.

6.11 Conclusions

CFD as a design tool for adsorbent bed design proves to be useful in estimating wall to fluid heat transfer parameters. It makes possible the modelling of a realistic case of an adsorbent bed using wire woven fin and flat fin heat exchangers. From the simulation comparisons of the copper wire woven finned and aluminium flat finned heat exchangers the wire finned heat exchanger has three advantages over the aluminium flat fin. The first advantage was the greater surface area as seen in figure.6.16 the second was a better heat transfer efficiency as

seen in figure 6.21 and the third advantage was the smaller volume of the heat exchanger as showed in figure.6.16.

It was observed from CFD simulation carried out on heat transfer on contact points between fin and porous adsorbents that the contact points between the adsorbent and heat exchanger had a significant effect to heat transfer. A poor heat transfer flow distribution can result in a lower heat transfer rate. Therefore, the optimisation of flow distribution is an essential step in heat exchanger design optimisation. CFD methods have demonstrated to have great potential in predicting the performance of both existing and newly developed adsorbent beds designs.

CHAPTER 7

SCALING UP THE EXPERIMENTAL INVESTIGATION OF A WIRE WOVEN HEAT EXCHANGER ADSORPTION BED PACK WITH SILICA GEL

Abstract

In the previous chapter a CFD comparison study was carried out on a copper wire woven finned and aluminum flat heat exchanger. The copper wire finned heat exchanger was considered to have good heat transfer performance compared to the aluminum flat fin. This chapter describer the experimental work performed on the scaled up adsorption cooling test rig. It begins with the introduction of the test rig design, its constituting components and data acquisition system. Performance curves of system components such as the evaporator, condenser and adsorbent beds are discussed. This chapter also outlines the system behavior under different operating conditions and a full system CFD simulation.

7.1. Introduction

This chapter prepares the foundation for chapter number 8 which deals with the modelling of two wires finned adsorbent beds adsorption cooling system. It gives an insight into the working of the wire woven heat exchanger adsorption cooling system. Procedure of installation of a test rig equipped with data logging system is given along with the calibration of sensors. Subsequently the method followed in conducting tests on a new configuration of adsorption cooling system. The purpose of the testing of the system is to ascertain systems viability and interaction of individual components. The tests also are carried out to obtain system parameter for use in the CFD simulation. Several performance curves are produced for such system components as adsorbent bed evaporator and condenser.

7.2 Experimental Set-Up

The adsorption test rig consists of a condenser, evaporator and adsorbent bed. The adsorbent bed contains a heat exchanger consisting of one silica gel filled copper wire woven fins and tube. The wire fins contains 0.5 kg of silica gel in total. A heating and cooling water tanks are used to provide the adsorption bed, condenser and evaporator with water at the desired temperatures. During the desorption stage of the cycle the adsorption bed is heated to temperature (80°C) while the condenser is kept at 25°C [82-91]. During the adsorption stage of the cycle the adsorption bed is cooled down to 25°C and the evaporator to 15°C [90, 91]. Valves with a timer are used to control the heating and cooling water between the cycles of operation of the adsorbent bed, evaporator and condenser [91].

7.2.1 Components

The experimental test rig set up for adsorption cooling system measurements consisted of the following components:

1. One adsorbent beds
2. Evaporator
3. Condenser
4. Three water tanks one hot water tank, one cooling water tank and one chilled water tank
5. Vacuum pump
6. Manually switchable valves, solenoid valves and one diaphragm valve
7. Sensors: Flow meters, pressure transducer and type K thermocouple
8. Measuring: data logger (multiplexes with digital converter) transferring data to a personal computer

This help to keep the water temperature more stable. One flow meter is installed in each water system. Valves V2 and V3 acts as controller for the flow rates. The heat source is provided by a Wire wound tubes tube heat exchanger that is heated by heating coil. Hot water temperature is controlled by valve V5. The temperatures of the chilled water and water, is controlled by valves V1. The controlled operation of the vacuum valves and the valves in heating and cooling water system is controlled by a Programme logic controller (PLC) system. The temperature of the cooling water is about 25ºC, and the hot water temperature is 80ºC.

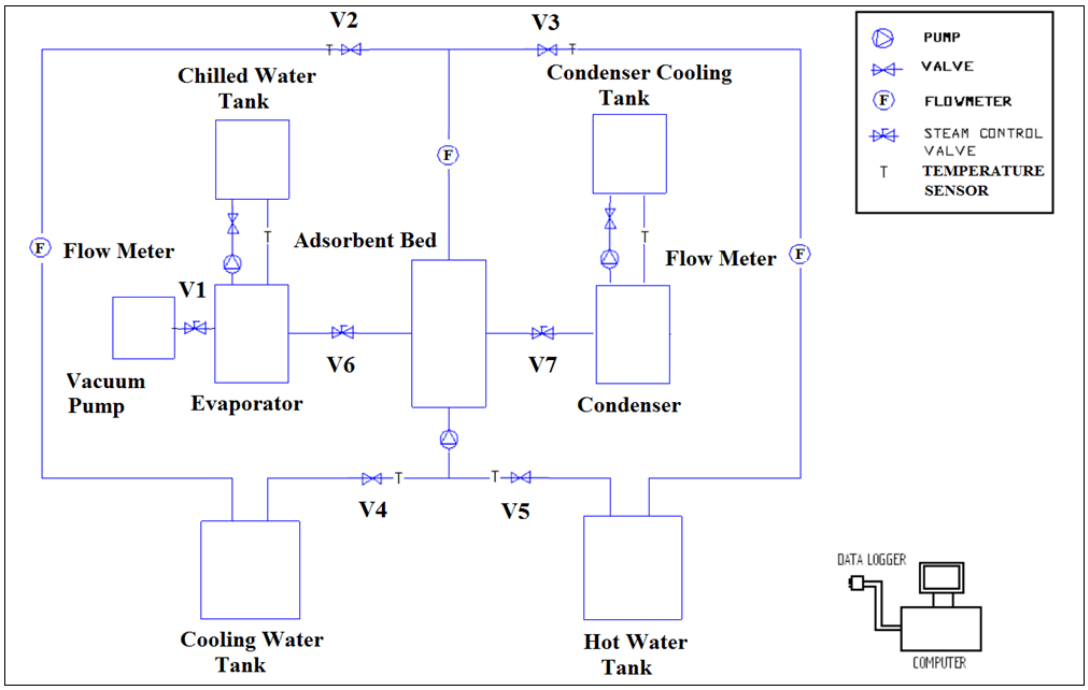

Figure 7.1 Schematic view of the adsorption cooling test rig with the wire woven fins.

7.3 Heat Transfer Coefficients and Performance Modelling

The heat transfer coefficients of the adsorption and desorption are evaluated from the experimentally measured temperatures of the adsorbent, the inlet and outlet temperatures of the heat transfer fluids entering the adsorbent beds during adsorption and desorption processes. The general formula for the heat transfer coefficient using log mean temperature difference is given by [63-91-114].

$$U_{overall} = \frac{Q_{des/ads}}{A_{Bed}\, LMTD} \tag{7.1}$$

where $U_{overall}$ is the overall heat transfer coefficient, $Q_{des/ads}$ is the desorption or adsorption heat, A_{Bed} the total surface area (including fins area) of the adsorbent bed and LMTD is the log mean T temperature difference which is calculated as,

$$LMTD = \frac{\left(T_{hw/cw} - T_{des/ads}\right) - \left(T_{hw/cw,out} - T_{des/ads}\right)}{In\dfrac{\left(T_{hw/cw} - T_{des/ads}\right)}{\left(T_{hw/cw,out} - T_{des/ads}\right)}} \tag{7.2}$$

The adsorption and desorption heat of the system are estimated using the inlet and outlet temperatures of the adsorbent beds and it is given by

$$Q_{des/ads} = \dot{m}_{hw/cw} c_P \left(T_{des/ads}\right)\left(T_{hw/cw,in} - T_{hw/cw,out}\right) \tag{7.3}$$

Here $\dot{m}_{hw/cw}$ is the mass flow rate of the hot water or cooling water flow into the adsorbent bed and Cp($T_{des\ ads}$) is the specific heat of the water at adsorber temperature. The overall heat transfer coefficients for adsorption and desorption processes are calculated from the cyclic-steady state temperatures of the AD cycle [3-10].

The performance of the adsorption cooling is accessed using key performance parameters namely the specific cooling capacity (SCC) and the coefficient of performance (COP) which are given as follows,

$$SCC = \int_0^{t_{cycle}} \frac{Q_{evap}\,\tau}{M_{sg}}\, dt \tag{7.4}$$

$$Q_{evap} = \dot{m}_{chilled}\, C_P \left(T_{evap}\right)\left(T_{chilled,in} - T_{chilled,out}\right) \tag{7.5}$$

$$COP = \int_0^{t_{cycle}} \frac{Q_{evap}\,\tau}{Q_{des}}\, dt \tag{7.6}$$

where $\dot{m}_{chilled}$ is the chilled water flow rate and Q_{evap} is the heat of evaporation. The heat of condensation is calculated using cooling water inlet and outlet temperatures and mass flow rate of the condenser and it is given as

$$Q_{evap} = \dot{m}_{cond} C_P (T_{cond}) (T_{cond,in} - T_{cond,out}) \quad (7.7)$$

7.4 Wire Wound Finned Tubes

A tube construction adopted for adsorbent bed heat exchangers makes use of surface in the form of wire helically wound fins. Copper wire is used to give high conductivity and thus make the most of the efficiency of this form of extended surface.

For the purpose of this experiment a copper wire-woven fin heat exchanger was manufactured from drawings to the specification shown in table 7.1, provided to P. A. K Engineering Limited who donated it for the purpose of this study.

Table 7.1.Specification for the Copper wire woven fins

a	Tube Diameter	15mm
	Tube material	Copper
b	Wire Material	Copper Wire
	Copper Thickness	0.7mm
	Loops per Turn	70 turns per fin pitch
	Length of Copper Wire	1400mm per fin pitch
	Maximum operation temperature	120°C

Table 7.1 shows the specification of the copper wire woven finned heat exchanger the copper tube diameter is 15mm and the thickness of the wire fin is 0.7mm. The wire are made up of 70 loops per turn 360 degrees the lenth of the wire per 360 turn is 1400mm one turn is the equivalent to one flat fin so two turns of wire fins is one pitch. Figures 7.2 and 7.3, show the

stages of preparing the copper wire woven fin heat exchangers covered with silica gel for the experiment.

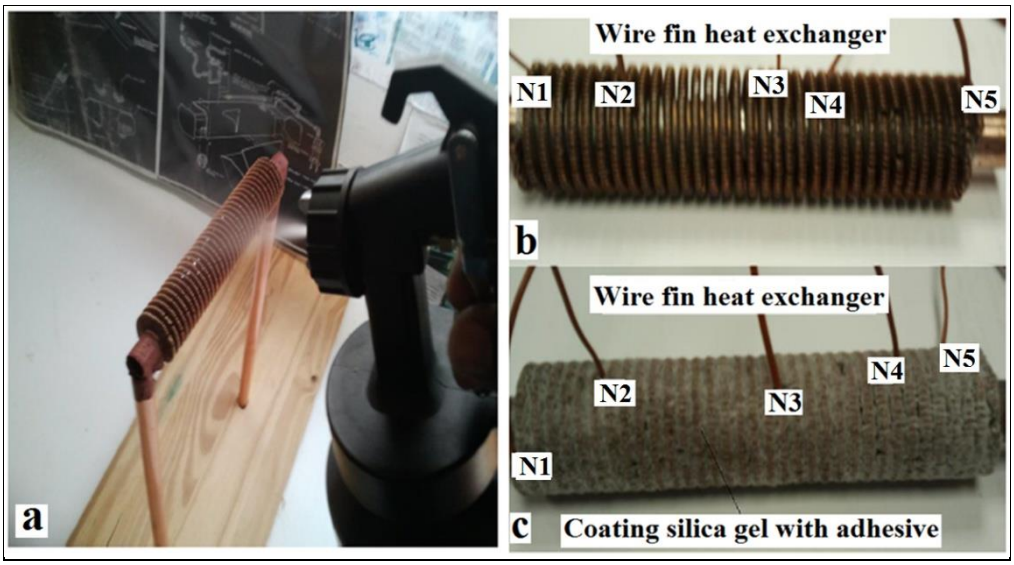

Figure.7.2 Wire wound heat exchanger being prepared for heat transfer testing (a),(b) and (c) epoxy was used to attach silica gel to wire fins this is a similar method used by (Source SorTech) [48].

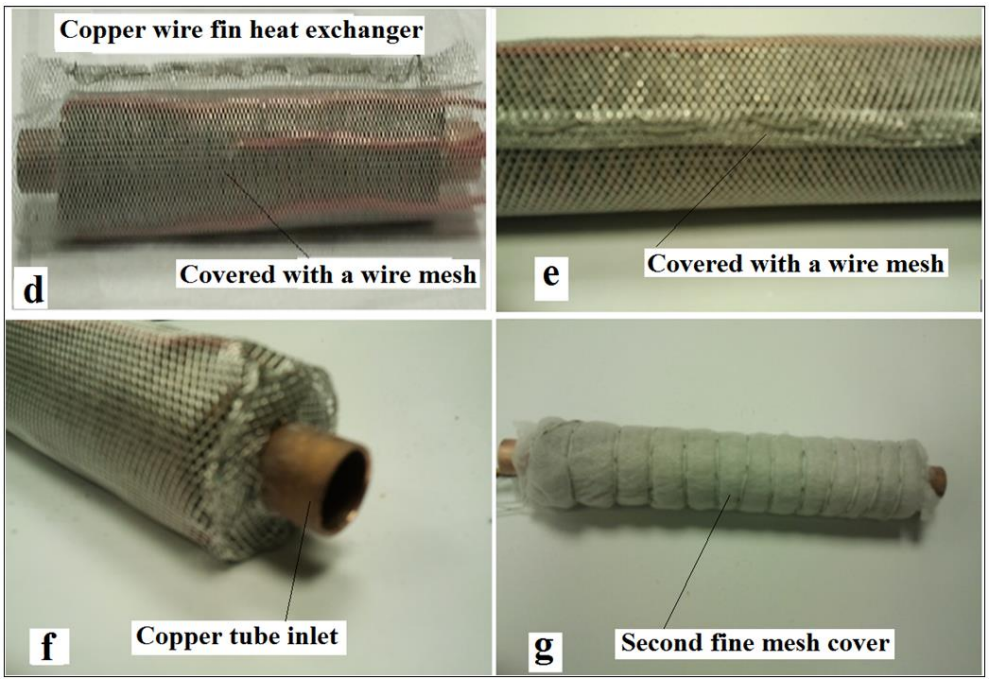

Figure 7.3 (d),(e) Wire aluminium mesh was used to cover epoxy attach silica gel (f) and (g) second covering of fine mesh.

The advantages of using the epoxy resin to attach the silica gel granule to the wire fin heat exchanger are: (1) improved speed of heat transfer (2) less volume and weight of silica gel (3) Improved vapour transport.

7.5 System Measuring Instruments and Measuring Points

The test rig incorporated several measuring instruments to produce a range of parameters boundary condition for the CFD Simulation. These are described, further on, in this section, where the various measuring points in the experiment are discussed.

7.5.1 Geometries of the Wire Fins and Thermocouples Location

The data collected for the heat transfer performance evaluation of the wire woven fins heat exchanger was measured by attaching five, K type thermocouples at various points on the wire woven fins as shown in figure 7.4.

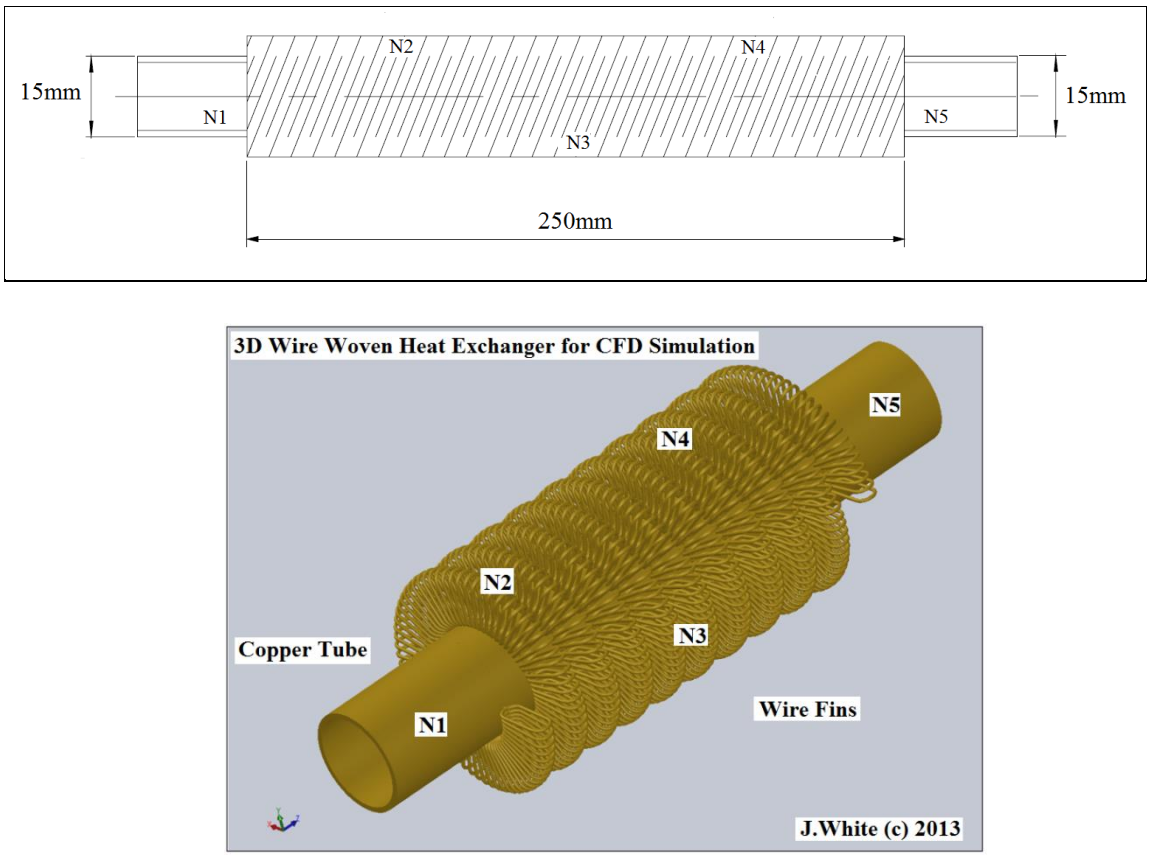

Figure 7.4 The location of the thermocouples used to investigation the heat transfer of wire fins to silica gel.

7.5.2 Temperatures

Listed here are the measuring point positioning in the experimental test rig:

1. Five measuring points on the wire wound tubes heat exchanger
2. Two measuring points at opposite outside surfaces of the adsorbent
3. One measuring point at the flange fitting of the adsorbent bed
4. Ambient temperature
5. Inlet and outlet temperatures of the three coolants
6. Temperature of the liquid in the evaporator

7.5.3 Temperature Sensors:

All five temperature sensors were thermocouple type K. These sensors were embedded in the wire wound tubes heat exchanger**.** The temperature range was from 25◦ C up to 80◦C. The sensors provided the current of 1 mA (also measured by the data logger through a high precision resistance) through a constant current supply.

7.5.4 Pressure Vacuum Gauge and Solenoid Valves

With vacuum pressure gauges, the pressures in the evaporator, in the adsorbent bed and in the condenser can be recorded one after another. For this system, the sensor had four outlets connected with solenoid valves to the components. The solenoid valves were controlled by the data transducer which has the control sequences from a PLC connected to a computer programme.

7.5.5 Flow Meters

In the coolant and heating circuits of the test rig flow meters are installed one turbine velocity flow meter and two acrylic water velocity flow meters.

7.5.6 The Data Logger

The measuring signals of all built in sensors were scanned through multiple data acquisition system channels by a data logger and then transmitted to a computer.

7.5.7 Vacuum Pumps

For low temperature evaporation of the working fluid a vacuum pump was necessary. The vacuum pump was connected to the evaporator and adsorbent bed. The vacuum pump was used to reduce the pressure below the vapour pressure of the water at ambient temperature.

7.6 Wire Woven Fins Heat Exchanger Adsorption Test Rig

An Adsorption test rig was designed with an evaporator and condenser of identical construction. The reasons for designing this adsorption test rig was to compare the heat transfer performance of silica gel adsorbent and water pairs on wire wound tubes and then to use data for CFD simulation.

Figures 7.5 shows a labelled photograph of the Adsorption test rig layout, the adsorbent bed and 3D CAD design are shown in figures 7.6 and 7.7, respectively. During the construction of the test rig there was difficulty in obtaining a full vacuum in the evaporator because of leakage in the gaskets. The experiment was almost abandoned due to this problem; however, this problem was resolved by using epoxy resin pasted onto the gasket and permanently sealing the gaskets enabling tests to be carried out. The drawback of this solution was that the evaporator was permanently locked. This was not a problem in this study because the test rig was a temporary prototype to generate data for the purpose of the CFD Simulation.

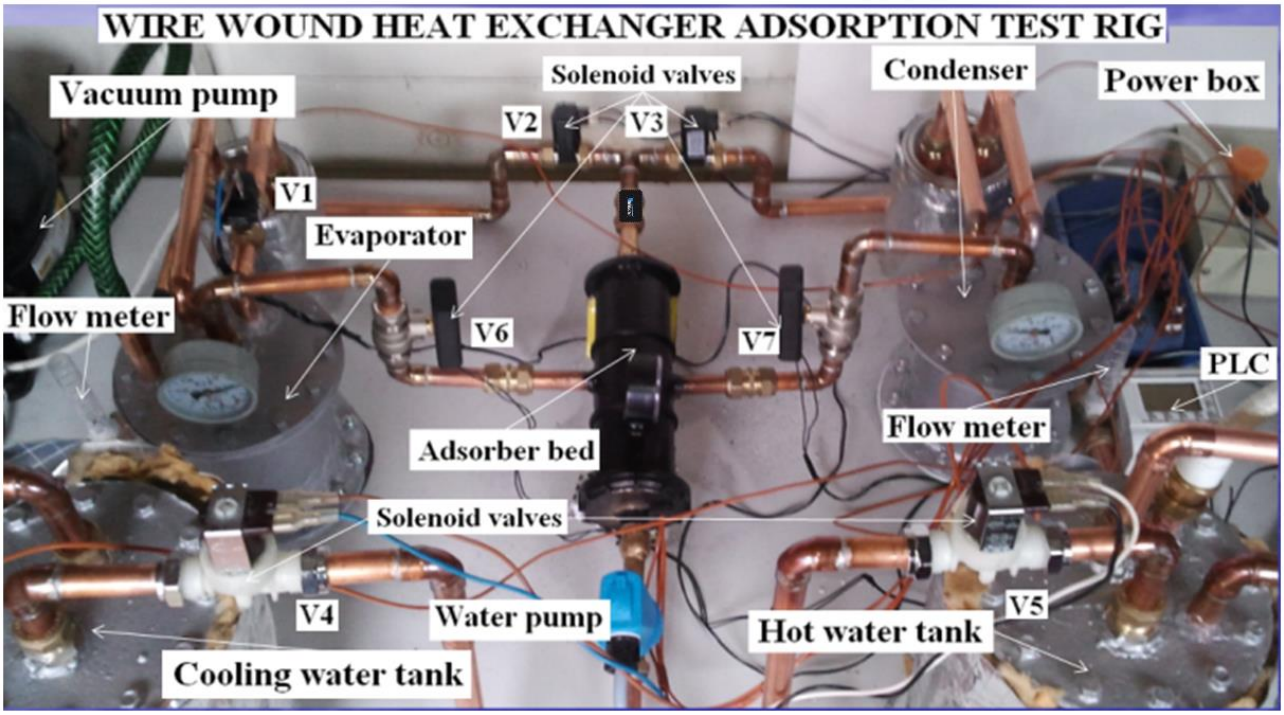

Figure 7.5 The adsorption bed test rig.

All the switch solenoid valves and vacuum pumps used in this adsorption cooling test equipment are controlled by a PLC programmer system connected to a computer. It is a automatically running prototype.

7.6.1 Testing Procedure

Prior to experiment, the test equipment (evaporator, condenser, adsorbent bed and piping systems) is first evacuated by a vacuum pump for one hour. During evacuation, hot water at 85°C is supplied to the adsorbent bed to heat-up the silica gel to remove moisture trapped in the adsorbent bed when all moisture is completely removed the test equipment is then ready for the experiment.

The adsorption cooling test rig is built with only one adsorbent bed an copper wire woven finned heat exchanger is used for this adsorbent bed. The adsorbent material (silica gel) is filled in the spaces between the wire fins. The connection to the evaporator, adsorbent bed and condenser is by valve 6 and valves 7. The evaporator is a cylindrical vacuum chamber.

At the bottom of the chamber a helix copper coil heat exchanger as shown in figure7.6 this helix coil is covered with water.

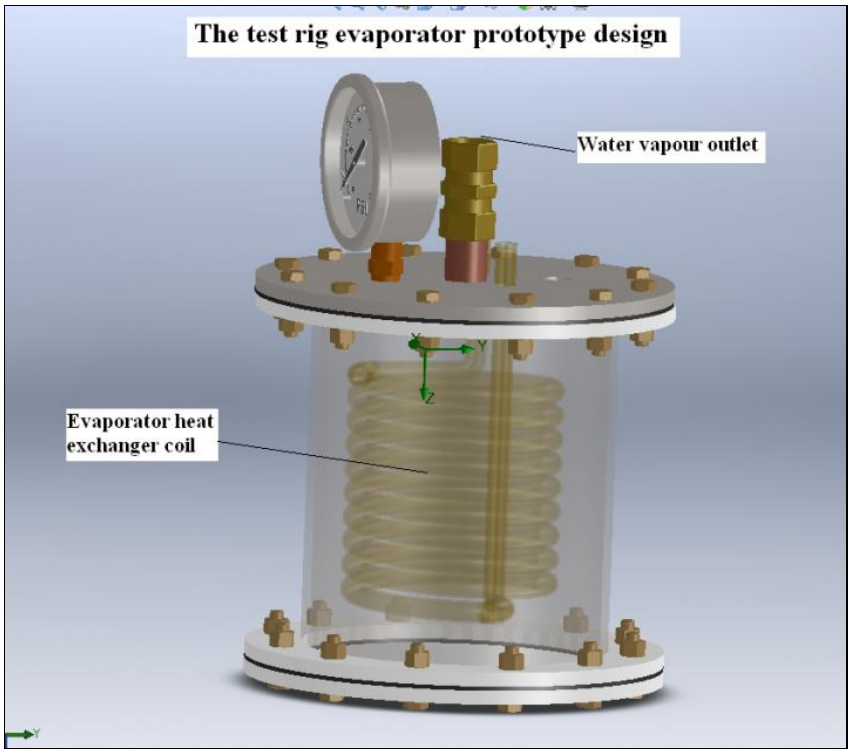

Figure.7.6 Helix copper coil heat exchanger (designed by J. White © 2012).

The condenser is also made of a helical coil heat exchanger in a cylindrical vacuum chamber. Throughout the adsorption process water vapour is adsorbed by the adsorbent material silica gel. Throughout this operation the valve 6 connected to the evaporator is opened and the valve 7 connected to the condenser is kept closed. At the same time the adsorbent bed is cooled and maintained at temperature of 25°C. After reaching the water vapour saturation conditions in the adsorbent bed the desorption process is initiated by means of hot water input at temperature of 80°C. This is done by switching on solenoid valves 5 and solenoid valves V3. At the same moment in time the solenoid valves 4 and 2 are closed and the valve connected to the condenser is opened. Water in the adsorbent bed will be desorbed due to the heat input. The water vapour desorbed from the silica gel flows through the valve 7 to the

condenser vacuum chamber. Here the water vapour is condensing on the surface of the condenser helical coil heat exchanger.

To simulate the experiment under rating conditions, the parameters of the standard operating condition employed in simulation code are shown in Table 7.2

Table.7.2 **Parameters of the standard operating condition employed in simulation code**

***T* in chilled water**	**15°C**
***T* in heating water**	**80°C**
***T* in cooling water**	**25°C**
Condenser pressure	**101325 (Pa)**
Adsorbent bed pressure	**101325 (Pa)**
Evaporator pressure	**101000 (Pa)**
Velocity	**0.5 (m/s)**
Time Cycle	**480s**
Time switching	**30s**

7.6.2 Considerations and Assumptions

- There is no refrigerant vapour or heat losses to the surrounding.
- Adsorbent, refrigerant and heat exchanger temperatures are instantaneously the same.
- Refrigerant exit from the evaporator at saturated vapour condition.
- Refrigerant exit from the condenser at saturated liquid condition.
- Flow through the expansion valve is isenthalpic flow.
- The isosteric heat of adsorption is assumed constant.

7.6.3 Adsorption Cooling System Simulation Stages

- Components simulation models (sub models)
- Evaporator, Condenser, Adsorbent beds
- Sub models validation study
- Integrating sub models to form Adsorption Cooling System simulation model
- Adsorption Cooling System simulation model validation study

7.7 Result and Discussion

7.7.1 Analysis under the Standard Operating Condition

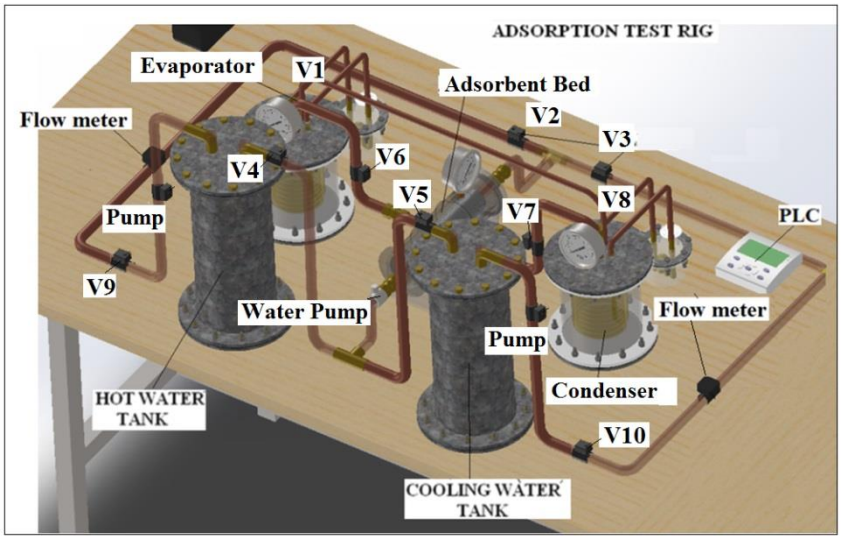

Figure.7.7 3D Model of test rig.

The test rig was first design by using 3D CAD then tested by CFD modelling to predict the heat transfer in the adsorbent bed. The simulation results were then validated with the experimental results. In this section the results of the simulating the adsorbent bed during adsorption and desorption will be discussed in comparison with the experimental results. Also the results of simulating the evaporator and condenser will be compared to experimental results. To simulate the experiment under typical conditions, the parameters of the standard operating condition employed in simulation code as shown in Table.7.4 are used.

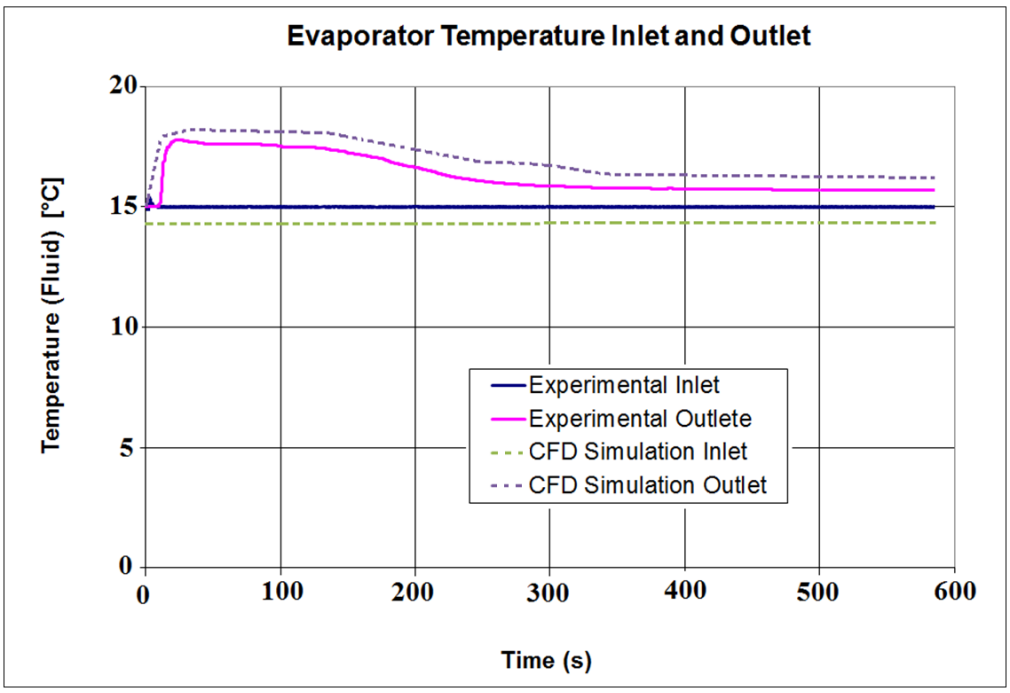

Figure 7.8 The refrigerant temperature in the evaporator.

Figure 7.8 depicts the refrigerant temperature variation in the evaporator. It can be observed that the output temperature increases first and decreases subsequently. Here, it is worthy to note that the evaporator outlet temperature varies within a range of 2-3 ^{o}C after stabilization.

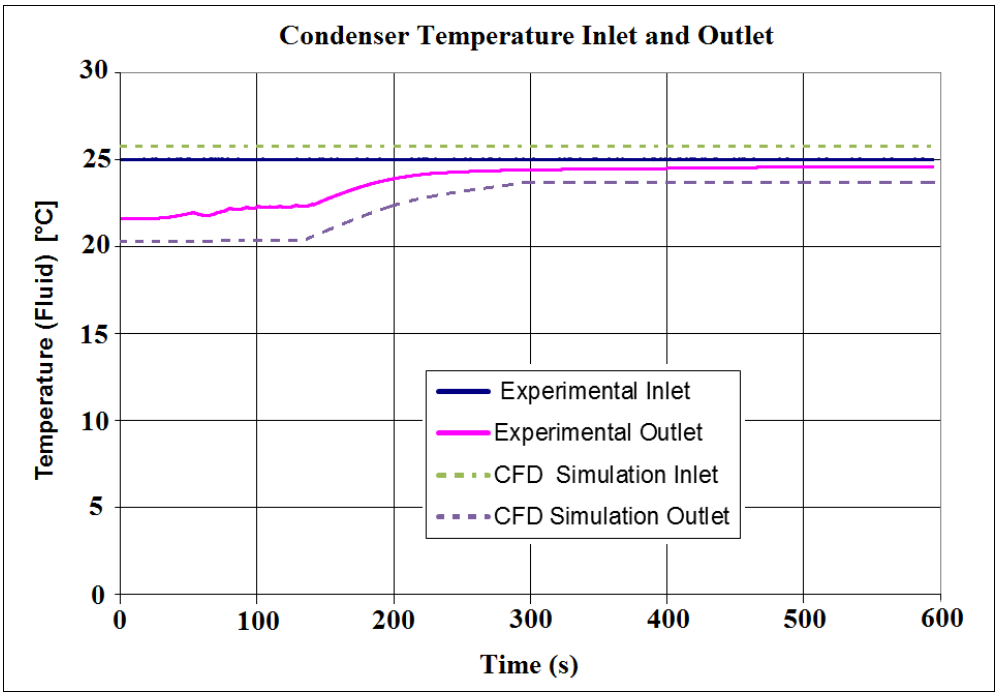

Figure 7.9 The refrigerant temperature in the condenser.

The experimental results from the condenser inlet and outlet refrigerant temperatures are compared to the CFD simulation inlet and outlet temperatures. It can be seen from figure 7.9 the CFD simulation results roughly agree with that of the experimental results.

Table 7.3 Temperature Data

Hot water cycle	Inlet temperature	60°C	°C
	Flow velocity	0.5	m/s
	Pressure	101325 Pa	Pa
Chilled water cycle	Inlet temperature	15	°C
	Flow velocity	0.5	m/s
	Pressure	101000 Pa	Pa
Cooling water cycle	Inlet temperature	25	°C
	Flow velocity	0.5	m/s
	Pressure	101325 Pa	Pa

The inlet water to the condenser has a temperature of 25 ^{o}C and that to the evaporator is 15 ^{o}C. These values decide that the pressure of condenser is held at 101325 Pa. At the inception of the adsorption-desorption period, pressure in the condenser increases and decreases subsequently.

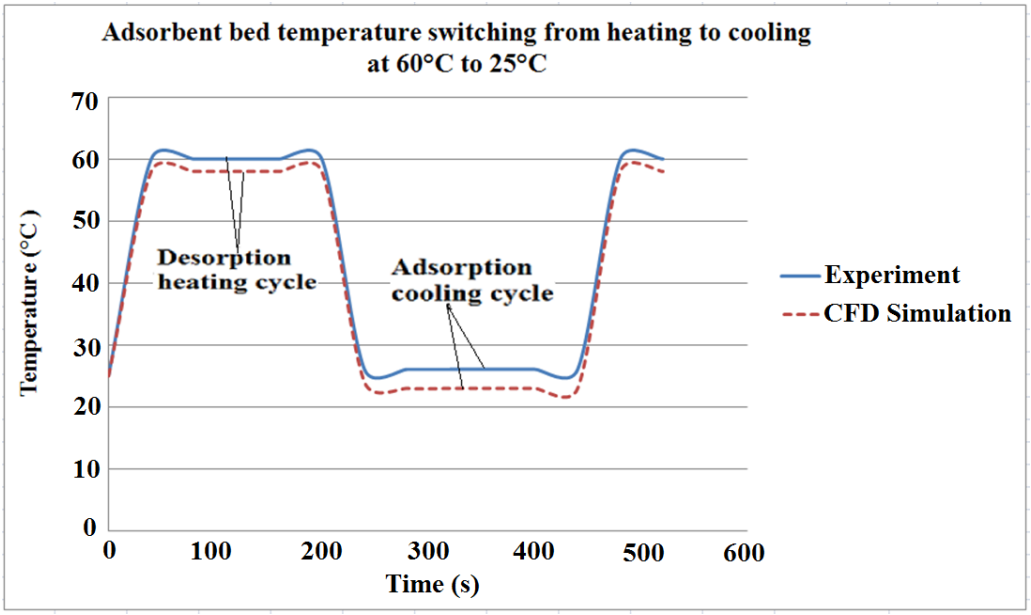

Figure 7.10 Comparison of the outlet temperature between the CFD simulation and the experiment data.

For an adsorption cooling system the operating temperatures are concerned of mainly two operating temperatures are observed in figure 7.10. These are the temperature of desorption heating and the adsorption cooling temperature. It may be important to note that the outlet temperatures of the adsorbent bed are affected by the time constant and error of the temperature sensors. The experimental result is in reality are a collection of the best results and not just a single perfect value of results.

Table.7.4 Temperature Data

Hot water cycle	Inlet temperature	70°C	°C
	Flow velocity	0.5	m/s
	Pressure	101325 Pa	Pa
Chilled water cycle	Inlet temperature	15	°C
	Flow velocity	0.5	m/s
	Pressure	101000 Pa	Pa
Cooling water cycle	Inlet temperature	25	°C
	Flow velocity	0.5	m/s
	Pressure	101325 Pa	Pa

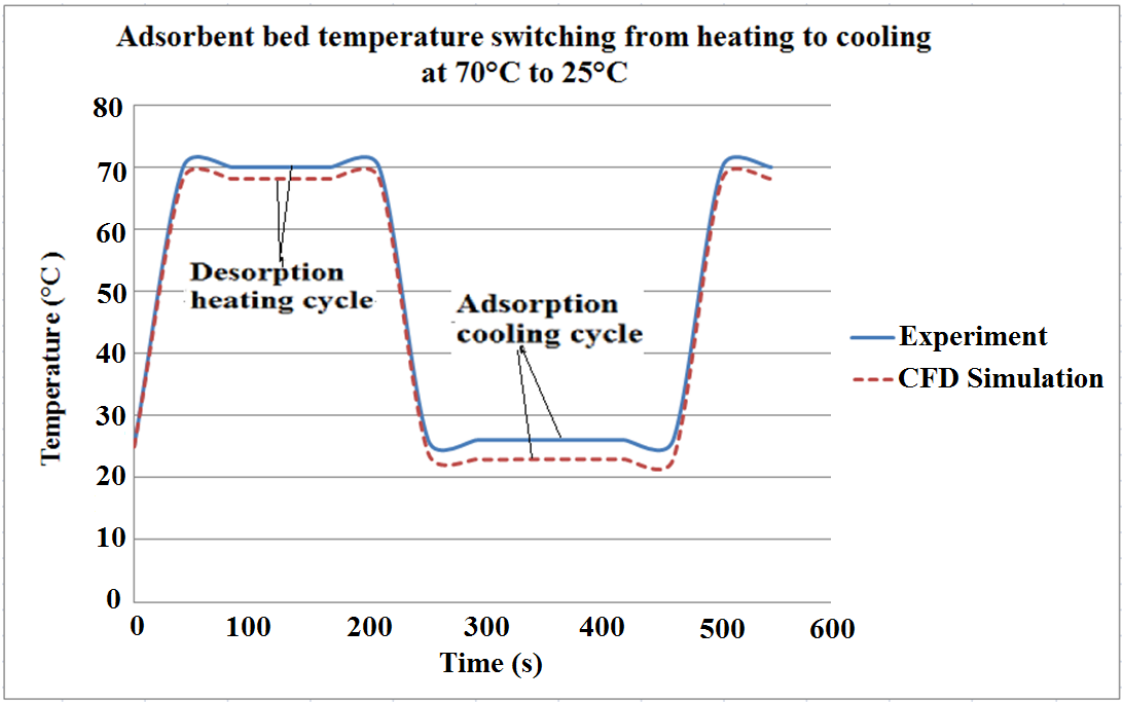

Figure 7.11 Comparison of the outlet temperature between the CFD simulation and the experiment data.

Table 7.5 Temperature Data

Hot water cycle	Inlet temperature	80°C	℃
	Flow velocity	0.5	m/s
	Pressure	101325Pa	Pa
Chilled water cycle	Inlet temperature	15	℃
	Flow velocity	0.5	m/s
	Pressure	101000 Pa	Pa
Cooling water cycle	Inlet temperature	25	℃
	Flow velocity	0.5	m/s
	Pressure	101325 Pa	Pa

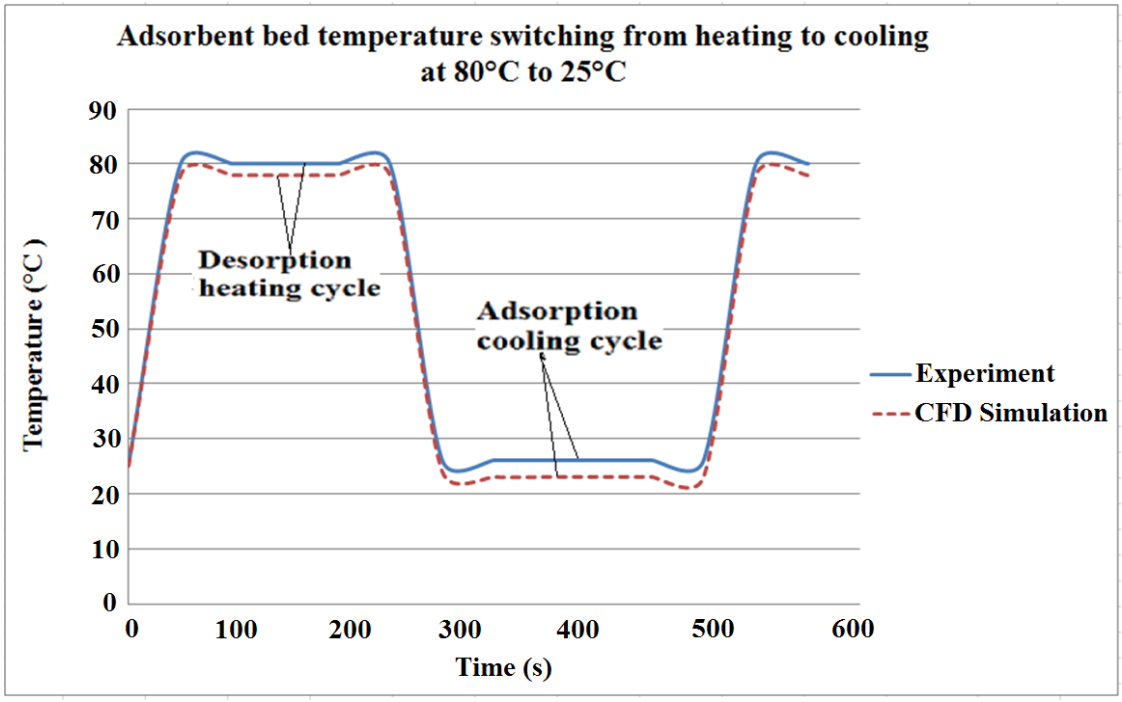

Figure 7.12 Comparison of the outlet temperature between the CFD simulation and the experiment data.

7.8 Validation of CFD Simulation Model

The CFD simulation model was validated with the help of experimental data obtained from tests conducted on the test rig. The flow diagram of the adsorption cooling system processes is shown. The photographic view of the wire fins adsorption test rig is shown in figure.7.5. Measurement results were used as input parameters for the CFD simulation model of the cooling system which was developed to evaluate the performance of this system at different temperature. In the validation of the model of the proposed wire woven fins adsorbent cooling system the test was run so as to accumulate the relevant data for the simulation. The average error between CFD simulation and the experimental data was determined as:

$$\varepsilon = \frac{1}{N}\sum \frac{\left|CalculatedValue - MeasuredValue\right|}{MeasuredValue}$$

Or in percentage

$$\varepsilon[\%] = \frac{1}{N}\sum \frac{\left|CalculatedValue - MeasuredValue\right|}{MeasuredValue}.100 \qquad (7.11)$$

Where

ε is the average error

N is the number of samples,

The system temperatures is an important variable input which influences the performance of the adsorption cooling system. Change occurring at the different temperature during the test was used to study its effect on the cooling capacity and COP of the system. The total cooling adsorption cooling and heating desorption temperature both from the test and simulation data of the system were used as dependent variable and drawn against the inlet temperature as independent variable. Figure.7.8, Figure.7.9, Figure.7.10, Figure.7.11 and Figure.7.12 show the experimental validation of the CFD simulated cooling and heating capacities under varying inlet temperature. The solid lines in all figures show the experimental outlet cooling

and heating temperature variation over time and dots represent the CFD cooling temperature variation over time. It is clear from the observation of these figures that both simulation and test results show same trend i.e., the cooling temperature were proportional. An agreement of validation was observed for most of the data error analysis showed a deviation of 6% and 3.4 % respectively.

7.9 Conclusion

The simulation code has been tested for stability in computation and is able to achieve CFD simulation of the wire woven fin heat exchanger and the different components of the adsorption cooling system. The comparison of CFD simulated results and experimental data proves that the CFD model is reliable tool.

With this simulation tool, the time and cost of designing an adsorption cooling system could be reduced for the design of a one adsorbent bed system as it provides valuable prediction for component performances. With minor modification, it can be extended for use on other configurations of multi-bed system.

CHAPTER 8

CONCLUSIONS AND PROSPECT FOR FUTURE WORK

8.1 Introduction

In addition to the conclusions drawn at the end of each chapter, this chapter sums up the important results and conclusions obtained from the detailed study of earlier works done in the area of adsorption cooling technologies. Additionally, this chapter also presents the main findings of present research. This is followed by relevant recommendations for future research and development.

8.2 Conclusions

The CFD simulation of the adsorption cooling system using copper wire woven finned heat exchanger packed with silica gel has been successfully simulated. CFD comparison study was carried out on a copper wire woven finned and aluminum flat finned heat exchanger. The copper wire woven finned heat exchanger was considered to have better heat transfer performance compared to the aluminum flat fin. The use of CFD simulation approach to simulate adsorption cooling system differs from most simulation work reported in the literature on adsorption cooling systems. The simulation code has been tested for capability of simulating adsorption system heat transfer. A comparison of simulated results and experimental data proves that the CFD simulation model is a reliable tool.

Due to the improvement in porous media CFD simulation, the water vapour uptake or off-take of the adsorbent beds can now be accurately simulated in terms of heat transfer and porous adsorbent bed design. Using CFD simulation code the time and cost of designing an adsorption cooling system could be reduced as it provides valuable prediction for component performances with minor modification.

8.3 Suggestions for Further Work

A solution to the need for a configuration with a larger surface area could be to redesign the adsorbent bed to accommodate a copper wire woven fins heat exchanger. This type of heat exchanger increases the surface area because of the fine wire configuration. The review of the literature indicates a lack of work being carried out on this type of heat exchanger in adsorption cooling systems, leading to the concept design by the researcher of a copper wire woven finned adsorbent bed and a lab test rig to test the performance of this type of heat exchanger. Copper wire woven finned heat exchangers are commonly used in oil heating system. This can be redesigned for adsorbent beds used in adsorption cooling systems and would solve one of the heat transfer problems of the heat exchanger.

In this study, CFD simulation modelling was used to help design a new copper wire woven finned and silica gel adsorbent bed. It is expected that the analysis of this will help contribute towards research and development of adsorption cooling technologies. For this to be achieved, additional research is needed to redesign a full adsorption cooling system that could be used, for example, as a cooler display unit. This system could then be tested against a mechanical vapour system, over a period of time, in order to validate its performance.
In order for this new full adsorption cooling system to have high performance in terms of coefficient of performance the following should be preferred.

1. A copper wire woven heat exchanger should be chosen rather than aluminium flat plate fin heat exchanger since copper has higher thermal efficiency than aluminium and wire fin have a lager surface area than a flat plate fin heat exchanger.

2. The CFD simulation models should be supported with experimental studies of the prototypes. The modelled cycles should be constructed and analysed to further verify the results of CFD simulation models.

3. The number of adsorbent beds in this new design can vary from a two adsorbent bed system up to an infinite number of adsorbent beds so as to improve the performance variables such as heat transfer.

4. Further studies could also be concentrated on the availability of different porous adsorbent refrigerant pairs that could be suitable to be used as packing with this type of copper wire woven heat exchanger. New adsorbent and refrigerant pairs that are available in the literature can be added to the current CFD simulation models in order to study the performance.

As a final remark it is believed that this study forms a basis for the design and development of guidelines for very promising technology within adsorption cooling systems. In the future, with the required research and developments, these systems will commercially be the commonly used air conditioning and refrigeration systems. A concept design of a full adsorption cooling system is shown in figure 8.1 and a basic layout is shown in figure 8.2.

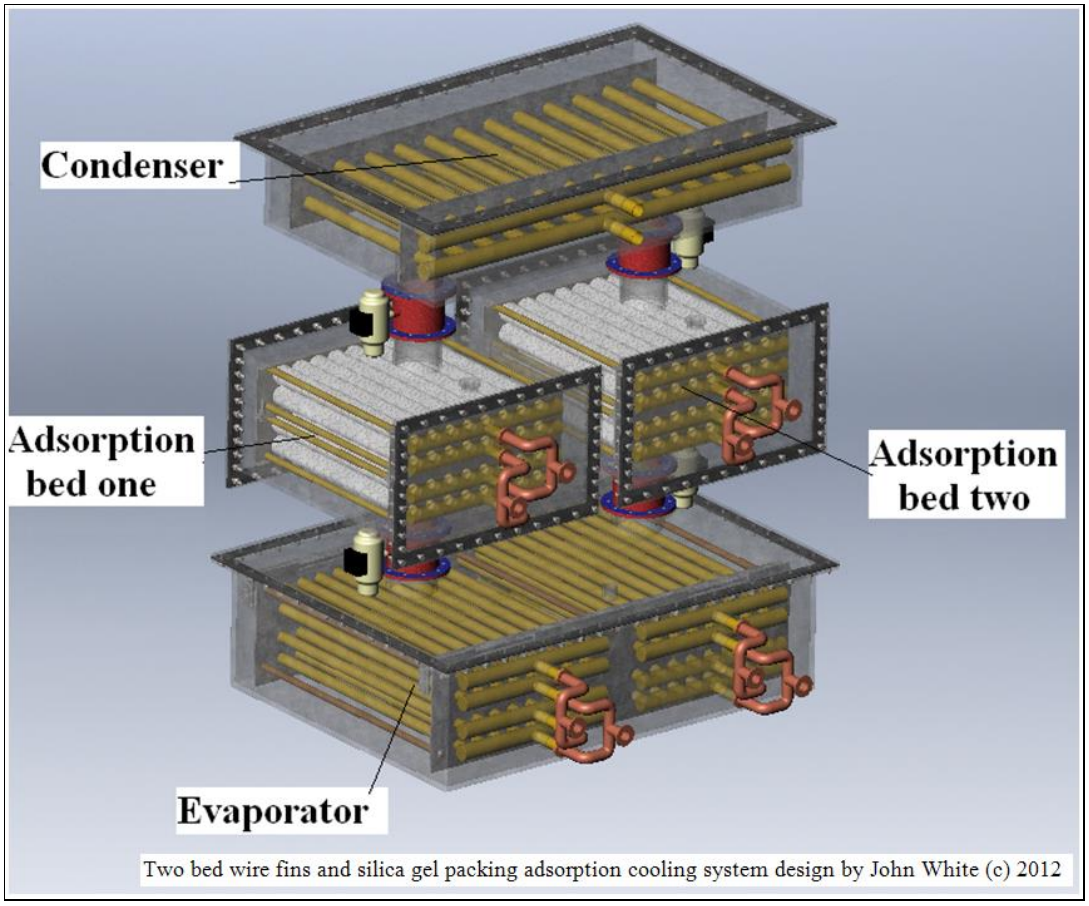

Figure 8.1 Design of Concept Design of adsorption cooling system

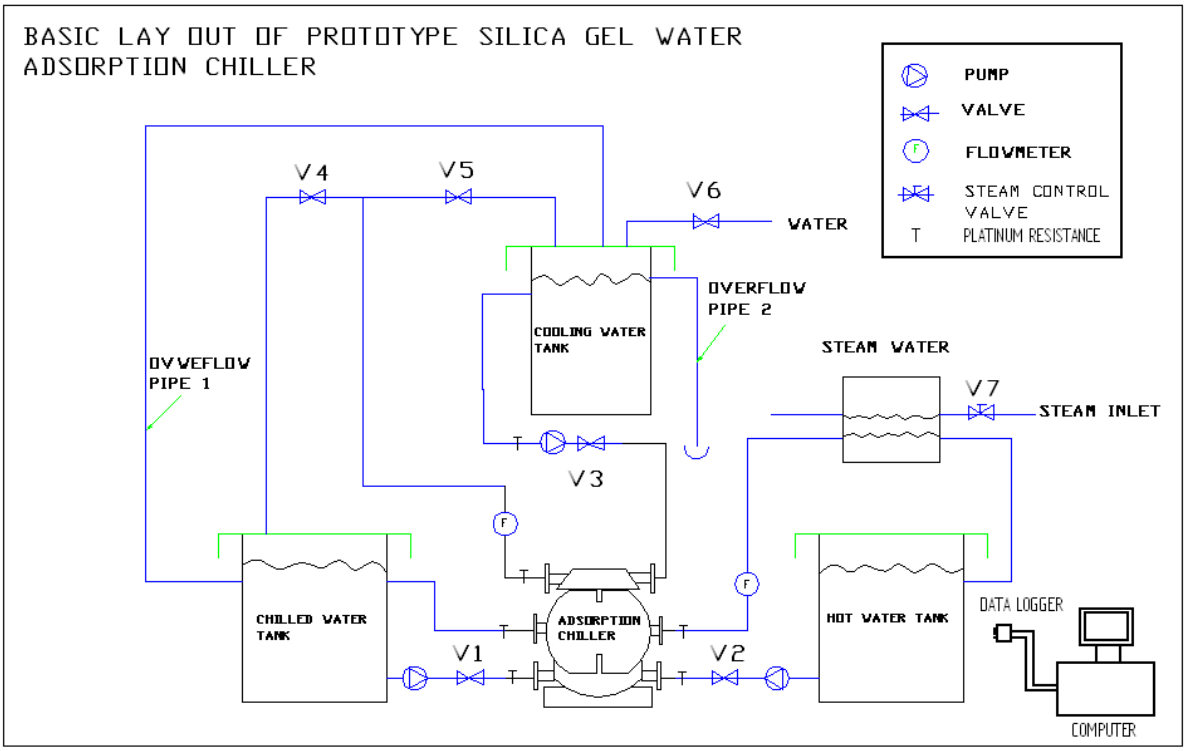

Figure 8.2 Schematic illustration of the adsorption cooling system design

REFERENCES

[1] Augier .F, Laroche .C., Brehon. E. (2008) Application of Computational Fluid Dynamics to Fixed Bed Adsorption Calculations: University of Science and Technology, Beijing.

[2] Mueller, G. E. (1992) Radial void draction distributions in randomly packed fixed bedsof uniformly sized spheres in cylindrical containers in, *Powder Technology*, Vol 72(3) pp. 269-275.

[3] Rahimi, M. and Mohseni, M. (2008) CFD modelling of the effect of absorbent size on absorption performance of a packed bed column in *Korean Journal of Chemical Engineering*, vol. 25, no. 3, pp. 395–401.

[4] Murakami, S, Kato, S., Ito, K. and Zhu Q. (2003) Modelling and CFD prediction for diffusion and adsorption within room with various adsorption isotherms. In *Indoor Air* 13, Supplement 6, pp.20-27.

[5] Critoph, R.E., (1996) Evaluation of alternative refrigerant-adsorbent pairs for refrigeration cycles. Applied Thermal Engineering,.16: p. 891-900.

[6] Kuipers, J.A.M., Van Swaaij, W.P.M., (1998) In Wei, J., Anderson, J., Bischoff, K., Denn, M., Seinfield, J., Stephanopoulos, G., eds.; *Advances in Chemical Engineering*. Academic Press, San Diego, p.227.

[7] Ranade,V., (2002) *Computational Flow Modeling for Chemical Reactor Engineering*. Academic Press, New York.

[8] Nuntaphan Atipoang, Vithayasai Sanparwat, Vorayos Nat, Vorayos Nattanee and Kiatsiriroat Tanongkiat. (2010) Use of oscillating heat pipe technique as extended surface in wire-on-tube heat exchanger for heat transfer enhancement *International Communications in Heat and Mass Transfer* Vol. 37, 287–292

[9] Miller, E.B. (1929) The Development of Silica Gel, Refrigerating Engineering in *The American Society of Refrigerating Engineers.* 17(4) pp. 103-108.

[10] IGT, (1972) Technical feasibility of solid adsorption cooling system, Institute of Gas Technology, Project HC-4-15, December.

[11] Tchernev, D.I., (1979) Solar Air Conditioning and Refrigeration Systems Utilizing zeolites. Proceeding of meetings of Commissions E1-E2, Jerusalem, Issued by International Institute of Refrigeration, pp. 209-215.

[12] Meunier, F. (2002) Sorption Contribution to Climate Change mitigation, in: Proceedings of the International Sorption Heat Pump Conference, Shanghai. September 24-27.

[13] Sakoda, A., & Suzuki, M., (1984) Fundamental study on solar powered adsorption cooling system. *Journal of Chemical Engineering*, Japan, Vol. 17, No. 1pp.52-57.

[14] Sakoda, A. and Suzuki M (1986) Simultaneous Transport of Heat and Adsorbate in Closed Type Adsorption Cooling System Utilizing Solar Heat *Journal of Solar Energy Engineering.* Vol.108, pp.239-245.

[15] Kluppel, R.P. and Gurgel, J.M.A.M. (1988) Solar Cooled Drinking Fountain. *Sunworld*, Vol 12, No 4, pp 113-4.

[16] Cho, S.H. and Kim, J.N., (1992) Modelling of a Silica Gel/Water Adsorption-Cooling System, *Energy*, Vol. 17, No.9, pp.829-39.

[17] Watabe, Y. and Yanadori M., (1994).Cooling characteristic of adsorpti refrigeration apparatus using silica gel-ethanol system. *Kagakii Kogakii Ronbunshu*, Vol.20, No.4, pp.589-593.

[18] Saha, B.B., Boelman, E.C., and Kashiwagi, (1995).T. Computational analysis of an advanced adsorption-refrigeration cycle, *Energy*, Vol. 20, No 10, pp.983-94

[19] Boelman, E.C., Saha, B.B., and Kashiwagi, T., (1997). Parametric Study of a Silica Gel-water Adsorption Refrigeration Cycle-the Influence of Thermal Capacitance and Heat Exchanger UAvalues on Cooling Capacity, Power Density, and COP. *ASHRAE Transactions*, Vol 103. No 1, pp.l37-48

[20] Alam et.al (2000) Heat exchanger design effect on the system performance of silica gel water adsorption system *International Journal of Heat Mass Transfer.* Vol.43. pp. 4419-4431.

[21] Anyanwu E.E., and Ezekwe C.I., (2003) Design, construction and test run of a solid adsorption solar refrigerator using activated carbon/methanol, as adsorbent/adsorbate pair, *Energy Conversion and Management* (44) pp 2879-2892

[22] Tanaka S., Hasegawa T., and Waki T. (1983) On the integrated solar collector-chiller using the intermittent adsorption cycle. *I.S.E.S. Solar World Congress,* August 14-19, Perth.

[23] Wang, R.Z., and Oliveira, R.G., (2005). Adsorption refrigeration An Efficient Way to Make Good Use of Waste Heat and Solar Energy *Proceedings of International Sorption Heat Pump* Conference, Denver, USA.

[24] Anyanwu, E.E, and Ogueke, N.V., (2005) Thermodynamic design procedure for solid adsorption solar refrigerator, *Renewable Energy* (30) pp. 81-96.

[25] Chang W.-S, Wang C.-C and Shieh C.-C (2005) Experimental study of a solid adsorption cooling system using flat-tube heat exchangers as adsorption bed Applied Thermal Engineering 27 2195–2199.

[26] Jakob, I., and Walter Mittelbach, W., (2008) Development and Investigation of a Compact silica gel/water adsorption chiller integrated in solar cooling systems, VII Minsk, International Seminar, "Heat, Pumps, Refrigerators, Power Sources". Minsk, Belarus, September 8-11.

[27] Rouquerol. J., et al (1994) Recommendations for the characterization of porous solids (Technical Report) *International Union of Pure and Applied Chemistry,* Vol.66, No.8, pp.1739-1758

[28] Liu, Y., Leong. K.C., (2005) The effect of operating conditions on the performance of zeolite/water adsorption cooling systems. *Technological University Applied Thermal Engineering*, Vol.25 (10) pp. 1403–1418.

[29] Menard D., Py X., Mazet N., (2005) Activated carbon monolith of high thermal conductivity for adsorption processes improvement Part A: Adsorption step, *Chemical Engineering and Processing* Vol 44(9) pp. 1029–1038.

[30] Saha, B.B., El-Sharkawy, I.I, Chakraborty, A., Koyama, S. (2007) Study on an activated carbon fiber–ethanol adsorption chiller. Part II, Performance evaluation. *Internation Journal Refrigeration,* Vol.30. (1) pp.96–102.

[31] Huang, J., et al., (2007) Adsorption studies of a water soluble dye, Reactive Red MF-3B, using sonication-surfactant-modified attapulgite clay. *Journal of Hazardous Materials* Vol.143, pp 541–548.

[32] Hai-Jun, C., .et al., (2008) Attapulgite based LiCl composite adsorbents for cooling and air conditioning applications, *Applied Thermal Engineering.* Vol. 28 pp. 2187–2193.

[33] Wang, L.W., (2009). A review on adsorption working pairs for refrigeration, *Renewable and Sustainable Energy.* Vol.13 (3) pp.518-534.

[34] Dabrowski, A., (2001) Adsorption-from theory to practice. *Advances in Colloid and Interface Science* Vol. 93 pp. 136-224.

[35] Fripiat, J.J., Gatineau, L., Van Damme, H (1986), Multilayer Physical Adsorption on Fractal Surfaces, *Langmuir,* Vol.2 (5) pp. 565-567.

[36] Qiu, S., and Zhu. G., (2009) Molecular engineering for synthesizing novel structures of metal–organic frameworks with multifunctional properties *Coordination Chemsistry Reviews,* Vol 253 (23) pp. 2892-2910.

[37] Aranovich, G., and Donohue, M., (1998) Analysis of Adsorption Isotherms: Lattice Theory Predictions, Classification of Isotherms for Gas–Solid Equilibria, and Similarities in Gas and Liquid Adsorption Behavior. *Journal of Colloid and Interface Science* Vol.200 (2), pp. 273-290.

[38] Sangwichien, C., Aranovich, G.L., and Donohue, M.D., (2002) Density functional theory predictions of adsorption isotherms with hysteresis loops. *Colloids and Surfaces A: Physicochemical and Engineering Aspects*, 206, pp. 313–320.

[39] Somorjai, G.A., (1972) *Principles of Surface Chemistry*, Prentice-Hall, Englewood Cliffs, N. J.

[40] San J.Y., Wei-Min Lin W.M, (2008) Comparison among three adsorption pairs for using as the working substances in a multi-bed adsorption heat pump, *Applied Thermal Engineering.* Vol 28, Issues 8-9, pp. 801-11-8.

[41] Sing, K.S.W., (2004) Characterization of porous materials: past, present and future, *Colloids and Surfaces A: Physicochemical Engineering Aspects*. 241, pp.3-7.

[42] Chua, H.T., Ng, K.C., Chakraborty, A., Nay, M.O. and Othman, M.A., (2002) Adsorption characteristic of silica gel + water systems, *Journal of Chemical and Engineering Data*, Vol. 47, pp.1177-1181.

[43] Rouquerol, J. Davy, L., (1978) Automatic gravimetric apparatus for recording the adsorption isotherms of gases or vapours onto solids, *Thermochemical Acta*, Vol. 24 (2), pp. 391-397.

[44] Yong, L., and Wang, R.Z. (2006) Adsorption Refrigeration: A Survey of Novel Technologies *Recent Patent on Engineering*, 2007 (1) pp. 1-21.

[45] Marletta, L., Maggio, G., Freni, A. , Ingrasciotta, M, and Restuccia, G., (2002) A non-uniform temperature non-uniform pressure dynamic model of heat and mass transfer in compact adsorbent beds *International Journal of Heat and Mass Transfer*, Vol. 45 pp. 3321-3330.

[46] Wang, R.Z. (2001) Adsorption refrigeration research in Shanghai Jiao Tong University. *Renewable and Sustainable Energy Reviews*; 5:1-37.

[47] Wang, R.Z, Oliveira, R. G., (2005) Adsorption Refrigeration - An Efficient Way to Make Good Use of Waste Heat and Solar Energy. *International Sorption Heat Pump Conference* June 22-24, Denver, Colorado, USA.

[48] Jakob, U., (2008**)** Development and Investigation of Compact Silica Gel Water Adsorption Chiller Integrated in Solar Cooling Systems, *Heat Pipes, Heat Pumps, Refrigerators and Power Sources,* Minsk, Belarus, September 8-11.

[49] Dunne, S. Carousel, (1996)Heat Exchanger for Sorption Cooling Process, US Patent No. 5503222, Issued, April 2, 1996.

[50] Critoph, R.E., and Zhong. Y., (2004) Review of Trends in Solid Sorption Refrigeration and Heat Pumping Technology *Invited Review Paper, Journal of Process* Engineering *Proc. IMechE, Part E* Vol 219 pp.285-300 .

[51] Fan,Y., Luo, L., Souyri, B., (2007) Review of Solar Sorption Refrigeration Technologies: Development and Applications. *Renewable and Sustainable Energy Revi*ews Vol. 11, pp. 1758–1775.

[52] Kopanidis, A. Theodorakakos (2008) Numerical Simulation of Fluid Flow and Heat Transfer with Direct Modelling of Microscale Geometry. *5th European Thermal-Sciences Conference,* The Netherlands.

[53] Augier, F., Doux F.I., Delenne, J.Y. (2010) Numerical Simulations of Transfer and Transport Properties inside Packed Beds of Spherical Particles a Process Modelling and Design Division, *Chemical Engineering Science,* Vo. 65. Pp 1055-1064

[54] Jiyuan Tu, Guan H.Y and Chaoqun Liu (2008) Computational Fluid Dynamics A Practical Approach, *Butterworth Heinemann Publication* ISBN 978-0-7506-8563-4

[55] Jafari, M. A., Zamankhan, P., Mousavi, S.M., . Pietarinen, K., (2008) Modelling and CFD Simulation of Flow Behaviour and Dispersivity through Randomly Packed Bed Reactors *Chemical Engineering Journal,* Vol. 144 (3) pp. 476-482

[56] Riffel, D.B. , Belo, F. A., (2007) Simulation of a Shell-and-Tube Heat Exchanger for Solar Adsorption Chiller., *Heat SET, Heat Transfer in Component and Systems for Sustainable Energy Technologies,* 18-20 April, Chambery, France

[57] Ahn, B. J., and Zoulalian, A., (1986) Axial Dispersion in Packed Beds with Large Wall Eeffect, *AIChE Journal* Vol. 32 (1) pp 170–174.

[58] Kwapinski, W., Winterberg, M., Tsotsas, E., Mewes, D., (2004) Modelling of the Wall Effect in Packed Bed Adsorption, *Chemical Engineering and Technology*. Vol. 27 (11) pp. 1179–1186.

[59] Wu, Y.X., Wang, X., Ching, C.B. (2002) Computational Fluid Dynamics Simulation of the Adsorption Separation of Three Components in High Performance Liquid Chromatography, *Chromatographia* Vol. 55 (7/8) pp. 439–445.

[60] Andersson, K. E. B. (1961). "Pressure drop in ideal fluidization",*Chemical Engineering Science,* Vol. 15, pp 276–297.

[61] Ergun, S. (1952) "Fluid flow through packed columns," *Chemical Engineering Progress*, vol. 48, pp. 89–94.

[62] Guo, G., , Dai. R. (2010) "Numerical Simulation of Flow and Heat Transfer in a Random Packed Bed", *Particuology"* Vol. 8 (3) pp.293-299.

[63] Dixon, A.G., and Cresswell, D. L. (1986) "Effective heat transfer parameters for transient packed-bed models," *AIChE Journal*, vol. 32, no. 5, pp. 809–819.

[64] Valdes- Parada, F,J., Ochoa-Tapia, J. A., and Alvarez-Ramirez , J. (2007) "Effective medium equations for fractional Fick's law in Porous Media" Francisco J. *Physica A: Statistical Mechanics and its Applications*, Vol. 373 pp. 339-353.

[65] Winterberg, M., and Tsotsas, E. (2000) "Impact of Tube-to-Particle-Diameter Ratio on Pressure Drop in Packed Beds", *AIChe Journal,* Vol 46 (5) pp. 108-188

[66] Murakami, S., Kato,S., Ito,K., and Zhu, Q. (2003) "Modelling and CFD prediction for diffusion and adsorption within room with various adsorption isotherms," *Indoor Air,* Vol. 13 (6) pp. 20–27

[67] Pozrikidis, C. (1997) Introduction to Theoretical and Computational Fluid Dynamics. New York/Oxford, Oxford University Press

[68] Tu, J., Yeah, G-H. and Lui, C. (2008) Computational Fluid Dynamics: A Practical Approach, Amsterdam/Boston: Butterworth Heinemann

[69] Kwapinski, W., Winterberg, M., Tsotsas, E., Mewes, D.,(2004) " Modelling of the Wall Effect in Packed Bed Adsorption", *Chemical Engineering and Technology*. Vol. 27 (11) pp. 1179–1186.

[70] Findenegg, G. H. (1983) *Fundamentals of Adsorption* (Engineering Foundation, New. York), pp. 207–218.

[71] Riffel, D.B. , et, al. (2007) "Simulation of a Shell-and-Tube Heat Exchanger for Solar Adsorption Chiller.", *Heat SET, Heat Transfer in Component and Systems for Sustainable Energy Technologies,* 18-20 April, Chambery, France.

[72] Guardo, A, Coussirat, M., Larrayoz, M. A., Recasens, F R. "CFD Flow and mass transfer simulation in a packed bed with supercritical solvent: Preliminary results " Chemical Engineering Department. Fluid Mechanics Department, Universitat Politècnica de Catalunya.Barcelona, Spain. *Online paper,*

[73] Yuana, Y, Hana, M., Chenga, Y, Wanga, D., Jina, Y. (2005) "Experimental and CFD analysis of two-phase cross/counter current flow in the packed column with a novel internal" *Chemical Engineering Science,* Vol. 60 (5) pp.6210-6216.

[74] Calis, H. P. A. et al. (2001) "CFD modelling and experimental validation of pressure drop and flow profile in a novel structured catalytic reactor packing." *Chemical Engineering Science,* Vol 56 pp. 1713–1720.

[75] Jafari , A., Zamankhan, P., Mousavi, S.M., Pietarinen. K. (2008) "Modelling and CFD Simulation of Flow Behaviour and Dispersivity Through Randomly Packed Bed Reactors" *Chemical Engineering Journal,* Vol. 144 (3) pp.476-482.

[76] Gu, A., Aibing, Y., Wright, B., and Zulli, P. (2006) "Simulation of Turbulent Flow in a Packed Bed" *Chemical and Engineering Technology"* Vol.29 (5) 596-603.

[77] Chandesris A. M., Serre, G., Sagaut, P. (2006) "Macroscopic Turbulence Model for Flow in Porous Media Suited for Channel, Pipe and Rod Bundle Flows" *International Journal of Heat and Mass Transfer,* Vol. 49 (15-16) pp. 2739 -2750.

[78] Salim .M. et. Al (2009) Strategy for Dealing with Wall-bounded Turbulent Flows *Proceedings of the International Multi Conference of Engineers and Computer Scientists 2009* Vol II IMECS 2009, March 18 - 20, Hong Kong.

[79] Siriboonluckul, N., and Juntasaro, V. (2007) "Turbulence Modelling for Wall-bounded Particle-laden Flow with Separation" Vol. 34. (3). pp.331-338.

[80] Kirkgoz, M. S., Oner A. A. Akoz, M.S. (2009) "Numerical Modelling of Interaction of a Current with a Circular Cylinder near a Rigid Bed" *Advances in Engineering Software* Vol.40 (3) pp.1190 -1199.

[81] White, J. (2012) "A CFD Simulation on How the Different Sizes of Silica Gel Will Affect the Adsorption Performance of Silica Gel", Modelling and Simulation in Engineering, vol. 2012, Article ID 651434, 12 pages. Hindawi Publishing Corporation. Published online January 2012.

[82] Bertil Andersson, K.E., (1961) "Pressure drop in ideal fluidization," *Chemical Engineering Science*, vol. 15, no. 3-4, pp. 276–297.

[83] Molerus, O.,and Schweinzer, J., (1989) "Resistance of particle beds at Reynolds numbers up to Re 104," *Chemical Engineering Science*, vol. 44, no. 5, pp. 1071–1079,

[84] Steger, J. L., and Benek, J.A (1987) "On the use of composite grid schemes in computational aerodynamics," *Computer Methods in Applied Mechanics and Engineering*, vol. 64, no. 1-3, pp. 301–320,

[85] A-Akahira, A., Amanul Alam, K.C., Yoshinori Hamamoto (2005), Atsushi Akisawa, and Takao Kashiwagi, "Experimental investigation of mass recovery adsorption refrigeration cycle," *International Journal of Refrigeration*, vol. 28, no. 4, pp. 565–572,.

[86] Chang, K.S., Chen, M.T., Chung, T.W., (2005) "Effects of the thickness and particle size of silica gel onthe heat and mass transfer performance of a silica gel-coated bed for air-conditioning adsorption systems," *Applied Thermal Engineering*, vol. 25, no. 14-15, pp. 2330–2340,.

[87] Liou, May-Fun, (2005) *A numerical study of transport phenomena in porous media*, Ph.D. thesis, Case Western Reserve University, 2005.

[88] Kopanidis, K., and Theodorakakos, A (2008) "Numerical simulation of Fluid Flow and Heat Transfer with Direct Modelling of Microscale Geometry," in *Proceedings of the 5th European Thermal-Sciences Conference*, The Netherlands, 2008.

[89] Anikeenko, A.V., Medvedev, N.N., Kovalev, M.K., and Melgunov M.S., (2009) , "Simulation of gas diffusion in porous layers of varying structure," *Journal of Structural Chemistry*, vol. 50, no. 3, pp. 403–410,

[90] Wang, D.C., Wu, J.Y., Xiaa, Z.Z., Zhaia, H., Wanga, R.H., and Dou, W.D. (2005) "Study of a novel silica gel - water adsorption chiller. Part II. Experimental study," *International Journal of Refrigeration*, vol. 28, no. 7, pp. 1084–1091

[91] Akahira, A., and K. C. A. Alam K.C.A., (2005) , "Experimental Investigation of mass Recovery Adsorption Refrigeration Cycle," *International Journal of Refrigeration*, vol. 28, no. 4, pp. 565–572

[92] Murakami, 5., Kato,S., Ito,K., and Zhu, Q., (2003) "Modeling and CFD prediction for diffusion and adsorption within room with various adsorption isotherms," *Indoor Air*, vol. 13, no. 6, pp. 20–27

[93] Akisawa, A., Saha, B.B., Ng, K.G., et al., (2001) "Experimental investigation of the Silica Gel-Water Adsorption Isotherm Characteristics," *Applied Thermal Engineering*, vol. 21, no. 16, pp. 1631–1642

[94] Hellstr¨om, J.G.I., and Lundstr¨om, T.S., (2006) "Flow through Porous Aedia at Moderate Reynolds Number," in *Proceedings of the 4th International Scientific Colloquium Modelling for Material Processing*, Riga, Latvia, June 2006.

[95] Sing, K.S.W., (1996) "Adsorption methods for the characterization of porous materials," *Advances in Colloid and Interface Science*, vol. 76-77, pp. 3–11

[96] Gelb, L.D., and Gubbins, K.E.,(1998) “Characterization of porous glasses: Simulation Models, Adsorption Isotherms, and the Brunauer-Emmett-Teller analysis Method,” *Langmuir,* vol. 14, no. 8, pp. 2097–2111

[97] Liou, M/F., (2005) *A numerical study of transport phenomena in porous media*, Ph.D. thesis, Department of Mechanical and Aerospace Engineering, Case Western Reserve University, 2005

[98] Inaba,H. Seo, J.K., and Horibe, A., (2004) “Numerical study on adsorption enhancement of rectangular adsorption bed,” *Heat and Mass Transfer,* vol. 41, no. 2, pp. 133–146.

[99] Horv´ath, C., and. Lin, H.-J., (1978) “Band Spreading in Liquid Chromatography: General Plate Height Equation and a Method for the Evaluation of the Individual Plate Height Contributions,” *Journal of Chromatography A*, vol. 149, pp. 43–70

[100] Goworek, J., and Stefaniak, W., (1992) “Investigation on the Porosity of Silica Gel by Thermal Desorption of Liquids,” *Materials Chemistry and Physics*, vol. 32, no. 3, pp. 244–248

[101] Lienhard, IV J. H., and Lienhard, V. J. H., (2005). “A Heat Transfer Text Book,” 3rd, Edition, Phlogiston Press, New York, p. 164,612,

[102] NQ, K.C., et al. (2001) “Experimental Investigation of the Silica Gel- Water Adsorption Isotherm Characteristics” *Applied Thermal Engineering,* Vol 21, pp.1631 – 1642

[103] Kopanidis, A., Theodorakakos, A. (2008) Numerical simulation of fluid flow and heat transfer with direct modelling of microscale geometry. Dept. of Engineering and Management of Energy Resources, University of Western Macedonia 5th European Thermal-Sciences Conference, The Netherlands.

[104] D.C. Wanga, J.Y. Wu. (2005) "Study of a novel silica gel–water adsorption chiller. Part II. Experimental Study" *International Journal of Refrigeration,* Vol. 28, pp. 1084 -1091

[105] Yovanovich M.M., Marotta E.E.,(2003) Thermal spreading and contact resistances, in: A. Bejan, D. Kraus (Eds.), Heat Transfer Handbook, John Wiley and Sons Inc., Hoboken, New York, USA, (Chapter 4).

[106] Lambert, M. A., and Jones, B. J., 2006, "Automotive Adsorption Air Conditioner Powered by Exhaust Heat. Part 1: Conceptual and Embodiment Design," *Proceedings of the Institution of Mechanical Engineers, Part D: Journal of Automobile Engineering*. **220**(7): pp. 959-972.

[107] Hellström J. G. I., Lundström T. S. (2006) "Flow through Porous Media at Moderate Reynolds Number" Modelling for Material Processing International Scientific Colloquium, June 8-9, 2006

[108] Inaba. H., Seo. J. K., Horibe. A. (2004) Numerical study on adsorption enhancement of rectangular adsorption bed. *Heat and Mass Transfer,* Volume 41, Number 2 pp. 133-146

[109] Liou. M-F. (2005) "A Numerical Study of Transport Phenomena in Porous Media Department of Mechanical and Aerospace Engineering" Case Western Reserve University" PhD, Thesis.

[110] Murakami, 5. Kato,S., Ito,K., and Zhu, Q., (2003) "Modeling and CFD prediction for diffusion and adsorption within room with various adsorption isotherms," *Indoor Air*, vol. 13, no. 6, pp. 20–27

[111] Wu, Y.X., Yu, H.W., and Ching, C.B. (2004) "A Computational Fluid Dynamics Study of Binary Adsorption Separation in Chromatography". *Chemical Engineering Technology,* Vol. 27 (3) , pp .955-966

[112] Steger, J. L., and Benek, J.A. (1987) "On the use of composite grid schemes in computational aerodynamics," *Computer Methods in Applied Mechanics and Engineering*, vol. 64, no. 1-3, pp. 301–320

[113] Zhang. L.Z. (2000) "Design and testing of an automobile waste heat adsorption cooling system", *Applied Thermal Engineering*, vol. 20 (2000) 103-114

[114] Kopanidis, K., and Theodorakakos, A. (2008) "Numerical simulation of Fluid Flow and Heat Transfer with Direct Modelling of Microscale Geometry," in *Proceedings of the 5th European Thermal-Sciences Conference*, The Netherlands, 2008

[115] NQ, K.C., et al. (2001) "Experimental Investigation of the Silica Gel-Water Adsorption Isotherm Characteristics" *Applied Thermal Engineering,* Vol.21, pp.1631 – 1642

[116] Akahira, A., et al. (2005), "Experimental investigation of mass recovery adsorption refrigeration cycle," *International Journal of Refrigeration*, vol. 28, no. 4, pp. 565–572

[117] Kopanidis, K., and Theodorakakos, A (2008) "Numerical simulation of Fluid Flow and Heat Transfer with Direct Modelling of Microscale Geometry," in *Proceedings of the 5th European Thermal-Sciences Conference,* The Netherlands, 2008

[118] Murakami, 5., Kato,S., Ito, K., and Zhu, Q. (2003) "Modeling and CFD prediction for diffusion and adsorption within room with various adsorption isotherms," *Indoor Air*, vol. 13, no. 6, pp. 20–27

[119] Wagner Wolfgang and Kruse Alfred (1998) "Properties of water and steam: the industrial standard IAPWS-IF97 for the thermodynamic properties and supplementary equations for other properties, Second edition ISBN 978-3-540-21419-9.

[120] Binder, R.C. (1973), Fluid Mechanics, 5th Edition. (Englewood Cliffs, NJ) Prentice-Hall, Inc

[122] Bellot JC , Condoret JS (1991) Liquid Chromatography Modelling: A Review. Process Biochemistry 26:363

[123] Guiochon G (1996) Book Review. Journal of Chromatography A 734:423.

[124] Reverchon E, Lamberti G. Subra P (1998) Modelling and Simulation of the Supercritical Adsoption of Complex Terpene Mixtures. Chemical Engineering Science 53:3537

[125] G.S.H. Lock (1994) Latent Heat Transfer: An Introduction to Fundamentals Oxford Engineering Science Series publications ISBN 13: 9780198562849

[126] C. A. Truesdell, III (1991) A First Course in Rational Continuum Mechanics. Vol. 1: General Concepts, 2nd ed., Academic Press. ISBN 0-12-701300-8. Sects. I.8-10.

[127] Ali, M. M. and Ramadhyani, S. (1992) Experiment on connective heat transfer in corrugate channels, Experimental Heat Transfer, Vol. 5, pp. 175-193.

[128] Beecher, D. T. and Fagan, T. J. (1987) Effect of fin pattern on the air-side heat transfer coefficient in plate finnedtube heat exchangers, ASHRAE Trans, Vol. 93, pp. 1961-1984.

[129] Ito, M., Kimura, H. and Senshu, T. (1977) Development of high efficiency air-cooled heat exchanger, Hitachi Review, Vol. 26, pp. 323-327.

[130] Rogers GFC, Mayhew YR. (1988) Thermodynamic and Transport Properties of Fluids: SI Units (4th Edition) ISBN-10: 0631902651

[131] Liu.Y.L., Wang R.Z. and Xia Z.Z. (2005) Experimental study on a continuous adsorption water chiller with novel design. *International Journal of Refrigeration 218–230*

Appendix A

CERTIFICATE OF ANALYSIS

Product name: SILICA GEL A TYPE, 0.5-1.5 MM BROKEN PIECES, MOISTURE CONTENT <1.5%
Lot No.: 487937
Report date: OCT. 13, 2008
Quantity: 20000KG
Contract No.:

Items		Standard	Results
Qualified ratio of particle size	>1.5 MM	<5.0	4.00
	<0.5 MM	<5.0	1.40
Adsorption capacity %	RH=20%, ≥%	10	11.2
	RH=40%, ≥%	21	23.7
	RH=80%, ≥%	32	35.1
Loss on heating, 180℃ ≤%		2	1.36
Qualified ratio of spherical granules, % ≥		---	---
Ph		4 - 8	4.1
Bulk density, g/l ≥		730	780
Specific Resistance, Ω. cm ≥		3500	8000

Date: OCT. 13, 2008
Name: Kang Liu
Signature :

Qingdao Winsorb Limited

No. 9, Shandong Road, Qingdao, China, P.C. 266071

Ph.: +86-532-82075033 Fax: +86-532-85847865

Email: Kang.Liu@winsorb.com

CERTIFICATE OF ANALYSIS

Product name: WHITE SILICA GEL, 1-2 MM BEADS
Lot No.: 811061 (787021)
Report date: NOV. 15, 2008
Quantity: 20000KG
Contract No.:

ITEMS		Standard	Results
Adsorption capacity %	RH=20%, ≥%	10.5	11.1
	RH=50%, ≥%	26	27.2
	RH=90%, ≥%	36	36.5
Loss on heating, 170℃ ≤%		2	1.50
Ph		4 - 8	4.25
Bulk density, g/l ≥		720	775
Qualified ratio of spherical particle, % ≥		95	96
Specific resistance, Ω,cm, ≥		4000	4500

Date: NOV. 15, 2008
Name: Liu Kang
Signature :

No. 9, Shandong Road, Qingdao, China, P.O. 266071
Ph.: +86-532-82075033 Fax: +86-532-85847865
Email: Kang.Liu@winsorb.com

CERTIFICATE OF ANALYSIS

Product name: WHITE SILICA GEL IRREGULAR GRANULES (A TYPE CRYSTALS), 1.0 – 3.0 MM
Lot No.: 487910
Report date: SEP. 02, 2008
Quantity: 16000KG
Contract No.:

Items		Standard	Results
Qualified ratio of particle size	>3.0 MM	<5.0	2.00
	<1.0 MM	<5.0	1.50
Adsorption capacity %	RH=20%, ≥%	10	10.6
	RH=40%, ≥%	21	22.4
	RH=80%, ≥%	32	36.8
Loss on heating, 170℃ ≤%		2	1.10
Qualified ratio of spherical granules, % ≥		---	---
Ph		4 - 8	4.4
Bulk density, g/l ≥		730	772
Specific Resistance, Ω. cm ≥		3500	4500

Qingdao Winsorb Limited

No. 9, Shandong Road, Qingdao, China, P.C. 266071

Ph.: +86-532-82075033 Fax: +86-532-85847865

Email: Kang.Liu@winsorb.com

CERTIFICATE OF ANALYSIS

Product name: ORANGE SILICA GEL 2.0-5.0 MM BEADS
Lot No.: 787987
Report date: OCT. 09, 2008
Quantity: 10000KG
Contract No.:

Items		Standard
Appearance		Semitransparent orange beads
Qualified ratio of beads, >= %		96.0
Absorption (%)	RH=20%, >= %	9.0
	RH=35%, >= %	15.0
	RH=50%, >= %	24.0
Loss on heating, <= %		2.0
Bulk density, g/L		750
Color Variation	RH=20%, >= %	Orange
	RH=35%, >= %	Light green
	RH=50%, >= %	Light blue

Qingdao Winsorb Limited

No. 9, Shandong Road, Qingdao, China, P.O. 266071

Ph.: +86-532-82075033 Fax: +86-532-85847865

Email: Kang.Liu@winsorb.com

CERTIFICATE OF ANALYSIS

Product name: SILICA GEL WHITE B TYPE, 2-4 MM BEADS
Lot No.: 5575149
Report date: DEC. 10, 2007
Quantity: 14200KG
Contract No.:

Items		Standard	Results
Adsorption capacity %	RH=20%, ≥%	3	6.0
	RH=50%, ≥%	10	14.4
	RH=90%, ≥%	50	76.1
Loss on heating, 170℃ ≤%		2	1.10
Qualified ratio of spherical granules, % ≥		---	---
Ph		4 - 8	6.9
Bulk density, g/l ≥		500 - 600	531
Specific Resistance, Ω. cm ≥		≥3000	5500

Appendix B

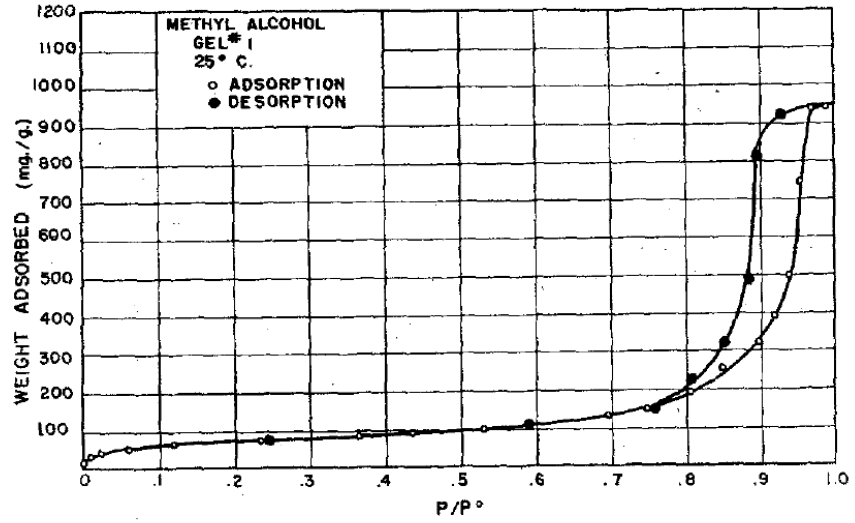

A

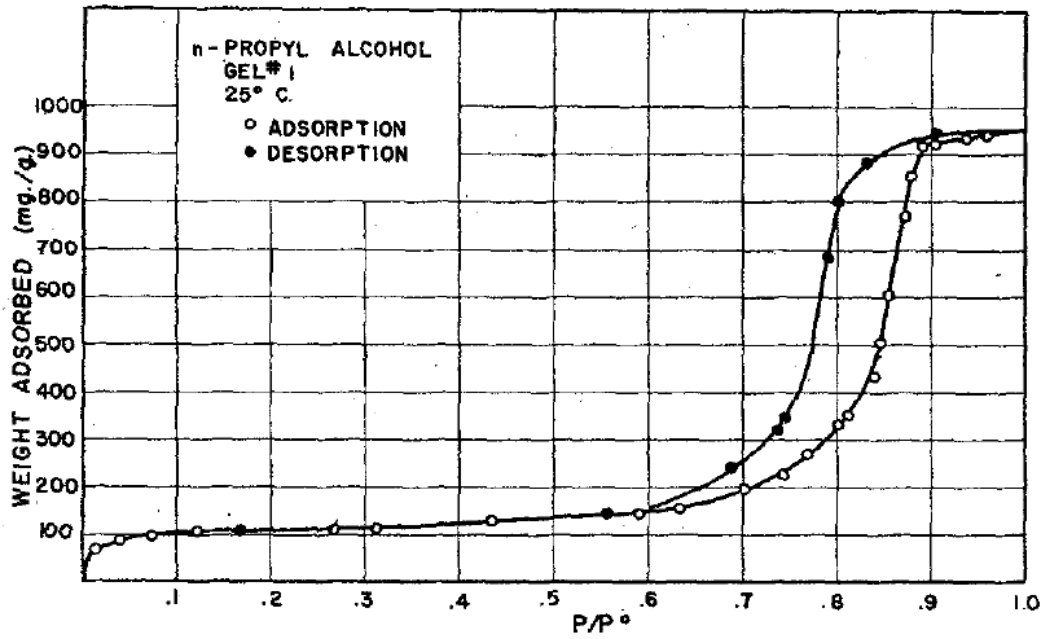

B

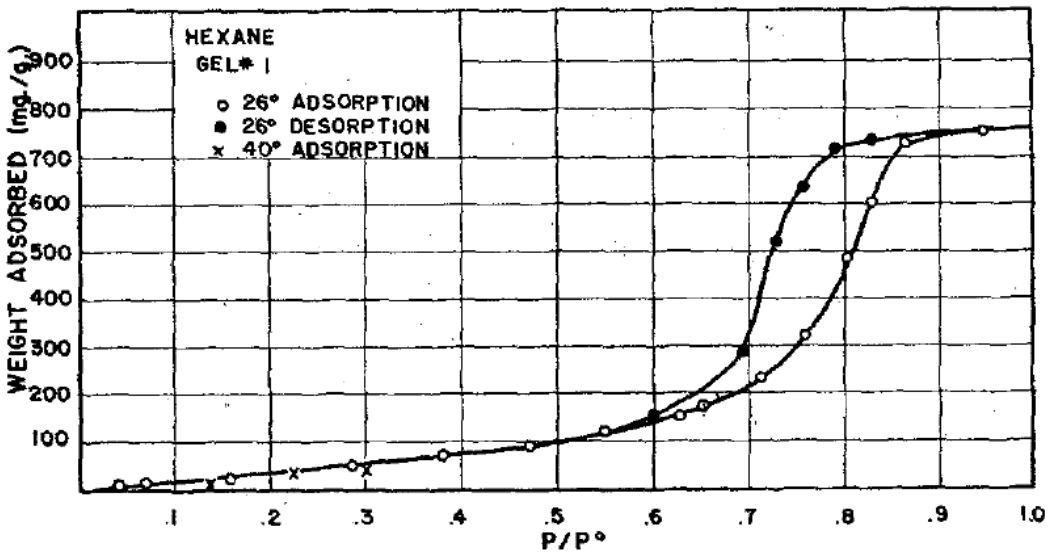
HEXANE
GEL# I
o 26° ADSORPTION
● 26° DESORPTION
× 40° ADSORPTION
WEIGHT ADSORBED (mg./g.)
100
200
300
400
500
600
700
800
900
.1
.2
.3
.4
.5
.6
.7
.8
.9
1.0
P/P°

C

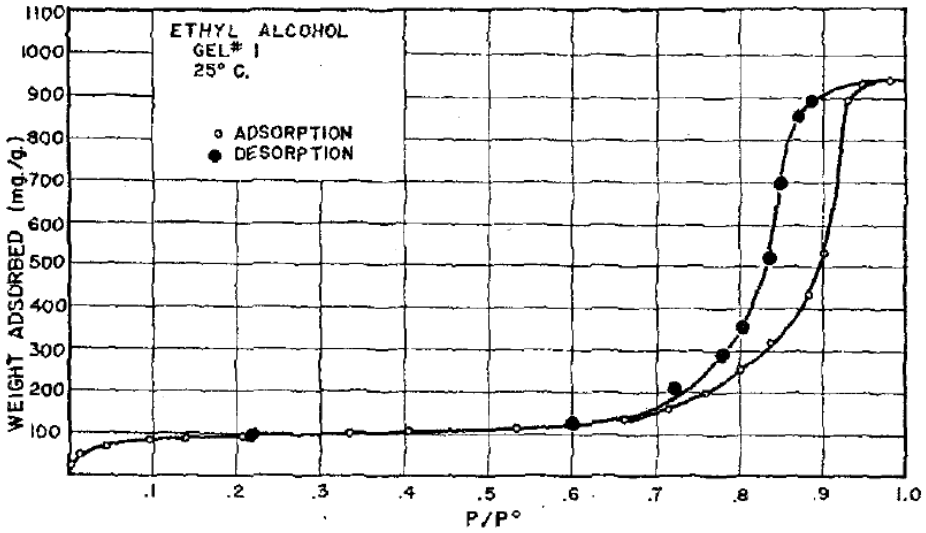
ETHYL ALCOHOL
GEL# I
25° C.
o ADSORPTION
● DESORPTION
WEIGHT ADSORBED (mg./g.)
100
200
300
400
500
600
700
800
900
1000
1100
.1
.2
.3
.4
.5
.6
.7
.8
.9
1.0
P/P°

D

Appendix C

A fluid flow model using flow simulation involves a number of basic steps that are shown in the following flowchart in figure 1

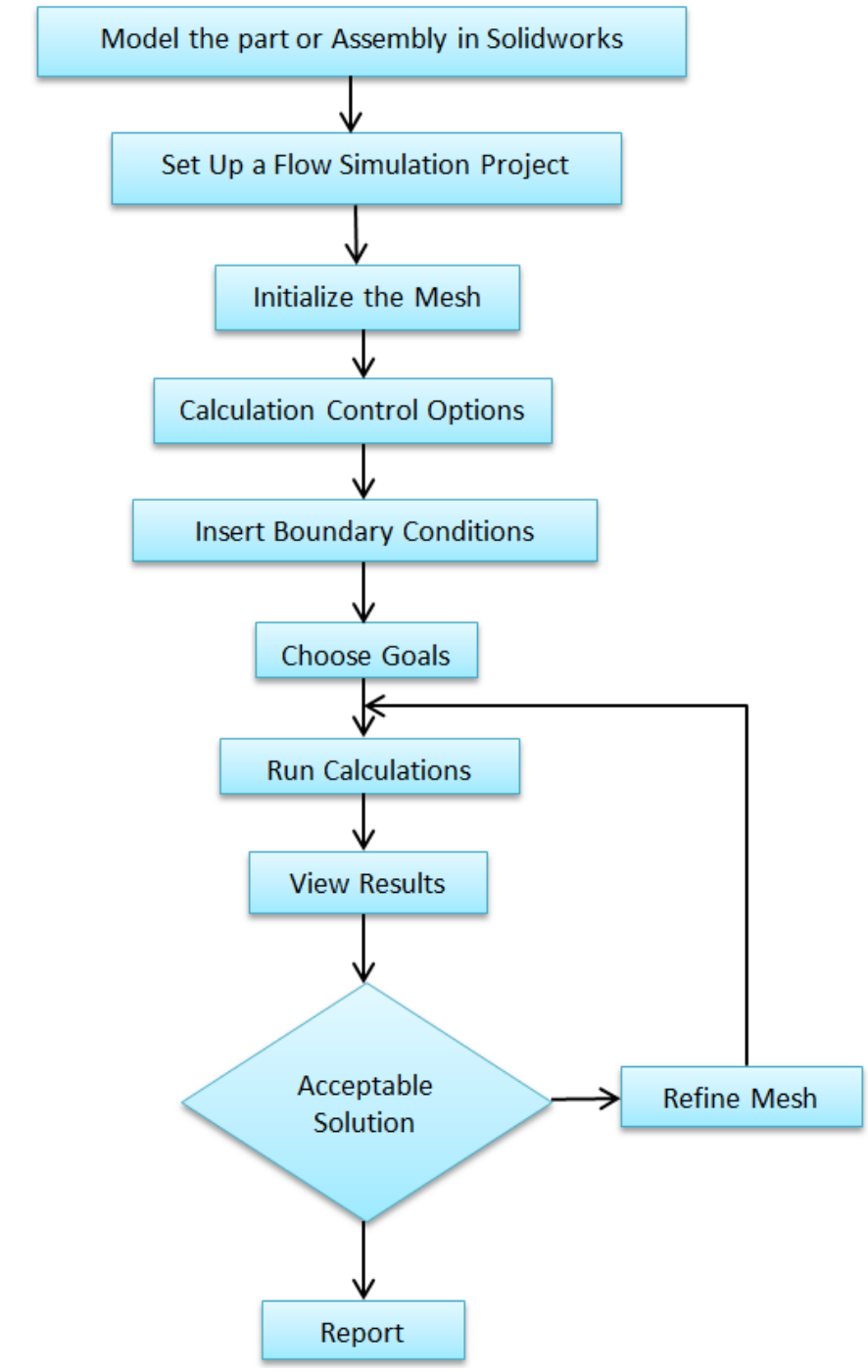

Figure.1. Flowchart for fluid flow analysis using Solidworks Flow Simulation